2006-01-01

# Design and Development in the Field of Alkaline Fuel Cell Technology

Steffen Schudt
*Technological University Dublin*

# Design and Development in the Field of Alkaline Fuel Cell Technology for Operation with Air

Steffen Schudt
Dipl.-Ing. Maschinenbau (FH)

Master of Philosophy (MPhil)

School of Control Systems and Electrical Engineering
Faculty of Engineering
Dublin Institute of Technology

Supervisors:
Dr. Eugene Coyle
Dr. David Kennedy
Professor Dr. James P. Hamilton
Professor Dr.-Ing. Heinz Schmidt-Walter

January 2006

I certify that this thesis, which I now submit for examination for the award of MPhil, is entirely my own work and has not been taken from the work of others save and to the extent that such work has been cited and acknowledged within the text of my work.

This thesis was prepared according to the regulations for postgraduate studies by research of the Dublin Institute of Technology and has not been submitted in whole or in part for an award in any other Institute or University.

The Institute has permission to keep, to lend or to copy this thesis in whole or in part, on condition that any such use of the material of the thesis be duly acknowledged.

Signature Stefan Schmidt Date 26th January 2006

Candidate

# Acknowledgements

I would like to thank Dr. Eugene Coyle, Dr. David Kennedy, Dr. James Hamilton and Dr. Heinz Schmidt-Walter for their advice during this research. Furthermore, I want to express my gratitude to Elmar for his effort with the translation, Lena for looking after my health, and my friends and family for their friendship and continuous support during the progress of the work.

Great thanks to Gerhard for being an excellent colleague and fellow researcher. I also wish to express my gratitude to the colleagues at Gaskatel who gave me a helping hand during the experimental work of this research and for their academic support.

# Abstract

This thesis is about the research on alkaline fuel cell (AFC) technology to investigate the long term operation with air. The aim was to solve the two main problems arising from long term operation and especially from operation with air:

- Dilution of the liquid electrolyte by the water from the reaction
- Cell damage due to the formation of carbonate

In recent years the development of fuel cells has gained a growing interest again. However the interest in alkaline fuel cells was low as the polymer electrolyte membrane fuel cell (PEMFC) seemed to be the superior system. One reason for this is the estimation that the AFC cannot be operated with air because of the reaction of $CO_2$ and the electrolyte potassium hydroxide solution (KOH). This research project shows that it is possible to operate the AFC with air and hydrogen in place of pure oxygen and hydrogen.

First of all tests were made with gas diffusion electrodes (GDEs) that are used to build the fuel cell. The electrodes were operated with air in a half cell. Even after thousands of hours in operation with unfiltered air no significant decrease of power was detectable. But testing electrodes in a half cell is only one part. The only way to get reliable results is to test the electrodes under real conditions: Long term operation in the alkaline fuel cell. For this purpose fuel cells were built with $O_2$-electrodes that were manufactured according to the results of the half cell tests. In addition, many changes had to be done to develop the fuel cell and adopt it to the demands of the operation with air.

The results are presented and discussed in this thesis. In the end it was possible to operate the AFC for several hundred hours with unfiltered air without damaging the cell. Proposals for future work are also given.

## List of Publications

| | |
|---|---|
| 23 June 2005 | Electrical Engineering Colloquium, University of Applied Sciences, Darmstadt, Germany; Presentation: Alkaline Fuel Cells |
| 4-6 October 2005 | Ninth Grove Fuel Cell Symposium, London, United Kingdom; Poster presentation: Long-term Operation of an Alkaline Fuel Cell with Air |
| 3-5 November 2005 | XII Symposium "Nutzung Regenerativer Energiequellen und Wasserstofftechnik" ("Utilisation of Renewable Energy Resources and Hydrogen Technology"), University of Applied Sciences, Stralsund, Germany; Presentation: Operation of an Alkaline Fuel Cell with Air containing $CO_2$ |

# List of Contents

# List of Symbols and Abbreviations

| | |
|---|---|
| $A$ | Cross-section of the conductor in cm² |
| $c_E$ | End concentration in M |
| $c_S$ | Start concentration in M |
| $F$ | Faraday constant |
| $I$ | Current in A (mA) |
| $I$ | Current density in A/cm² (mA/cm²) |
| $l$ | Total length of the conductor in cm |
| $M$ | Molar mass in kg/kmol |
| $m$ | Mass in kg |
| $P_{FC}$ | Power of the fuel cell in Watt |
| $p$ | Pressure in bar |
| $p_S$ | Partial pressure in bar |
| $R$ | Electrical resistance in Ω |
| $T$ | Temperature in °C |
| $t$ | Time in s |
| $V$ | Voltage in V (mV) |
| $V_{Drop,\,KOH}$ | Voltage drop for the electrolyte KOH solution in V (mV) |
| $z$ | Number of electrons |
| $x_S$ | Moisture content |
| $\varphi$ | Relative humidity |
| $\kappa$ | Electrical conductivity in S/cm |
| $\lambda$ | Air ratio |

| | |
|---|---|
| AFC | Alkaline Fuel Cell |
| $Ag_2O$ | Silver oxide |
| CE | Counter electrode |
| $CO_2$ | Carbon dioxide |
| $CO_3^{2-}$ | Carbonate ion |
| DLR | Deutsches Zentrum für Luft- und Raumfahrt (German Aerospace Center) |
| DMFC | Direct Methanol Fuel Cell |
| $e^-$ | Electron |
| EF | EloFlux |
| G 1/8" | Pipe thread |
| GC | Gas Chromatograph |
| GDE | Gas Diffusion Electrode |
| $H^+$ | Hydrogen ion |
| $H_2$ | Hydrogen |
| $H_2O$ | Water |
| $H_2O$ g | Water gaseous |
| $H_2O$ l | Water liquid |
| $HCO_3^-$ | Hydrogen carbonate (bicarbonate) |
| HRE | Hydrogen Reference Electrode |
| IEC | Ion Exchange Capacity |
| IKA | Manufacturer for laboratory and analytical technology |
| $K^+$ | Potassium ion |
| $K_2CO_3$ | Potassium carbonate |
| $KHCO_3$ | Potassium bicarbonate |
| KOH | Potassium hydroxide |
| MCFC | Molten Carbonate Fuel Cell |
| $N_2$ | Nitrogen |
| NASA | National Aeronautics and Space Administration |
| $OH^-$ | Hydroxide ion |

| | |
|---|---|
| $O_2$ | Oxygen |
| Oxag | Gaskatel name for electrodes with $Ag_2O$-catalyst |
| PAFC | Phosphoric Acid Fuel Cell |
| PEMFC | Proton Exchange Membrane Fuel Cell |
| PESU | Polyether Sulphone |
| PTFE | Polytetrafluorethylene |
| RE | Reference electrode |
| Silas | Oxygen electrode with silver catalyst and asbestos |
| Silflon | Name of a catalyst (Company Krupp Uhde, Germany) |
| SOFC | Solid Oxide Fuel Cell |
| WE | Working electrode |

# 1 Introduction

With fossil energy resources becoming more and more depleted it is essential to intensify research into alternative energy sources. Fuel cells can make an important contribution towards a renewable energy supply. Fuel cells will certainly not provide the solution to all future energy problems, however owing to high inherent efficiency fuel cell technology will allow the breaking of new ground in energy supply thus helping to conserve energy resources and the environment.

Research is ongoing on a variety of fuel cell types and a suitable system can be designed depending on the actual purpose and application required. Fuel cell technology is already more than 100 years old and a significant body of research was carried out during the 1960s [1-1]. Despite this, research on fuel cells is still relatively young and has regained relevance in recent years in the field of renewable energies technology. Many questions remain to be solved and answered.

The research presented in this thesis is concerned with alkaline fuel cells (AFC). When compared with other types of fuel cells, AFC technology offers a number of advantages. There is no need for expensive catalytic converters or membranes; the system required to operate an AFC is comparatively simple. AFCs also achieve very high efficiency values. The liquid potassium hydroxide (KOH) solution used as electrolyte could be considered a disadvantage. However, the handling of this electrolyte can be managed if suitable materials and sealing techniques are used (a comparison is the use of lead-acid batteries).

When investigating AFCs it soon becomes apparent that they can only be operated using pure gases, namely pure oxygen and pure hydrogen. In the literature it is commonly stated that it is not possible to operate an AFC with air in place of pure oxygen: "However, a major disadvantage is the $CO_2$ sensitivity of the alkaline electrolytes as carbonates are formed. In strong alkaline environments, the solubility of carbonates is rather poor. This leads to the formation of

carbonate crystals, capable of blocking electrolyte pathways and electrolyte pores." [1-2]. It is contended that the $CO_2$ contained in the air will react with the potassium hydroxide solution and will form the less soluble potassium carbonate. The electrodes in an AFC are gas diffusion electrodes (GDE), and the structure can be compared with a micro-porous sponge. It is easy to imagine that the pores would be clogged by the generated carbonate thus blocking the reaction. Since the carbonate cannot simply be flushed out of the cell this would mean the destruction of the fuel cell. It is the aim of this work to show that it is possible to operate an AFC with air (i.e. untreated). Another problem mitigating against long-term operation is the generated reaction water. The reaction of hydrogen and oxygen in the fuel cell generates electricity and - as a "by-product" - water. Over time, the reaction water will dilute the electrolyte. This needs to be prevented, otherwise the electrical conductivity of the potassium hydroxide solution will decrease and hence the capacity of the cell will also decrease. In addition, the electrolyte volume will also increase which will eventually cause an overflow of the storage vessel.

## 1.1 Research in the Field of AFC Technology

Nowadays only a few companies or research institutes still do active research on AFC technology. Even if this technology showed its reliability in the past, i.e. during the Apollo Mission of the NASA, other types of fuel cells seemed to be superior. But in the recent years more and more publications concerning the AFC technology can be found. And again, the main point of interest is the $CO_2$ sensitivity of the electrolyte KOH solution.

Often the research is about the testing of the electrodes used to build the AFC in a half cell. In a publication of the DLR (Deutsches Zentrum für Luft- und Raumfahrt, German Aerospace Center) [1-3] results of their half cell tests are presented. Here, oxygen electrodes were operated in a half cell for several thousand hours. The air supplied was additionally enriched with $CO_2$. During the overall test duration no significant degradation of the electrodes was observed.

Further assumptions with regards to $CO_2$-absorption and the formation of carbonate respectively can be found in a work of the Penn State University, USA [1-4]. Here, the topic is the development and test of a $CO_2$-tolerant AFC, in this case a methanol/air-operated AFC. However, the assumptions should also hold for $H_2$/air-operation. As one conclusion it was found that a significant decrease in the current output starts to occur only after about 60 % of KOH has been converted to $K_2CO_3$.

To find solutions to prevent a dilution of the electrolyte by the water from the reaction is obviously not seen as critical. In recent publications only the exchange of the electrolyte is mentioned; especially in order to prevent precipitation of carbonate [1-4].
However, in older publications methods are presented to prevent a dilution by the water of reaction. In a report of Siemens-Varta [1-5] the development of a so-called diffusion gap reconcentrator is presented. The reaction water is extracted from the cell via the electrolyte. In the diffusion gap reconcentrator the reaction water is extracted from the electrolyte.

## 1.2 Overview of Thesis Research

In this work attempts were made to find solutions for both problems. In order to operate an AFC with air, a filter could be used to remove the $CO_2$ from the air which would be the easiest solution. However, depending on its dimensions a filter has to be changed from time to time and the functionality of the filter will require monitoring. A desirable feature and aim at the outset of the research was to develop a maintenance-free, continuously operating system to regenerate the electrolyte.
The use of electrodialysis had earlier been considered [1-6]. With this method it is possible to regenerate the KOH electrolyte thus preventing an excessive carbonate concentration and preventing damage of the AFC. Another advantage of this

method would be the possibility of removing the reaction water from the electrolyte. In this way both problems could be solved using one method.
The tests carried out for the long-term operation of an AFC with air lead to some unexpected results. An oxygen electrode supplied with unfiltered air was tested in a half cell for more than 5500 hours. Neither the performance of this electrode declined significantly, nor it was destroyed. Using the results of the half cell tests, electrodes were manufactured for the use in the fuel cell. The fuel cells constructed for the tests utilised nickel as catalyst for the hydrogen electrode and silver for the oxygen (air) electrode. Both electrodes were manufactured using a rolling process.
For the operation with air in place of bottled oxygen the gas supply system had to be re-adjusted to the new conditions. If air is used instead of oxygen the gas flow through the cell has to be considerably higher (air has approximately 21 % $O_2$).
These experiments showed that there was no formation of insoluble carbonate in the electrodes. Over the duration of the experiments there was no serious drop in the fuel cell's performance characteristics. This effect is closely related to the construction and the production process of the oxygen electrode. It appeared that the formation of potassium carbonate was no longer the main problem.
The remaining problem was the reaction water. It was not deemed reasonable to utilise a process such as electrodialysis; it appeared much simpler to extract the generated reaction water through the air stream rather than through the electrolyte. Consequently, a variety of experiments were conducted to influence the water balance. Tests showed that by raising the operation temperature a portion of about 40 % of the produced reaction water could be extracted via the air flow. Due to mechanical problems the air flow rate was limited; otherwise an even higher portion of reaction water extraction could have been expected.
Finally, it was shown that the operation of an alkaline fuel cell with air is possible. Further problems that occurred during the research are discussed and ways to find a solution are presented.

## 1.3 Structure of the Thesis

Chapter 2 provides an overview of fuel cell technology. Firstly, a general introduction to fuel cells is presented. The alkaline fuel cell is explained and finally the system developed by Gaskatel is presented. The use of air for fuel cell operation is described and different approaches to solving problems arising are addressed.

Chapter 3 describes the practical part of the research. The manufacturing of the fuel cells and the achieved modifications are elaborated. Furthermore, the measurement instruments and measurement methods employed are described.

In chapter 4 the results of the experiments carried out are presented. The aim of this research was to examine the long term operation of an AFC with air. For the operation with air, the main focus is the commonly known problem of the incompatibility of the electrolyte KOH with $CO_2$. Furthermore, special attention has to be paid to the water in the cell for long term operation.

In chapter 5 the measurement results of the experiments presented in Chapter 4 are discussed. Initially, the half cell tests are covered which primarily served the examination of the basics and the selection of the electrodes. This is followed by a discussion of the results with the fuel cells and the measurements with the gas chromatograph.

Chapter 6 concludes this work and gives recommendations for future research.

# 2 Background

This chapter provides an overview of fuel cell technology. Firstly, a general introduction to fuel cells is provided, the alkaline fuel cell is explained and finally the system developed by Gaskatel is presented. The use of air for fuel cell operation is described and different approaches to solving problems arising are addressed.

## 2.1 Fuel Cells

The functional principle of fuel cells is based upon the controlled electrochemical reaction of hydrogen and oxygen to produce water with the purpose to harnessing the electric energy produced. This principle was introduced in 1839 by Sir William Grove, who described a hydrogen/oxygen fuel cell with liquid sulphuric acid as electrolyte [2-1].

Fuel cells make it possible to directly convert the chemical energy of a fuel into electricity. Unlike batteries, the fuel is supplied continuously and is not contained within the system. If the supply is used up it can be replenished. Contrary to thermal processes, the efficiency of fuel cells is not limited by the Carnot efficiency.

### 2.1.1 Fuel Cell Types

A variety of different fuel cell types exist. They are distinguished by the operating temperature, the electrolyte or the fuel used for operation.

**Proton Exchange Membrane Fuel Cell - PEMFC**

The PEMFC is a low temperature fuel cell. Its operating temperature is in the range of 50 °C to 100 °C. A solid polymer membrane is used as electrolyte (i.e. Nafion). It is permeable to protons, but it does not conduct electrons. A transport of $H^+$ ions is possible through this membrane, Hydrogen molecules can't pass it.

The transport of charge is done by the $H^+$ ions. The PEMFC is operated with hydrogen and oxygen. Air can also be used as source for oxygen.

**Alkaline Fuel Cell - AFC**

A description of the AFC is given in the next section (2.2)

**Direct Methanol Fuel Cell - DMFC**

The DMFC is similar to the PEMFC except that in place of pure hydrogen a mixture of methanol and water is employed as the fuel. Its operating temperature is in the range of 50 °C to 100 °C.

**Phosphoric Acid Fuel Cell - PAFC**

The PAFC is a high temperature fuel cell. Its operating temperature typically is about 160 °C to 200 °C. As electrolyte phosphoric acid of high concentration (~85 wt%) is used. The electrolyte is fixed in a membrane situated in between the anode and the cathode. Charge is transported by $H^+$ ions. The PAFC is operated with hydrogen and oxygen. The use of air as source for oxygen is also possible.

**Molten Carbonate Fuel Cell - MCFC**

The MCFC is also a high temperature fuel cell. Its operating temperature is about 500 °C to 650 °C. A mass of molten potassium carbonate ($K_2CO_3$) is employed as the electrolyte. Charge is transported by $CO_3^{2-}$ ions. The MCFC is operated with hydrogen, natural gas or biogas.

**Solid Oxid Fuel Cell - SOFC**

The SOFC is a high temperature fuel cell. Its operating temperature is about 750 °C to 1000 °C. As electrolyte solid zirconium dioxide ($ZrO_2$) is used. The SOFC is operated with hydrogen, natural gas or biogas.

This research is concerned with alkaline fuel cells and this type of fuel cell will therefore be addressed in this thesis.

## 2.2 Alkaline Fuel Cells (AFC)

Alkaline fuel cells are characterised as low-temperature fuel cells as their operational temperature is between 60–80 °C. AFCs consist mainly of the electrodes (anode and cathode), the separator electrically isolating the two electrodes, and potassium hydroxide solution as electrolyte. The fuel gases supplied to the cell are hydrogen and oxygen.

An advantage of AFCs is the use of inexpensive catalytic converters (e.g. Raney-nickel) and membranes. AFCs can reach very high efficiency values, typically up to 70 %. The liquid potassium hydroxide solution as electrolyte could be seen as a disadvantage, however careful handling solves this problem. AFCs incompatibility with $CO_2$ is still presented in technical literature to justify use for specific military or space research applications only [2-2].

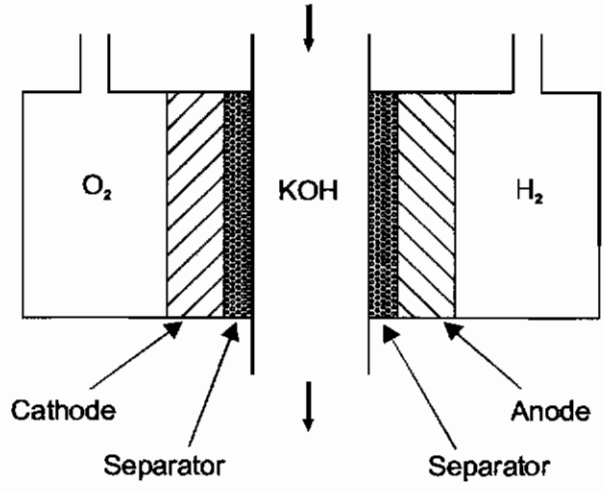


**Figure 2-1:** Schematic representation of a "classic" AFC

There are various constructions of alkaline fuel cells which are categorised by the kind of electrolyte supply.

The "classic" design shown in Figure 2-1 belongs to the type of cells with freely moving electrolyte, as does the EloFlux-AFC (shown in Figure 2-3) and which is described in the following section (2.3).

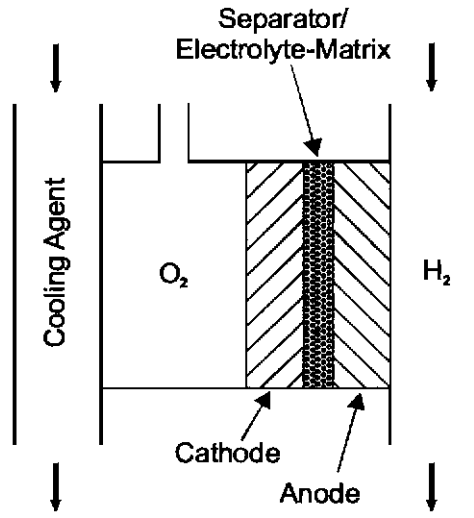


**Figure 2-2:** Schematic representation of a Matrix-cell AFC

Another category of AFC is that in which the electrolyte is fixed in the porous structure of the electrodes and the separator, so-called Matrix-cells. A schematic representation of a Matrix-cell with gas circulation is shown in Figure 2-2.

## 2.3 EloFlux-AFC

A unique AFC is the EloFlux-AFC that was utilised in the current research.

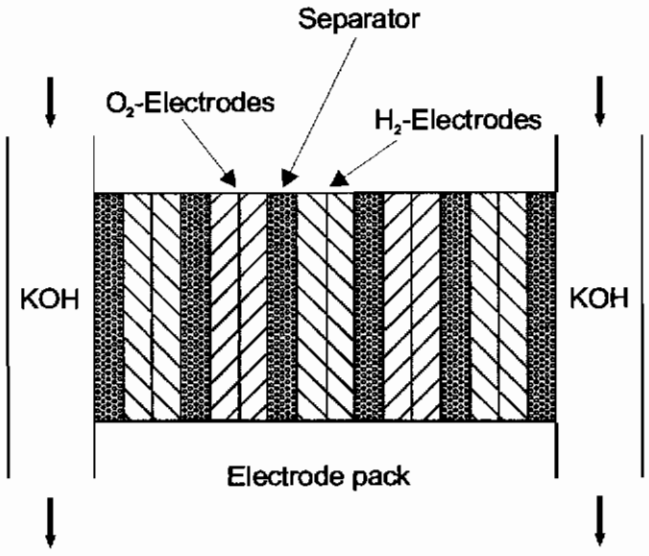


**Figure 2-3:** Schematic representation of an EloFlux-AFC

The EloFlux-AFC was developed and patented by Professor Winsel in 1971 [2-3]. In the 1970's the research and development was conducted by the Varta battery company (Varta Batterien AG) in Kelkheim, Germany. Later, research was carried out at the University of Kassel, Germany, in co-operation with Varta.
From 1997 the Gaskatel company has worked on the development of the EloFlux-fuel cell and electrolysers.

### 2.3.1 Construction of an EloFlux-AFC

Components of an EloFlux-AFC

**Electrodes**

In the fuel cell gas diffusion electrodes (GDE) are used. The catalyst used for the hydrogen electrode is Raney-nickel which is a very porous nickel. For the oxygen electrode silver is generally used [2-4]. The electrodes are manufactured in a rolling process using the catalyst and polytetrafluorethylene (PTFE) as a binding agent. In order to drain the current from the electrodes the electrode material is rolled onto a metal lattice [2-5, 2-6]. In order for a reaction to take place three phases have to be present: the reaction gas, the electrolyte and the catalyst. The location where the reaction takes place is called a triple phase boundary. The materials used and the manufacturing process result in a porous electrode structure. Two different pore systems are created: hydrophilic pores through which the electrolyte is transported, and hydrophobic pores through which the gas flows.

**Separator**

In an EloFlux-AFC the anode and the cathode are not separated by an electrolyte compartment, as is the case in a common AFC, but by a separator. The anode and cathode are placed directly on top of each other and are electrically isolated by the separator. However, an ion flow through the separator has to be possible. Additionally, the separator prevents a mixing of the gases. Plastic foils with corresponding properties are used. A distinction is made between active and passive separators. The active separators are located between anode and cathode, and the ion transport takes place through them during the reaction between the hydrogen and the oxygen electrode. The passive separators are located between the electrolyte compartment and the electrodes, and the electrolyte transport takes place through them; they are not involved in the actual reaction.

### Electrolyte

The electrolyte used is an aqueous potassium hydroxide solution (KOH). Conductivity and corrosiveness determine the concentration of the KOH solution.

### Housing

The housing of EloFlux-AFCs consists of epoxy resin; all components are cast together into a single block. This provides mechanical stability to the cell and supports the gas and electrolyte connectors.

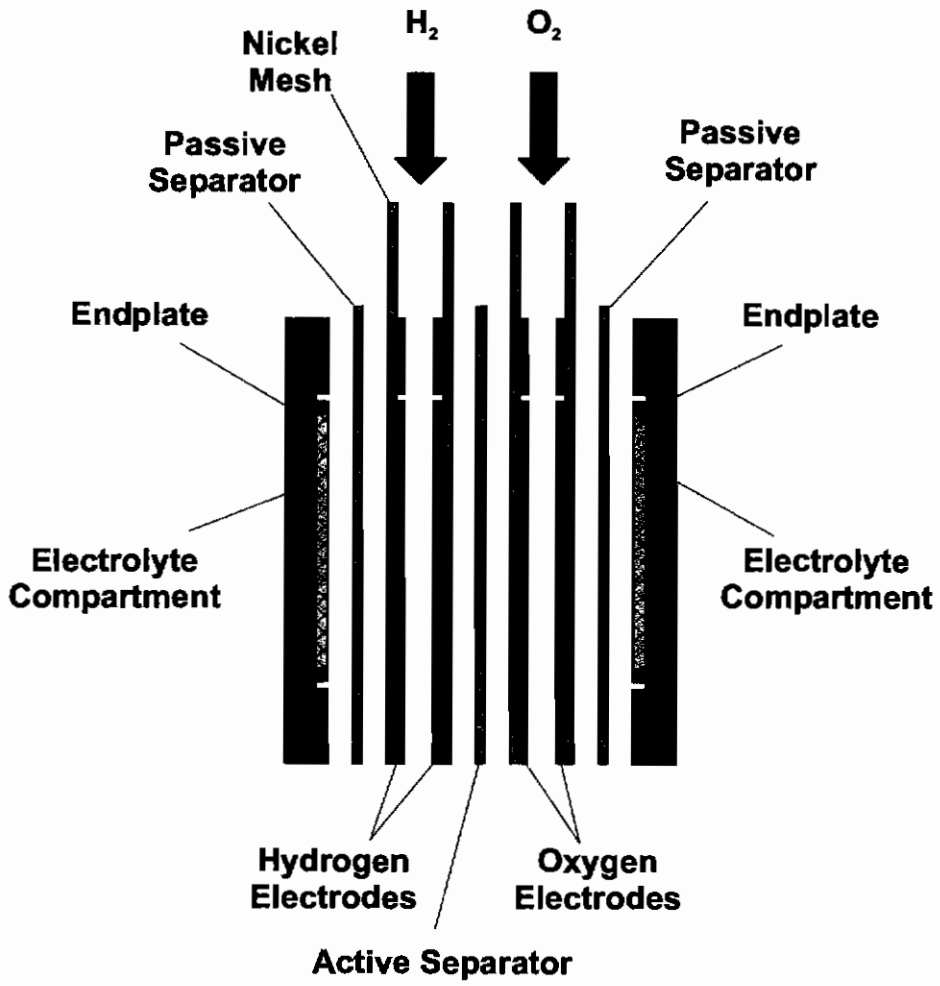


**Figure 2-4:** Construction of an EloFlux-AFC (one cell unit)

### 2.3.2 Electrochemical Reactions in an AFC

In an alkaline fuel cell hydrogen and oxygen react to form water. During this reaction energy is released. The overall electrochemical equation of the fuel cell is:

$$2\,H_2 + O_2 \rightarrow 2\,H_2O \qquad \text{(Eq. 2-1)}$$

The overall equation can be split into the partial reaction equations of the hydrogen and the oxygen electrode.

**Reaction at the hydrogen side (anode):**

$$2\,H_2 + 4\,OH^- \rightarrow 4\,H_2O + 4\,e^- \qquad \text{(Eq. 2-2)}$$

The hydrogen supplied is oxidised. The $H_2$ molecule is separated into two H ions. Each H ion reacts - while releasing its electron - with an $OH^-$ ion to form a water molecule. The electrons are conducted outside the cell where they can supply power to a load and are then conducted back to the cathode (electron flow outside the cell). Since electrons are released during the reaction an electron excess occurs; the hydrogen electrode is hence the minus pole of the fuel cell.

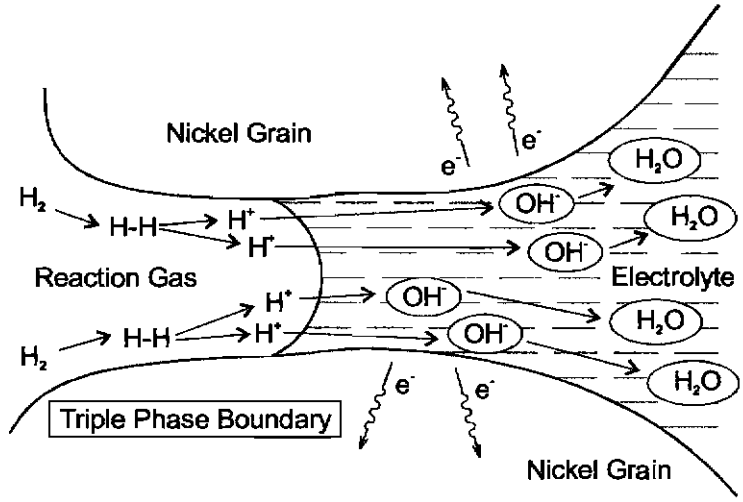


**Figure 2-5:** Reaction kinetics at the triple phase boundary of an $H_2$-electrode

**Reaction at the oxygen side (cathode):**

$$O_2 + 2H_2O + 4e^- \rightarrow 4OH^- \qquad \text{(Eq. 2-3)}$$

The oxygen supplied is reduced, it reacts with one water molecule to form two $OH^-$ ions. For this, two electrons are required which are supplied from the anode via the external electric circuit. At the oxygen side there is a lack of electrons; the oxygen electrode is hence the plus pole of the fuel cell.

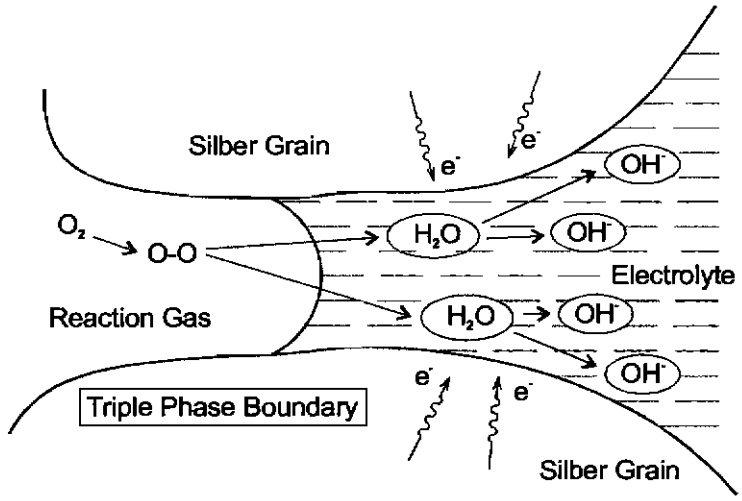


**Figure 2-6:** Reaction kinetics at the triple phase boundary of an $O_2$-electrode

A mass transport of $OH^-$ ions and water molecules takes place through the electrolyte. $OH^-$ ions migrate to the cathode whilst $H_2O$ molecules migrate to the anode. This transport takes place through diffusion. In an EloFlux-AFC the transport is superimposed by a pressure-dependent flow. A schematic representation of the mass transport in the fuel cell is shown in Figure 2-7.

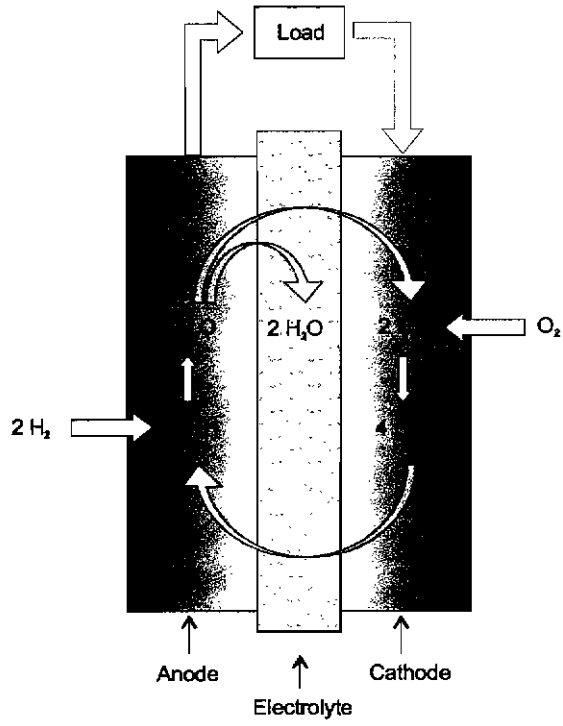


**Figure 2-7:** Mass transport in an AFC

### 2.3.3 Specific Features of the EloFlux-AFC

The difference of the EloFlux-AFC when compared to common AFCs or fuel cells with liquid electrolytes lies in a different electrolyte flow through the cell.

A conventional AFC consists of three partitions: one for hydrogen, one for oxygen or air and one for the electrolyte potassium hydroxide solution (see Figure 2-1).

The electrodes usually feature a polytetrafluorethylene (PTFE) layer at the gas side in order to prevent an intrusion of KOH into the gas compartment. The KOH flows along the electrode surface. KOH is brought into the electrode through diffusion and KOH and the reaction water are brought out of the electrode.

In an EloFlux-cell the anode and the cathode are grouted to each other, separated by a non-conducting, porous separator. This separator is lyophilic and is permeable for KOH, but under operating conditions it is impermeable for gases [2-7] due to capillary depression. The bubble-point of the separator can be higher

than 3.0 bar, depending on the chosen material. The Anode and the cathode are bi-porous and behave like a micro-porous sponge.

If the electrolyte-soaked electrode is exposed to a small gas over-pressure, then a part of the pores gets filled with gas while the rest remains filled with KOH. It is thus possible to pump the electrolyte through a stack of electrodes and separators.

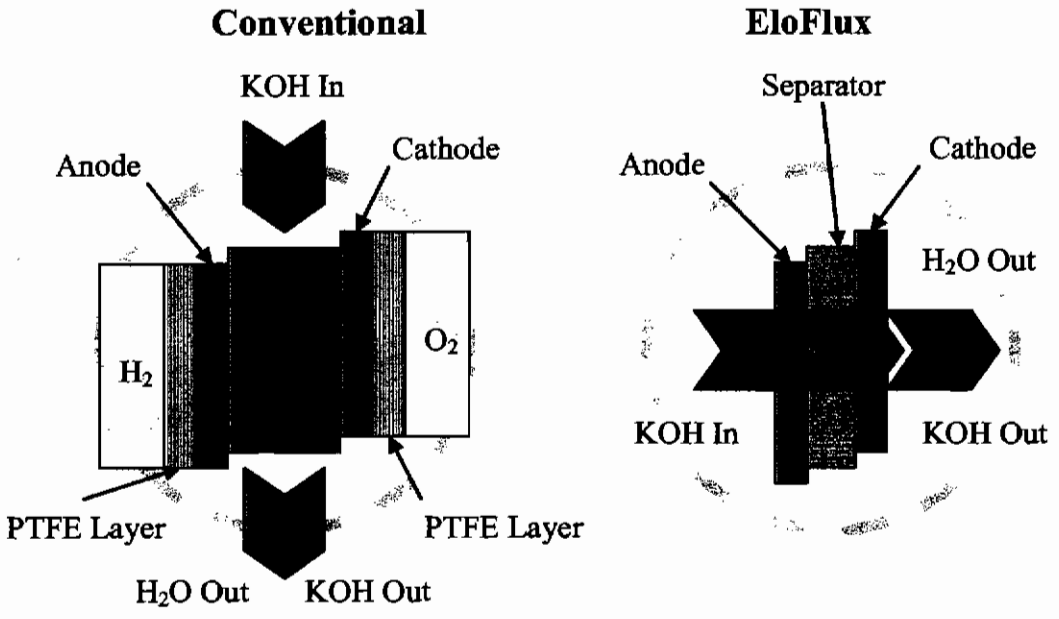


**Figure 2-8:** Electrolyte flow in a conventional AFC (left) and in an EloFlux-AFC (right)

Advantages of the EloFlux-System:

- compact construction due to the absence of separate partitions
- low internal cell resistance due to small distance between the electrodes
- ion transport through diffusion and an imposed convective flow
- simple temperature and water regulation due to a liquid electrolyte
- differential pressure between gas and electrolyte adjustable between circa 0.0 and 1.0 bar without an intrusion of gas into the electrolyte

### 2.3.4 EloFlux-AFC System for Air Operation

The system required to operate an EloFlux-AFC is comparatively simple. For the cell's electrolyte supply a reservoir is required, a pump for the KOH circulation

and the corresponding ducts and connectors. For the gas supply ducts and connectors are required as well, and if necessary a choke valve after the cell to adjust the flow rate. For operation with pure gases the cell would then be ready for operation.

In case the AFC is to be operated with air instead of pure oxygen the fuel cell and the system need to be adapted to the new conditions. The same holds for long-term operation, especially if it is to be achieved without a major maintenance effort.

A fundamental difference between oxygen and air operation is the different amount of gas to be supplied to the cell. With an oxygen proportion of 21 %, the gas amount has to be circa five times larger than compared to pure gas. In order to ensure a sufficient oxygen supply to the electrode an even larger surplus of air is chosen. The gas transport rate has to be increased as well to make sure that the portion of non-required gases does not inhibit the reaction. The gas distribution structure of a common EloFlux-AFC is not specified for these requirements. The modifications applied to the cell are described in chapter 3.

Modifications concerning the system are also necessary when using unfiltered air, i.e. air containing $CO_2$. For the long-term operation a solution has to be found on how to remove the produced reaction water from the system.

## 2.4 Problems of long-term Operation with unfiltered Air

The reaction of KOH with $CO_2$ contained in air results in the formation of carbonate and water:

$$CO_2 + 2KOH \rightarrow K_2CO_3 + H_2O \qquad \text{(Eq. 2-4)}$$

The electrodes used in EloFlux-AFCs can be thought of as micro-porous sponges. The $CO_2$ contained in air reacts with the potassium hydroxide and forms potassium carbonate which is initially in solution. When more and more $CO_2$ is introduced into the cell with the air and the solubility limit of carbonate in KOH

is exceeded, the carbonate forms a solid precipitate that can block the pore system of the electrode. The reaction in the electrode cannot take place any more and the cell is destroyed.
During the operation of an AFC the reaction of hydrogen and oxygen produces water (see Eq. 2-1).

This reaction water dilutes the electrolyte which causes a decrease of the conductivity of the potassium hydroxide solution. This needs to be prevented since it has negative effects on the mass transport in the cell and hence also influences the cell efficiency. Over time, the reaction water produced would also cause an overflow of the storage tank.

### 2.4.1 $CO_2$-Problem

Descriptions of alkaline fuel cells are mostly accompanied by a remark on the $CO_2$-incompatibility of the electrolyte KOH. The $CO_2$ introduced with the air reacts with the potassium hydroxide to form potassium carbonate. In case the potassium carbonate portion exceeds the solubility limit it will form a precipitate that can block the porous structure of the gas diffusion electrodes. This can be read in almost every publication on AFCs [2-8]. However, it is difficult to find detailed references about research carried out on that topic, or the results thereof. Mostly, it is only described as if it was a fact or should be one. As an example the following quote about a hydrogen/air element for alkaline electrolytes is presented: "*The carbon dioxide contained in air is not removed beforehand, so that carbonate is formed in the electrolyte... 11 to 17 l per minute air are supplied to the battery. The electrolyte used is 12 N KOH. In an experiment lasting 225 h the cells were loaded with circa 100 mA/cm² at 0.7 V at a temperature of 40 °C. Due to the carbonate formation in the electrolyte (1.7 N after 225 h) the KOH concentration decreased to 7.8 N. Simultaneously, the power was reduced from 75 to 64 mW/cm².*" [2-9]
There are, however, other indications in the relevant literature pointing in a different direction. Karl Kordesch writes in his work "Das Wasserstoff-Sauerstoff-Luft Brennstoffelement mit Kohleelektroden" ("The hydrogen-oxygen-air fuel cell

element with carbon electrodes") the following: "*The absorption of $CO_2$ from the air progresses amazingly slowly. During the work with air-depolarised cells it was observed, that the carbon electrode effectively prevented the electrolyte carbonisation through the carbon dioxide contained in air. After an operating time of two years the function of the cell is not affected by the content of 20 % carbonate in the potassium hydroxide electrolyte*" [2-10]. It is also elsewhere mentioned that it is possible, through a choice of suitable electrodes or electrode materials, to counteract the carbonate formation. On the other hand, potassium hydroxide solution also absorbs $CO_2$ from the ambient air and potassium carbonate is formed, even if the cell is not operated with air. This effect could be verified during tests with a fuel cell as well as during tests with a half cell [2-11].

In recent research the $CO_2$-problem is again increasingly tackled. Ways are shown to develop an AFC tolerant to $CO_2$. In most cases the research is about tests of the electrodes in a half cell. The work of the DLR (Deutsches Zentrum für Luft- und Raumfahrt, German Aerospace Center) has to be mentioned in this context. Here, oxygen electrodes in a half cell were operated in oxygen consumption mode for several thousand hours. The supplied air was additionally enriched with $CO_2$. During the overall test duration no significant degradation of the electrodes was observed [2-12].

Further work on this topic exists by Bram de Ruiter, at the Helsinki University of Technology, where experiments were conducted on the $CO_2$-absorption of the potassium hydroxide electrolyte. For this, two half cell experiments were set up, each with the same oxygen electrode. One cell was loaded while the other cell was not loaded. This was done to clarify also whether the operation has an influence on the $CO_2$-absorption. In both cases the progression of the increase of carbonate concentration in the electrolyte was similarly fast; the progression of the increase was linear over the experiment duration. It is assumed that the concentration gradient causes the $CO_2$ to diffuse into the electrode where it reacts with the potassium hydroxide. The carbonate formed is then found in the electrolyte. However, no statements were made on the effects this had on the electrodes [2-13].

In any case, the experiments can be considered questionable since both half cells had an open electrolyte reservoir. This means that the potassium hydroxide solution used had contact with the ambient air throughout the experiment. It is well known that KOH can absorb $CO_2$ in this way leading to carbonate formation.

Further assumptions with regards to $CO_2$-absorption and the formation of carbonate respectively can be found in a work at Penn State University, USA. Here, the topic is the development and test of a $CO_2$-tolerant AFC, in this case a methanol/air-operated AFC. However, the assumptions should also hold for $H_2$/air-operation. Here, the following path of the $CO_2$ is shown: firstly, the $CO_2$ in the air is solubilised in the water. It reacts to form carbonic acid which in turn dissociates stepwise. If KOH now is added to make an alkaline solution the carbonic acid reacts with the potassium hydroxide to form potassium carbonate and water.

$$H_2CO_3 + 2KOH \rightarrow K_2CO_3 + 2H_2O \qquad \text{(Eq. 2-5)}$$

This equation can be simplified since there are sufficient amounts of KOH present and the overall result is not changed by this:

$$CO_3^{2-} + H_2O \rightarrow HCO_3^- + OH^- \qquad \text{(Eq. 2-6)}$$

The ionic equilibrium depends on the solution pH and temperature. If the pH value is more acidic than 6.4, then the carbonic acid dominates. Between pH-values of 6.4 to 10.3 hydrogen carbonate dominates and above a pH-value of 10.3 pure carbonate dominates.

During operation a reduction of the current was always detected. If circa 60 % of KOH were converted into $K_2CO_3$ the current was significantly reduced. It was suggested to use this value as an indication to change the electrolyte. However,

there was no report about serious damage to or even destruction of the cell. Furthermore, during this work various membranes were tested to filter the $CO_2$ out of the air [2-14].

In the publication of Pascal Gouérec et al. further data can be found with regards to the $CO_2$-problem. They found that $K_2CO_3$ only precipitates at high concentrations (7.9 M at 20 °C and 9.67 M at 70 °C respectively). In order to achieve these concentrations, a KOH concentration of 15.8 M at 20 °C and 19.3 M at 70 °C respectively was required in the electrode. These concentrations are, however, very close to the solubility limits of KOH which are at 20.3 M (at 20 °C) and 27.1 M (at 70 °C) respectively. If this KOH concentration is reached anywhere in the electrode the KOH precipitates and can block the porous structure of the electrode. They suppose that an excess of the solubility limit is meant to be prevented by maintaining a thorough liquid transport in the cathode [2-15].

As presented in the previous paragraphs, during the literature research several hints were found concerning the $CO_2$ problem. But still the question remains unsolved, what actually happens with the $CO_2$ in the fuel cell when the latter is operated with air.

In the current work two models were investigated to explain the mass transport of water in the oxygen electrode. Two possible directions of flow can be imagined:

A – the water flows as a liquid from the electrode towards the counter electrode.
B – the water flows as a gas through the electrode towards the gas compartment.

Variant B is the desired direction of flow with regards to the extraction of the reaction water.

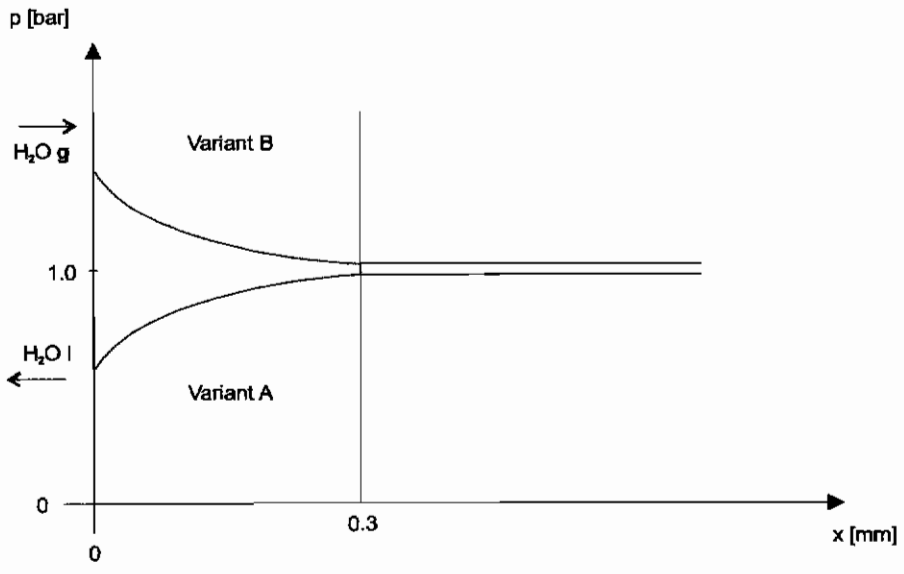


**Diagram 2-1:** Potential flow direction of the reaction water in the electrode

Diagram 2-1 shows the pressure distribution in the pores of the electrode as a function of the electrode thickness.

Variant A would cause a depression through the water flowing out which would provide for the replenishment of air and hence $CO_2$ from the gas compartment. In variant B the flow could, however, inhibit the intrusion of air. Exhausted oxygen would diffuse into the electrode, driven by the concentration difference. Additionally, the water can also absorb $CO_2$ and thus probably transport it from the electrode. The removal of the reaction water and the diffusion of the oxygen into the reaction zones must not interfere with each other.

How the water transport in the cell finally adjusts depends on the operating parameters and on the electrode properties.

Considering the mass transport through diffusion the following models can be identified. Diagram 2-2 shows the progression of the concentration as a function of the electrode thickness. The gas compartment is filled with air and hence the mass proportions of the gases in the electrode towards the gas compartment are initially identical with the mass proportions of air. During operation the oxygen is "used up", one $O_2$ forms two $H_2O$. The reaction can also be considered at the oxygen electrode alone, where one $O_2$ forms two $OH^-$. Under those conditions and the requirement of an equilibrium of the present particles the concentration of air

components in the electrode has to decrease towards the opposite electrode. The exhausted oxygen is replaced and the concentration gradient ensures a replenishment through diffusion. All other air components not partaking in a reaction have no stimulation to intrude into the electrode. Two possible scenarios can then be imagined for the $CO_2$ contained in the air. If it reacts with the electrolyte KOH to form $K_2CO_3$ - which is initially dissolved in the electrolyte - then more $CO_2$ will follow from the gas compartment. In case a reaction is prevented no $CO_2$ will intrude into the electrode from the gas compartment.

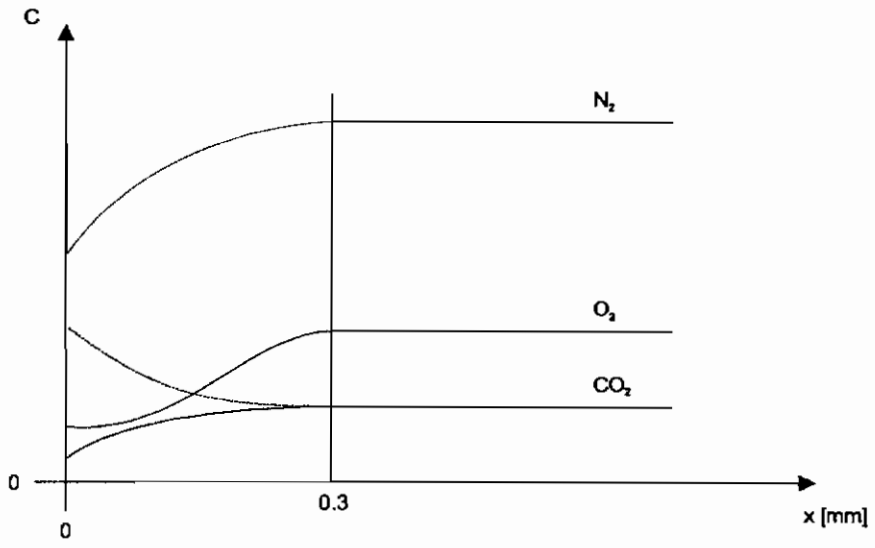


**Diagram 2-2:** Possible progression of the concentration inside the electrode

The following sections give an overview on how to solve the above described problems linked with the long-term operation with unfiltered air.

### 2.4.2 Removing the $CO_2$

**Filtration**

The easiest method to counteract the problem of carbonate formation would be the use of filters to remove the $CO_2$ from the air before it is conducted into the fuel cell where it can react with the KOH. To achieve this there are different methods, e.g. the absorption of $CO_2$ from the air using activated carbon or calcium oxide filters, or the use of potassium hydroxide wash bottles (see Figure 2-9). All of these methods do, however, require a certain effort for maintenance, such as monitoring and filter replacement on a regular basis.

In order to meet the specifications to ensure a nearly maintenance-free operation a continuously operating procedure was sought.

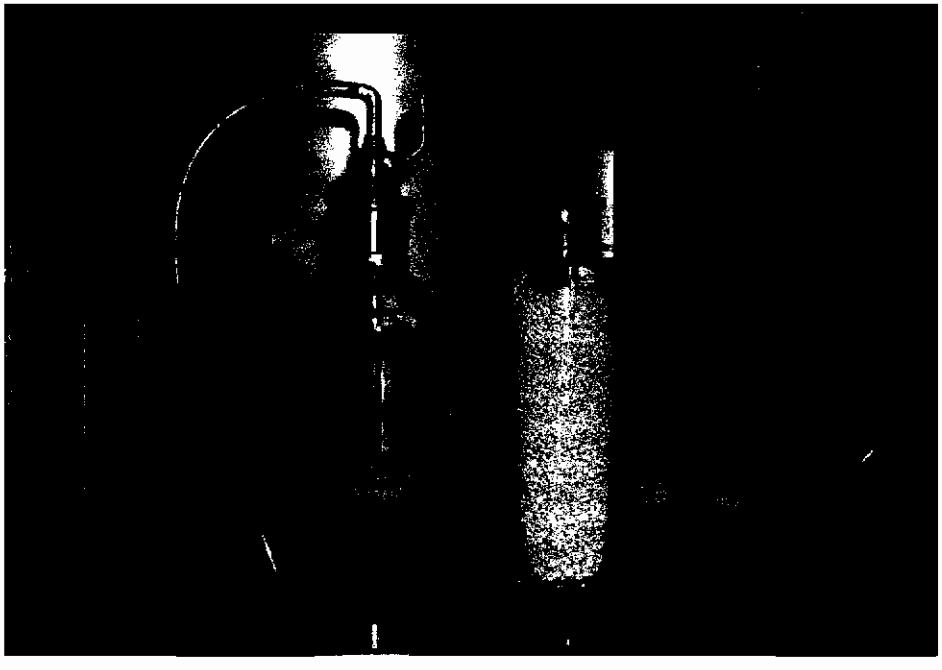

**Figure 2-9:** Fritted wash bottle with KOH solution (left) and calcium oxide-filter (right) to remove $CO_2$ from the air

Kordesch and Simader describe the use of soda lime to reduce the $CO_2$ contents from 0.03 % to 0.001 % before the air enters the cell [2-16]. This method was, for instance, used by the Zevko company [2-17].

## Electrodialysis

A system already considered previously is electrodialysis. Electrodialysis is a method to separate electrolytes from a solution [2-18].

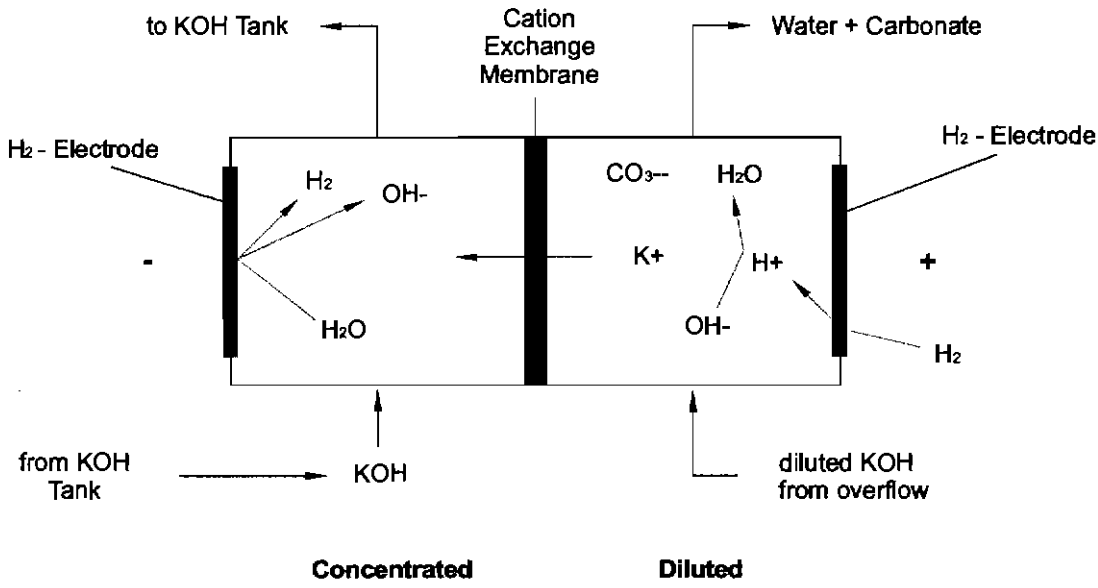


**Figure 2-10:** Schematic representation of a two-chamber electrodialysis cell

The simplest form of an electrodialysis cell is the two-chamber method shown in Figure 2-10. Driven by the electric field the ions migrate through conducting, permiselective membranes. For the application to electrolyte regeneration only the potassium ions have to be retrieved from the diluted electrolyte. At the concentrated side the electrolyte is conducted from the tank for reconcentration; at the diluted side the electrolyte is conducted from the overflow to reduce the concentration further. The $H_2$-electrodes produce hydrogen on the concentrated side, and consume $H_2$ on the diluted side. $K^+$ ions migrate from the diluted side through the cation exchange membrane to the concentrated side and there form KOH with the $OH^-$ ions. The carbonate remains in the anode compartment, in which additional water is formed. The reaction water from the overflow also remains on the diluted side. With this, carbonate and reaction water can be removed from the system. This makes the procedure suitable to solve both problems associated with long-term operation with one method.

In addition to the already mentioned procedures to remove the $CO_2$ several further descriptions were found during the literature review for this research. They are mentioned for completeness; however, further indications other in reference [2-19] were not found.

**Electrochemical extraction of carbonates**

In case an AFC is loaded with high current densities the concentration of $OH^-$ ions at the anode is reduced. Simultaneously carbonate-ions migrate to the anode. This causes the formation of an acidic solution with hydrogen carbonate as the main component. If the current density is further increased the hydrogen carbonate is split into water and $CO_2$. Pratt and Whitney have used this method [2-20].

**Liquid hydrogen**

Ahuja and Green describe the possibility to condense $CO_2$ from the air with the aid of liquid hydrogen. For this a model for a suitable heat exchanger was developed [2-21, 2-22].

**Alkaline solid state membranes**

The use of membranes is under discussion in which the alkaline electrolyte is bound in a solid state. Since no free potassium-ions are present even the feeding in of $CO_2$ with the air should not lead to carbonate formation [2-23, 2-24].

In general it can be stated that the operating parameters have an influence on the $CO_2$-sensitivity of the cell. For higher operating temperatures the solubility of $K_2CO_3$ in the electrolyte is increased. The precipitation of carbonate can hence be delayed [2-25]. It is also stated, that a circulation of the electrolyte increases the $CO_2$-tolerance of an AFC significantly [2-26].

### 2.4.3 Reaction Water Extraction

**Evaporation**

A very simple method to extract the reaction water can be realised through evaporation. For this, two approaches are in principle imaginable. The KOH reservoir could be heated directly. This, however, could cause problems if the KOH-circulation is to be operated under pressure. It is also imaginable to use a second tank which is supplied by the overflow of the main reservoir. From time to time the enriched potassium hydroxide would have to be conducted back into the system. In both cases it is, however, necessary to heat the reservoir. The required energy has to be supplied by the fuel cell. This is not sensible for low power ranges. Increasing the operating temperature of the fuel cell is also not possible due to the used materials. It is also envisaged that during operation the cell is heated without external heating. For multi-cell systems it might then become necessary to cool the cells (e.g. with an increased KOH throughput). In this case is seems not very sensible to heat up the potassium hydroxide solution on the one hand, and on the other hand use it for cooling.

**Diffusion gap reconcentrator**

Another possibility to extract the reaction water is by using a diffusion gap reconcentrator. Here, the reaction water is extracted from the cell via the electrolyte. This procedure was already tested and used by Varta during their research on AFCs [2-27]. At one side the heated potassium hydroxide is conducted into the cell and at the other side cold water is conducted into the corresponding compartment of the reconcentrator. In between the compartments is either a gas compartment ($H_2$ serves as carrier gas for the water vapour in the procedure), or, even better, a separating layer of hydrophobic material, e.g. PTFE. The pore system of the separating layer has to fulfil certain conditions under which water vapour can diffuse from the KOH side to the cold water side where the vapour condenses [2-28].

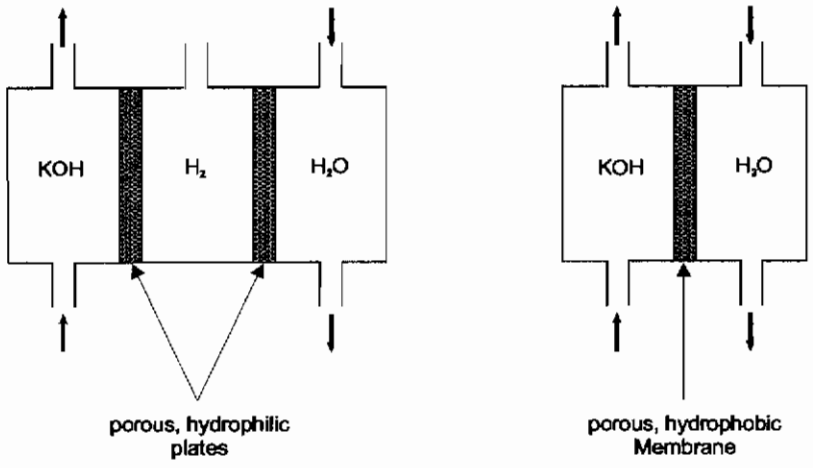


**Figure 2-11:** Schematic representation of a diffusion gap reconcentrator (left: with a gas compartment, right: with a hydrophobic membrane)

### Electrodialysis

As already described, the reaction water can also be extracted from the electrolyte using electrodialysis.

### Extraction with the hydrogen

Since the reaction water is produced at the hydrogen side (as explained in Eq. 2-2) it is obvious to extract it from the cell with the hydrogen. However, for this further components are required in the fuel cell system. It does not make sense to adjust an accordingly high throughput rate for the hydrogen and to emit it unused into the environment together with the extracted reaction water. The hydrogen has to be conducted in a circulation and the reaction water is removed from the hydrogen with a condenser. The system becomes hence much more complicated. This method is used by the NASA for the space shuttle fuel cells [2-29].

### Extraction with the air

Another possibility to extract the reaction water is with the air stream. Since a much larger amount of gas passes into the cell when operated with air instead of oxygen it can be assumed that the air stream absorbs a part or the total amount of

produced water which is then transported off with the air. For this, an estimation follows for the theoretically possible water absorption of dry air up to saturation at 30 °C:

Water absorption of dry air (T = 30 °C, p = 1.013 bar)

saturated state $\varphi = 1$

$$x_s = \frac{m_{H2O}}{m_{air}} = \frac{M_{H2O}}{M_{air}} \cdot \frac{p_S}{p - p_S} = 0.622 \cdot \frac{p_S}{p - p_S} \qquad \text{(Eq. 2-5)}$$

$$x_s = 0.622 \cdot \frac{0.04241}{1.013 - 0.04241} = \underline{\underline{0.0256}} \qquad \text{(Eq. 2-6)}$$

where

| | | |
|---|---|---|
| $x_s$ : | moisture content |
| $m_{H_2O}$ : | water mass in kg |
| $m_{air}$ : | air mass in kg |
| $M_{H_2O}$ : | molar mass water in kg/kmol |
| $M_{air}$ : | molar mass air in kg/kmol |
| $p$ : | pressure in bar |
| $p_s$ : | partial pressure in bar |

xs denotes the moisture content as the load of water (water vapour and also water) in the dry air for a saturated state. According to this calculation 1 kg of dry air can absorb 0.0256 kg water. This value now has to be put in relation to the produced reaction water. For the conversion of 1 kg hydrogen the fuel cell requires 34.2 kg air while 8.94 kg water are produced. Putting the given values into relation yields that the required 34.2 kg of air can absorb 0.88 kg of water. According to this the fuel cell needs to be operated at a temperature of 30 °C with a tenfold excess of air

($\lambda = 10$) in order to extract the produced reaction water completely via the air stream.

Since the partial pressure of water vapour $p_s$ changes with the temperature, each temperature will yield a different value for $\lambda$. In the table below these values are given for a temperature range of 10 °C to 60 °C.

| T [°C] | $P_{FC}$ [W] | $H_2O$ [mol/min] | $p_s$ [bar] | $x_s$ [-] | $\lambda$ [-] |
|---|---|---|---|---|---|
| 10 | 50 | 0.02 | 0.01227 | 0.0076264 | 34.28 |
| 20 | 50 | 0.02 | 0.02337 | 0.0146885 | 17.80 |
| 30 | 50 | 0.02 | 0.04241 | 0.0271783 | 9.62 |
| 40 | 50 | 0.02 | 0.07375 | 0.0488395 | 5.35 |
| 50 | 50 | 0.02 | 0.12335 | 0.0862403 | 3.03 |
| 60 | 50 | 0.02 | 0.19920 | 0.1522517 | 1.72 |

**Table 2-1:** Lambda values for reaction water extraction at different temperatures

With this purely theoretical calculation it seems possible to extract the produced reaction water from the cell with the air stream. Corresponding experiments are to verify this assumption.

## 2.5 Methodology and Procedures

At the beginning of the research the principle of electrodialysis seemed most suitable to overcome the two already described problems when using a fuel cell with air in long-term operation. Suitable ion changer membranes were investigated and tested; basic dimensioning calculations for an electrodialysis cell to be integrated in the AFC system were carried out [2-30].

The fuel cells that were built for the experiments initially exhibited faults. Therefore, a major part of the work was spent to locate and finally solve these problems.

The experiments dedicated to the fuel cell operation with air showed that the used oxygen electrodes with silver catalysts did not suffer any apparent damages. Such electrodes were tested over an extended period in a half-cell as well as in a fuel cell. This effect is caused by the consistency of the electrodes. Apparently it is possible through the choice of suitable materials and an adequate manufacturing process to produce electrodes that are suitable for the operation with air. Similar results were also reported by other institutes. A publication from 2003 in the "Journal of Power Sources" by the DLR (Deutsches Zentrum für Luft- und Raumfahrt, German Aerospace Center) reports on the long-term operation of gas diffusion electrodes for AFCs with gases containing $CO_2$ which did not result in a noticeable drop of the cell capacity [2-31].

In case an AFC with appropriate electrodes could be operated with air without any consequences from the $CO_2$ and the produced potassium carbonate respectively, then the use of a technique such as electrodialysis is no longer reasonable. For the extraction of the reaction water there are simpler and certainly more economical techniques available. It was decided to investigate the extraction of the reaction water using the air flow.

It was nevertheless important to know what happens with the $CO_2$ introduced into the cell. For this certain assumptions exist. According to an investigation by Jose D. Giner there exists the theory, that inside the cell a $CO_2$ circulation is established and that the $CO_2$ leaves the cell with the hydrogen. In order to obtain information about this the focus was set to the analysis of the gases [2-32].

# 3 Experimental

Chapter 3 describes the practical part of the research. The manufacturing of the fuel cells and the achieved modifications are elaborated. Furthermore, the measurement instruments and methods employed are described.

## 3.1 Construction of an AFC

An alkaline fuel cell mainly consists of the electrodes (anode and cathode), the separator electrically isolating the two electrodes, the oxygen and the hydrogen gas supplies and the liquid electrolyte KOH. The following text describes the EloFlux cell as one particular type of AFC in more detail. It can easily be imagined that, in order to build a complete fuel cell, further components are required. The above mentioned parts need, for instance, to be kept in place. Connectors for the supply with the gases and the electrolyte are required and the cell needs to be fitted with electrical terminals. Finally, the whole system has to be sealed in order to prevent potassium hydroxide solution from leaking out.

The different components the EloFlux AFC consists of are now described in more detail. The essential modifications worked out and realised in the progression of the project are also described here.

At the beginning of this work in April 2003, no satisfactorily working fuel cells were available at Gaskatel. The hitherto used separator, made from a material containing asbestos, was not produced any longer, and a long test series was carried out until separators were found that fulfilled the fundamental requirements. The cells built with these separators repeatedly exhibited faults, which could be traced back to casting problems. These problems could be solved; however, with the consequence, that nearly each part of the fuel cell had to be modified. Ultimately, the redesign resulted in many cases in a simplification of the manufacturing process of the individual parts.

### 3.1.1 Design of the EloFlux-AFC

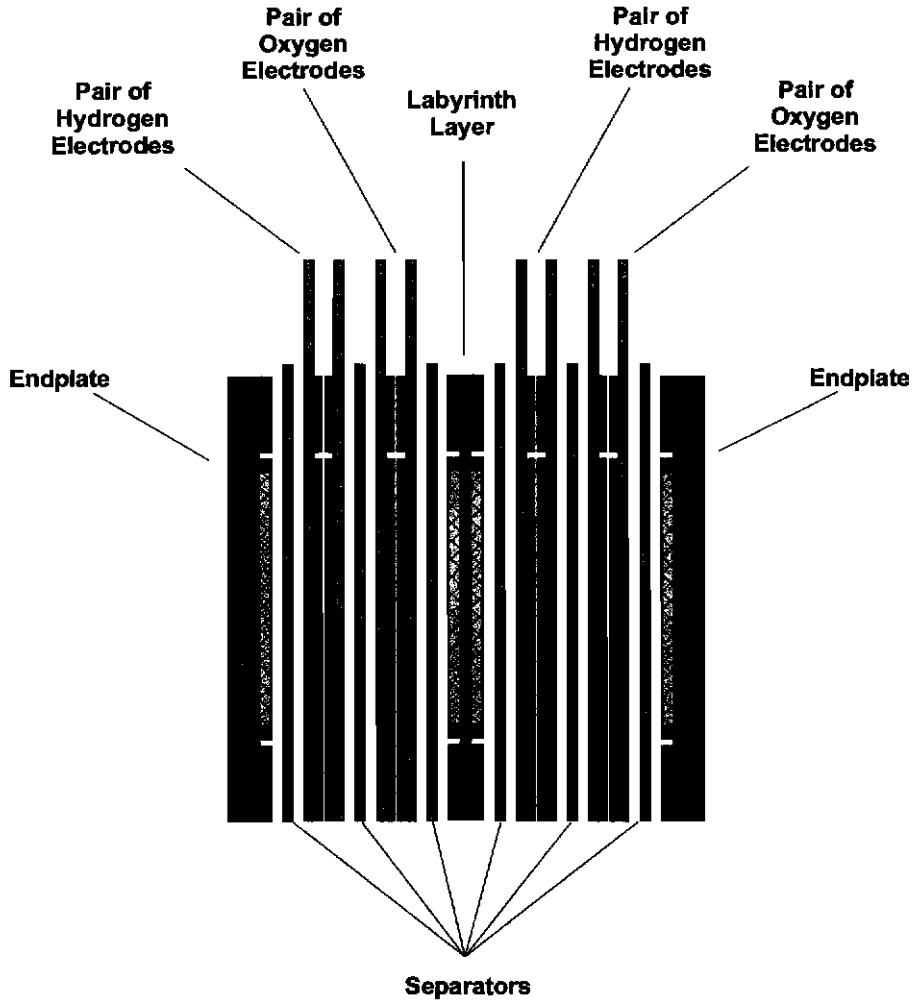


**Figure 3-1:** Schematic representation of the design of an EloFlux-AFC (two cell unit)

Figure 3-1 shows the design of two cell unit EloFlux-AFC. Specific for the design of a unit with more than one cell is the labyrinth layer between the single cells. To build up a one cell unit two pairs of electrodes, three separators and two endplates are used. By using the labyrinth layers it is easy to multiply the number of cells per unit.

In the following paragraphs the endplates and the labyrinth layer is described in more details. Further Information is given about the casting, the electrodes and the gas compartment for air operation.

### 3.1.2 Endplates

Front and back of an EloFlux AFC are each formed by the endplates. They provide mechanical stability to the cell and keep the parts placed in between them in position when the assembly is mounted in the casting mould. The endplates are cast from epoxy resin.

Initially, a plate with a thickness of 5.0 mm was cast, onto which a polyether sulphone (PESU) frame was glued on in a further process step. The space formed by the frame towards the electrode is the electrolyte distributor which distributes the potassium hydroxide solution across the entire active area. The endplates had borings for the gases and the electrolyte respectively. With these endplates the cells needed to be fitted with connector plates or with adequate devices equipped with the necessary conduit connectors.

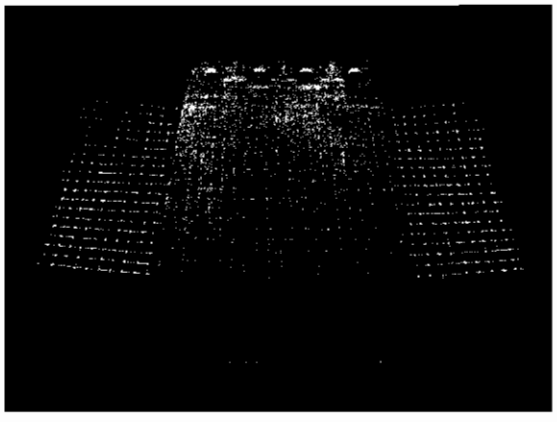

**Figure 3-2:** Old endplate (without frame)

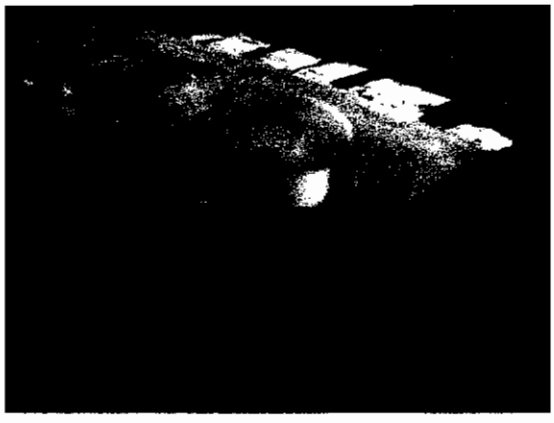

**Figure 3-3:** Fuel cell with glued-on connectors

The next step was the casting of connectors with inside threads which were directly glued onto the cell (see Figure 3-3). The connectors were also cast from epoxy resin and featured a continuous thread (G 1/8"). However, this procedure is very laborious and occasionally the connectors broke off again when carrying out assembly work.

Modifications on the casting mould led to the realisation of a new form of endplate. The base plate of the mould determining the shape to the outer form of the endplate was retained, while the frame and the back were modified. By

inserting an 8.0 mm polypropylene frame the thickness of the endplates was increased to 10.0 mm. This provides enough space to directly bore connector threads (G 1/8") into the endplate. The inward shape of the end plates was realised with a new back of the casting mould. The new endplate now features a frame on the inward side thus eliminating the laborious post-process of glueing a frame in. Based on the results of numerous test castings, which were done to solve casting problems, the sealing surfaces holding the separator were reduced in size. This resulted in more space through which the resin can flow during the casting. This has positive effects on the safe sealing between the individual gas and electrolyte channels (see also Section 3.1.4, *Casting*). In order to provide mechanical stability to the endplate, a fibre glass fleece and a fibre glass mesh are cast into the plates. When assembling the block, the mesh also reinforces the whole assembly.

**Figure 3-4:** New end plate with cast-on frame and threads

### 3.1.3 Labyrinth Layer

When manufacturing multi-cell fuel cells, a so-called labyrinth layer is added between each cell, which is used to distribute the electrolyte.

For cell stacks, a special focus has to be on the electrolytic resistance between the individual cells. In case it is too low, the resulting shunt-current reduces the overall efficiency of the AFC. To prevent this effect it is necessary to have a high electrolytic resistance. For that reason the design of the labyrinth layer was developed with long but narrow pathways for the electrolyte.

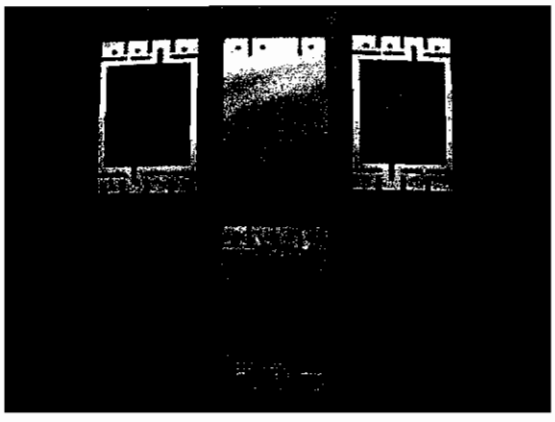

**Figure 3-5:** Old labyrinth layer consisting of three individual parts

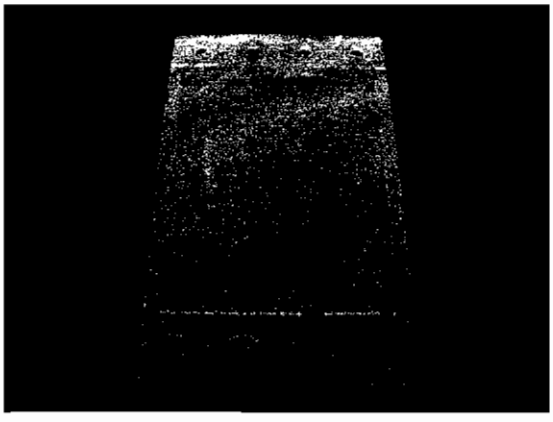

**Figure 3-6:** New, cast labyrinth layer

The labyrinth layers are also cast from epoxy resin and feature an electrolyte distributor (like the endplates) on each side and the openings for the gases and the electrolyte. With an appropriate layout a parallel as well as a serial supply of the individual cells with KOH can be achieved. Originally, these labyrinth layers were manufactured in an elaborate process by gluing several parts (base plate, frame, etc.) together (see Figure 3-5). By building a suitable casting mould, here the manufacturing effort could also be reduced. Figure 3-6 shows the cast labyrinth layer; the dimensions of the frame and of the seal faces correspond to those of the endplates.

### 3.1.4 Casting

Extensive work was also carried out in the area of casting and resins. A fundamental problem of the used resin Araldite GY 240 of the Vantico company was its crystallising, which is a property of bisphenol-A-based resins. This effect could be compensated by using a different temperature (storage at T > 30 °C); however, the necessary effort for this is inadequately high. Furthermore, an expensive adaptation of the used casting machine would have been necessary. This problem alone was reason enough to search for a resin-hardener combination which was easier to handle.

For the selection of a new resin-hardener combination various test series were carried out until a suitable replacement was found [3-1].

Various requirements (parameters) had to be met:

- resistant to potassium hydroxide
- temperature resistant up to 80 / 90 °C
- oxidation resistant
- cold hardening
- very low shrinkage
- low brittleness at temperatures down to –40 °C
- low thermal expansion
- flexibility, in order to facilitate the different expansions of the different materials
- no tendency towards crystallisation
- suitability for machining
- good clearing of air bubbles
- good adhesion of several layers
- no tendency towards stress cracks
- when using fillers: resistant to KOH, non-conducting

Several resins with different viscosities were tested and the influence of the temperature was investigated. The viscosity and the pot life are important parameters for the selection. The longer the resin is capable of flowing the easier it can intrude into the parts thus guaranteeing a good sealing. Air bubbles trapped in the resin can also rise and completely clear from the resin. However, the viscosity of the resin should not be as low that it can intrude into areas where it is not desired, for instance, the gas and electrolyte compartments, the gas supply structure or the active electrode area. This could happen, for example, if the resin could penetrate the porous structure of the electrodes or the separator. In order to keep the processing effort low, it would be useful if the resin did not require warming up.

During the experiments also resins with fillers were tested, with the intention to influence the mechanical stability and the thermal conductivity respectively. However, for the casting of the blocks resins with fillers are not suitable since they have a negative influence on the flow behaviour, in particular due to the small cross-sectional areas between the individual parts. The used metal lattices of the electrodes also pose a problem for these resins. However, the endplates, for instance, could be manufactured using filled materials.

The tested resins were a mixture of bisphenol-A and bisphenol-F resins, which do not tend to crystallise, independent of the temperature.

The resin-hardener combination currently used (resin: Ebalta AH 5 and hardener: Huntsman Aradur 145) can be used at room temperature. It is suitable for use in a casting machine (Hilger and Kern, ELDO-MIX); even at low temperatures the resin does not crystallise any more. The results achieved during the casting led to the conclusion, that the viscosity and the pot life of this resin-hardener combination were suitable for the manufacturing of fuel cells using casting techniques. After the casting, the cell hardens at room temperature. In order to reduce internal stresses the cell is then tempered at a temperature of 80 °C.

Further problems occurred during the casting of the cells. Initially, many of the manufactured blocks exhibited leakages between the electrolyte and the gas

borings: gas intruded into the electrolyte circulation, and in the worst case both gases mixed; this has to be absolutely prevented. The cause for this was assumed to be due to faults occurring during the casting.

In order to eliminate leakages due to mechanical damages to the, for instance, separator, many cells were opened. Indications of a destruction of the separator

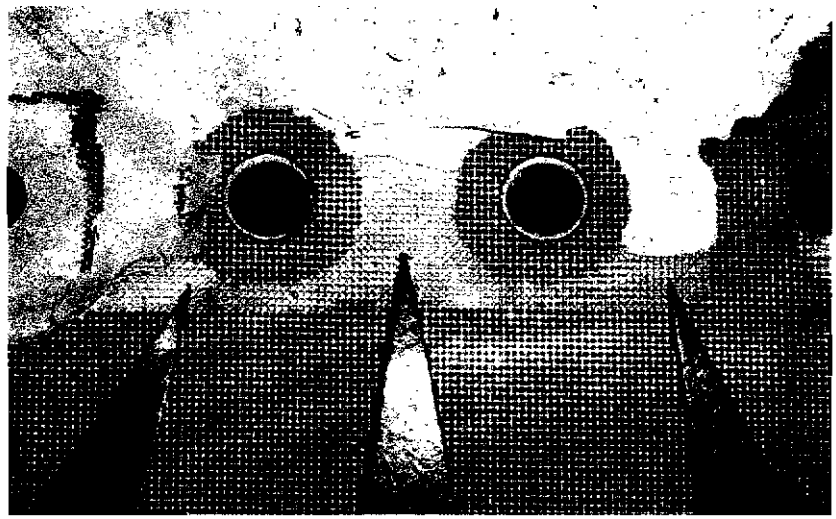

**Figure 3-7:** Casting fault between the gas and the electrolyte borings

could not be found. However, there were regions that had not been filled with resin during the casting. This confirmed the assumption about problems with the casting of the cells. As previously described, the cell is assembled from different parts, which are mounted and finally cast in epoxy resin. The resin not only has to form the housing of the cell, but also seals the different compartments of the cell towards each other and glues the individual parts together. The sealing between the gas and the electrolyte borings of the cell is very important. The gases must neither intrude into the electrolyte nor must they mix with each other. Figure 3-7 shows the region of the electrolyte and the gas borings of an opened cell (Gaskatel No. 0072), that exhibited heavy leakages during the experiments. The red arrows indicate the regions which the resin did not reach. The metal lattice of the electrode is still completely visible. Only further towards the top remains of the separator can be seen. At these regions, a solid compound of resin, electrode and separator was formed.

Another problem was that in some cells resin had intruded into the gas and the electrolyte channels (Figure 3-8), and even as far as into the electrolyte distributor and the gas supply structure of the electrodes (Figure 3-9), thus leaving the cells unusable. Here, also remains of the separator were found which was clotted with the resin which had intruded the channels.

**Figure 3-8:** Electrolyte channel filled with resin

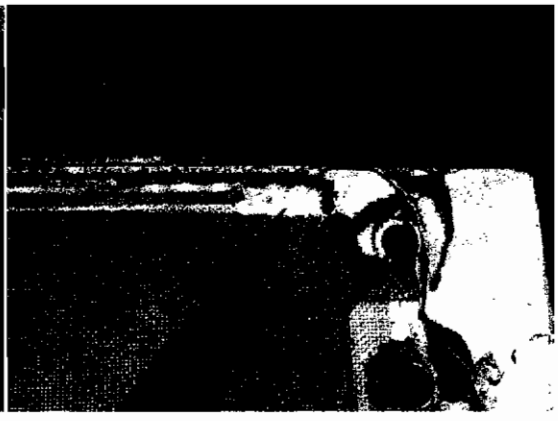

**Figure 3-9:** Main gas supply channel blocked by a resin intrusion

In order to eliminate these faults further experiments were undertaken to investigate the flowing properties of the resin. In a simple set-up with a casting mould made of Perspex different test blocks were cast. With this set-up, it could be observed during the casting how the resin flowed through the prepared paths or where problems might occur.

The design of these test blocks was focused on the following components:

- 1 electrode
- separator
- labyrinth layer
- separator
- 2 electrodes (electrode pair like in a block)

All test blocks were cast with a simple set-up called "Amanda" without using a casting machine.

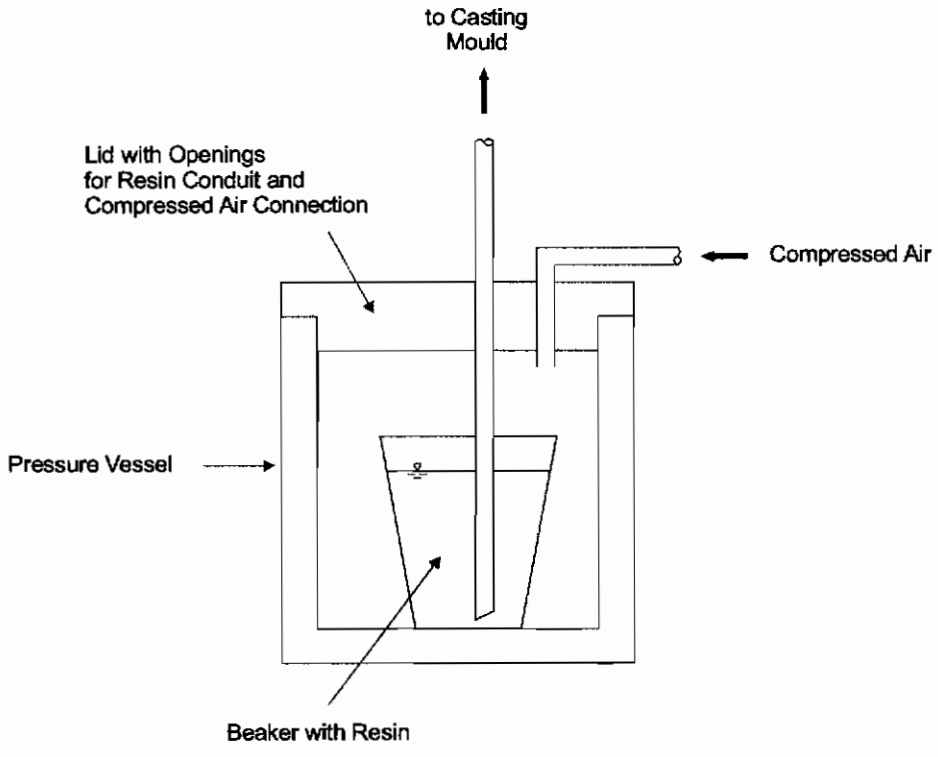


**Figure 3-10:** Schematic representation of the casting set-up "Amanda"

For the casting experiments different resins were used and the temperature was varied respectively. The resin and the hardener were initially mixed in a beaker with a mixer by company IKA at a low rotation speed. The beaker containing the resin is then placed inside a pressure vessel (see Figure 3-10). When pressurising the closed vessel with compressed air the resin is pressed through a conduit reaching into the beaker into the casting mould. During the tests it became clear, that with the old shape of the electrode the resin never completely flowed through the small channels to ensure the sealing of the gas and the electrode regions (see Figure 3-11).

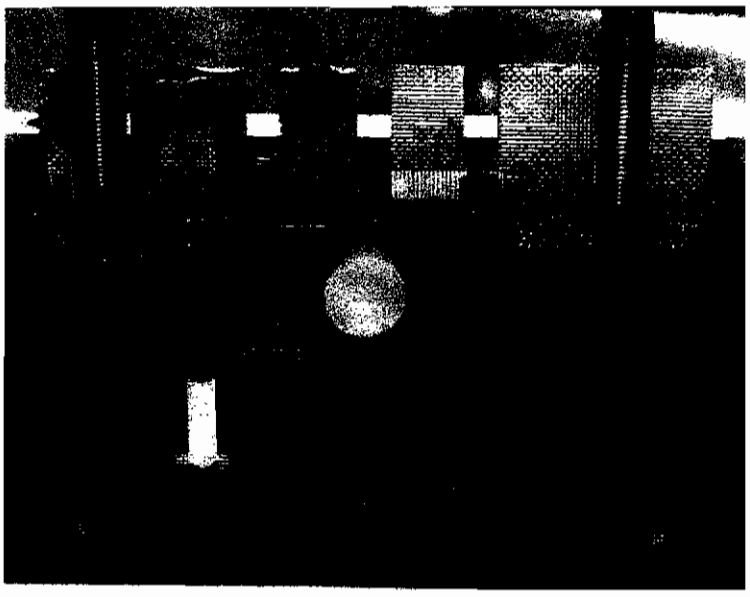

**Figure 3-11:** Casting test – fault between the gas and the electrolyte channel; the resin (blue) did not flow completely through the prepared channel

In the end, not only a new resin-hardener combination could be found; with the cumulated results and findings a new electrode shape was developed, achieving better sealing as well as preventing the intrusion of resin into the gas supply structure of the electrode (see Figure 3-15).

However, with this set-up it could not be determined why the resin can intrude into the gas and the electrolyte borings of the block. Further experiments with all parts of the fuel cell were carried out in the casting mould with inserted pressure sensor films (Fuji Pressurex) between the endplate and the separator-electrode stack. These sensor films change their colour when exposed to pressure. Sensor films of the "low" type were used, with a corresponding pressure range of 2.41 to 9.65 N/mm². The expected result of this experiment was an image of the seal faces of the used endplates, as indicated in Figure 3-12 by the black coloured areas. The colouring of the sensor film indicated that some areas were not pressed sufficiently when the parts were mounted under pressure in the casting mould. The pressure distribution resulting from the pressure-mounting of the parts in the casting mould is shown in Figure 3-13. The regions with a low mounting pressure at the frame of the electrolyte distributor and at the seal faces around the electrolyte and gas borings (indicated by red arrows) are clearly visible. An effective sealing against

the intrusion of resin is not achieved with this. On the other hand, the regions marked by the blue arrows cannot be considered as faults. A colouring of the sensor film cannot occur in these locations as the electrolyte channels of the end plates are located there. An intrusion of the resin is not to be expected due to the construction of the seal faces, and could not be observed so far.

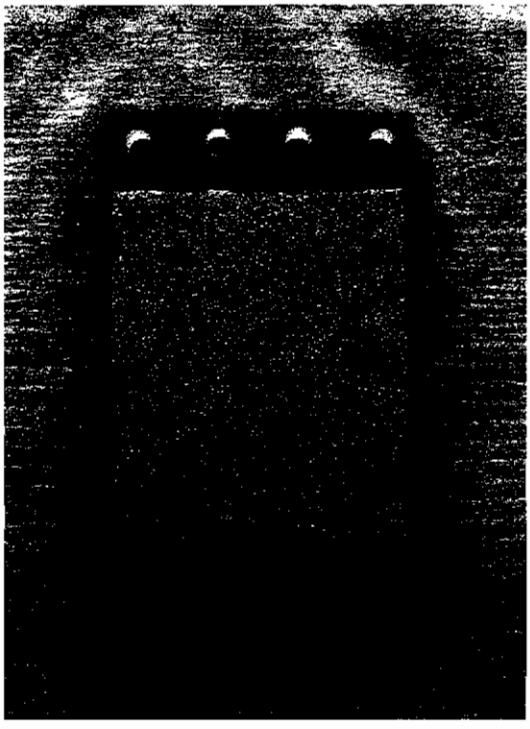

**Figure 3-12:** Seal faces of the endplate

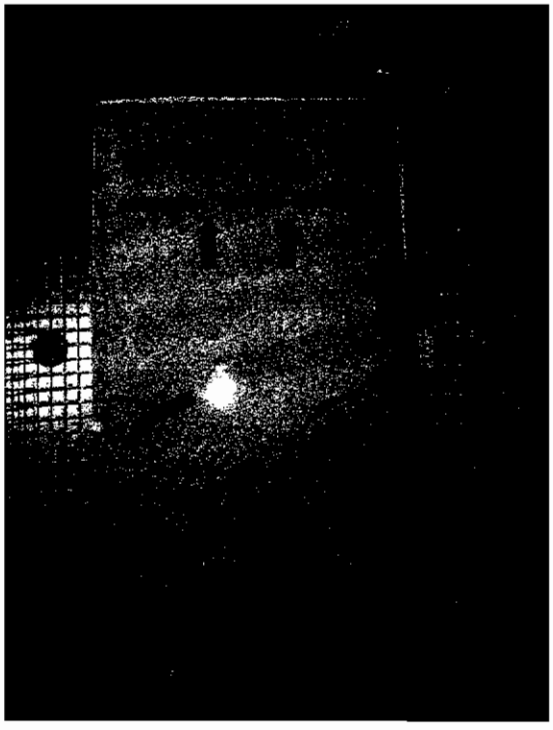

**Figure 3-13:** Sensor film after testing the pressure-mounting in the casting mould

The cause of this was identified in the endplate, which -due its thickness- was too inflexible to level out eventually occurring irregularities. This effect did not stand out so much when manufacturing multi-cell fuel cells, since the large number of parts balances irregularities. For single cells with accordingly fewer parts the mentioned resin intrusion occurred. During the experiments with the sensor film it became apparent, that an increase of the pressure when pressure-mounting the parts in the casting mould was not beneficial. On the contrary, it actually caused further problems, since the pressure could destroy the porous electrode structure or damage the separator. The following procedure was proven to be practicable: all parts are placed in the casting mould and are initially mounted with a moderate

pressure (fastening torque of all 4 screws 300 Ncm). Then the casting mould is placed in an oven at 50 °C for several hours. The influence of the temperature makes the endplates more flexible. Only then are the bolts for the pressure mounting of the casting mould tightened with the final torque of 500 Ncm. In this manner the fundamental faults of the casting could be eliminated.

### 3.1.5 Electrode and Electrode Shape

As already mentioned, the casting experiments showed that the hitherto used electrode shape caused problems during the casting. For use in a fuel cell, the rolled electrode material needs to be cut to shape and has to be fitted with the appropriate cuttings. The electrode shape results from air-blasting the electrode material from the metal lattice. Initially, only small channels were air-blasted for the resin to flow through. This was done using a special blasting template. The electrodes are mounted between two metal plates featuring channels for compressed air supply. During the casting experiments it became apparent that regions repeatedly did not completely fill with resin thus enabling the gases to intrude into the electrolyte, or even the gases mixing. These faults could be corrected by modifying the blasting template. In Figure 3-14 and Figure 3-15 the old and the new electrode shape are compared. More space was created around the gas and electrolyte channels, so that the resin does not have to flow through narrow channels. In order to realise this only a ring of electrode material is left around the cuttings for the gas and electrolyte channels when air-blasting; the dimensions of the ring correspond to the dimensions of the seal faces of the endplates. Additionally, the position of the main gas supplies was moved towards the electrode centre. The modifications would cause a leakage point if the old position of this gas channel were used. Another modification introduced during the research was the position of the contact plate. It is now located always above the gas channel with the terminal on top.

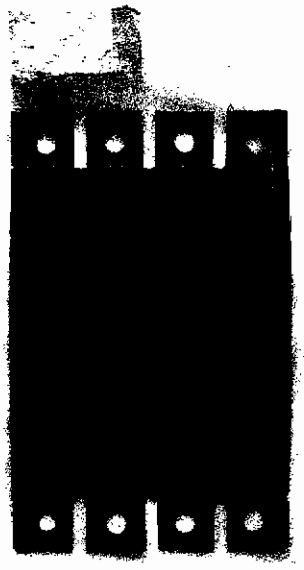

**Figure 3-14:** Old electrode shape

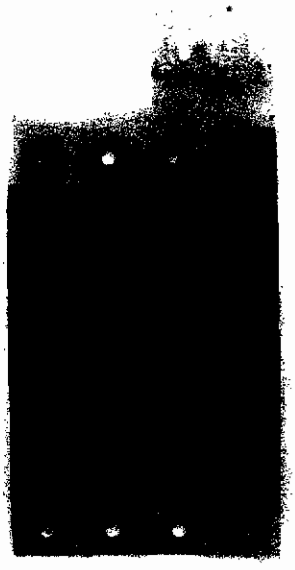

**Figure 3-15:** New electrode shape

For the use of air instead of oxygen further modifications are necessary. The required gas flow through the cell theoretically has to be circa 5 times larger than compared to operation with oxygen. This corresponds to a lambda value of $\lambda = 1$. Considering that the electrode region that is supplied last with air almost only gets nitrogen supplied to it, it makes sense to work with an excess of air. In order to ensure the oxygen supply of the entire electrode an air excess of $\lambda = 2$–3 is used. This aim could not be achieved using the original gas supply structure. In common EloFlux AFCs, a channel structure is rolled into the electrode material using a metal grid starting from the gas channel in order achieve a better gas distribution across the active electrode area. While this channel system is sufficiently large for use of hydrogen and oxygen, considerably larger cross-sectional areas are required for air operation. Therefore, the vertical gas channels were widened initially and further channels were scraped across into the active areas of the electrode in addition to the rolled-in channel system. It is of great importance that the scraped channels are not continuous from the gas inlet to the gas outlet. In this case the pore system of an electrode could not be blasted free by gas pressure in case the electrode had filled completely with electrolyte. With this the electrode would be dysfunctional since gas could not reach the reaction zone.

Further modifications of the electrode shape are not sensible since additionally scraped channels would result in too large a loss of active material. Instead, the use of a gas distributor or a gas compartment is recommended.

### 3.1.6 Gas Compartment for Air Operation

As already mentioned the usual gas supply structure of the electrode is not sufficient to operate the AFC with air. A gas compartment between the oxygen electrodes is meant to remedy this. For this, a polyether sulphone (PESU) frame is placed in between the electrodes of an electrode pair. The dimensions correspond to those of the electrolyte distributor frame in order to ensure a tight sealing. A first experiment was carried out with a simple frame into which a nickel foam with the according thickness was inserted (see Figure 3-16). The insertion of an appropriate material is necessary as otherwise the electrodes could lift off the separator. A disruption of the electrolyte film and an interruption of the mass transport would arise thus preventing the fuel cell from functioning.

The inserted nickel foam initially worked very well. However, with increasing operating time a malfunction occurred: due to the high air flow rate and due the extraction of water, deposits of potassium hydroxide were formed in the area of the air inlet channel (see Figure 3-17). The nickel foam enhances this effect due to its net-like structure in which the potassium hydroxide accumulates. The air flow was rapidly reduced and finally stopped completely. It was not possible to find an effective prevention of this effect with the construction employed. This could probably be achieved with a polytetrafluorethylene (PTFE) foil which would have to be placed on the electrode towards the gas compartment. Gaseous water (reaction water) could permeate through the PTFE foil into the gas compartment and be extracted by the air flow. Fluids, on the other hand, cannot penetrate the foil and hence potassium hydroxide cannot enter the gas compartment. It has to be ensured that the reaction water is produced in a gaseous state and stays gaseous until it has passed the PTFE foil. During the progress of this research experiments were not carried out on this issue.

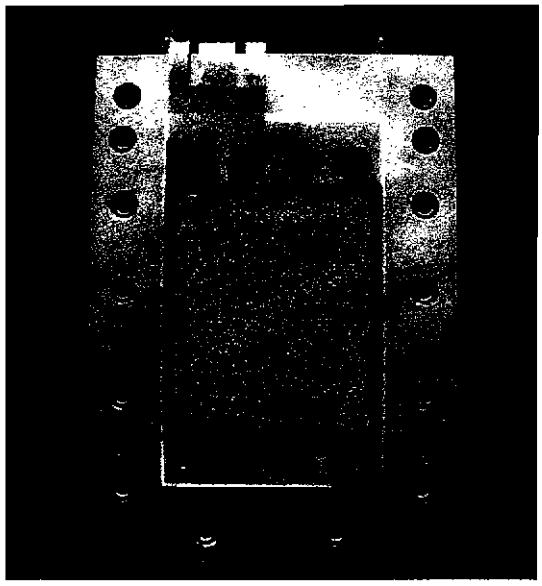

**Figure 3-16:** Gas compartment with PESU frame and nickel foam

**Figure 3-17:** Blocked gas supply channel (Experimental setup to simulate gas compartment in the fuel cell)

For the next experiment a PESU frame was used featuring a labyrinth-shaped air channel (see Figure 3-18). The bars are to prevent a lifting of the electrodes; their area corresponds to half of the open area. This is to keep the loss of active area small.

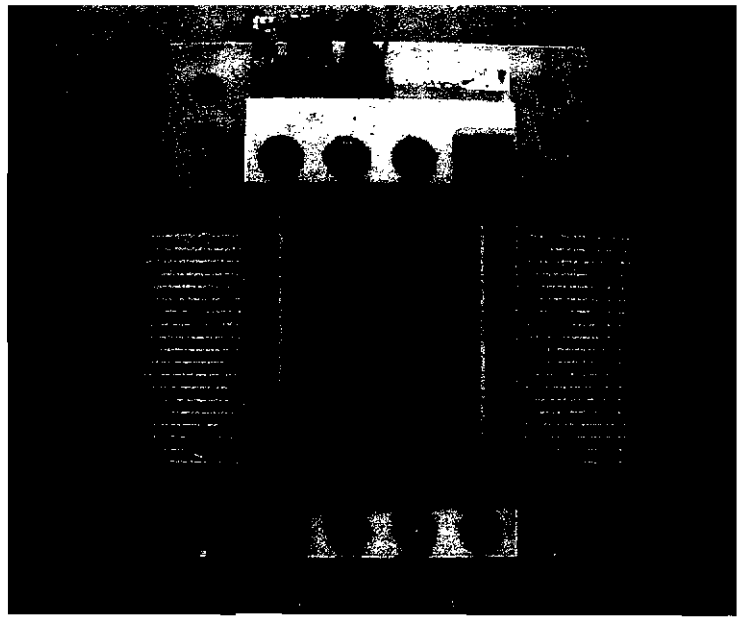

**Figure 3-18:** Gas compartment with labyrinth-shaped air channel

### 3.1.7 Fuel Cells built for this Research

#### Gaskatel Nr. 0068 – EF FC 1x (4/2/2)

The first tests with a fuel cell were made with Fuel Cell 0068. It was a conventional EloFlux-AFC without any adoption to the operation with air in place of pure oxygen.

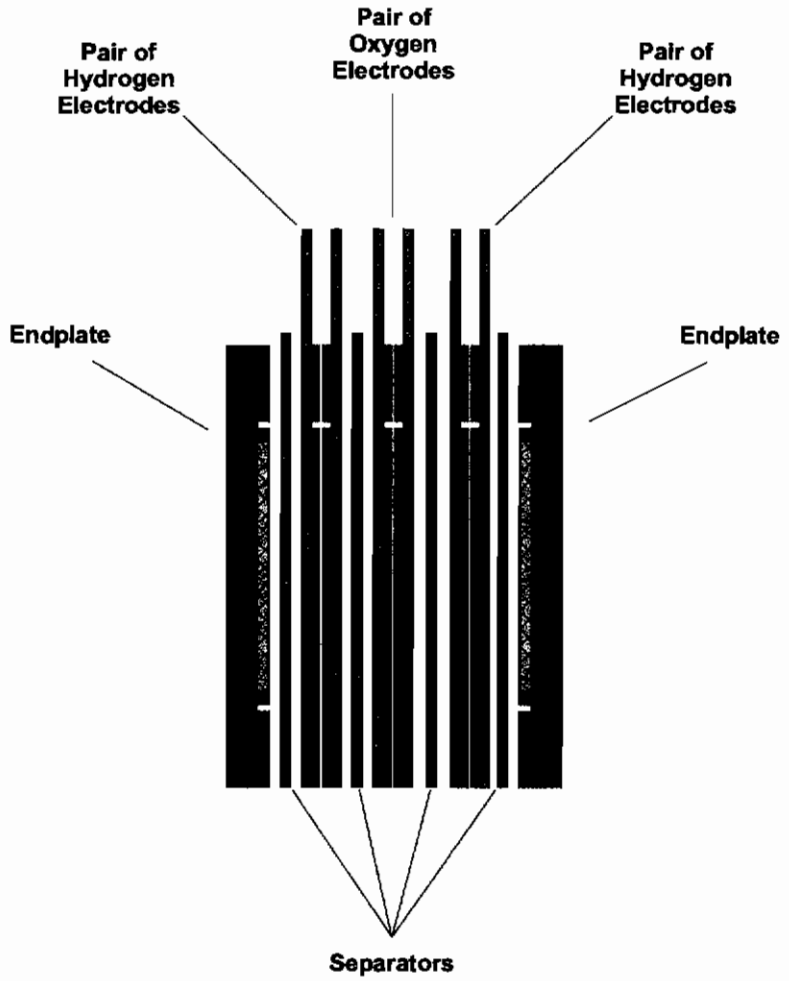


**Figure 3-19:** Schematic representation of the design of Fuel Cell 0068

Figure 3-19 shows the design of Fuel Cell 0068. At the hydrogen side four nickel electrodes of type #314 were used and at the oxygen side two silver electrodes with Silflon-catalyst were used. The anode consists of four electrodes, the cathode of two electrodes. The separator used was a PALL Supor 800 with 0.8 $\mu$m pore size.

### Gaskatel Nr. 0096 - EF FC 1x (4/2/2)

Fuel cell 0096 was the first cell featuring a special gas compartment for the air operation. For this, a frame with an inserted nickel foam as air distributor was placed between the oxygen electrodes (see Figure 3-16).

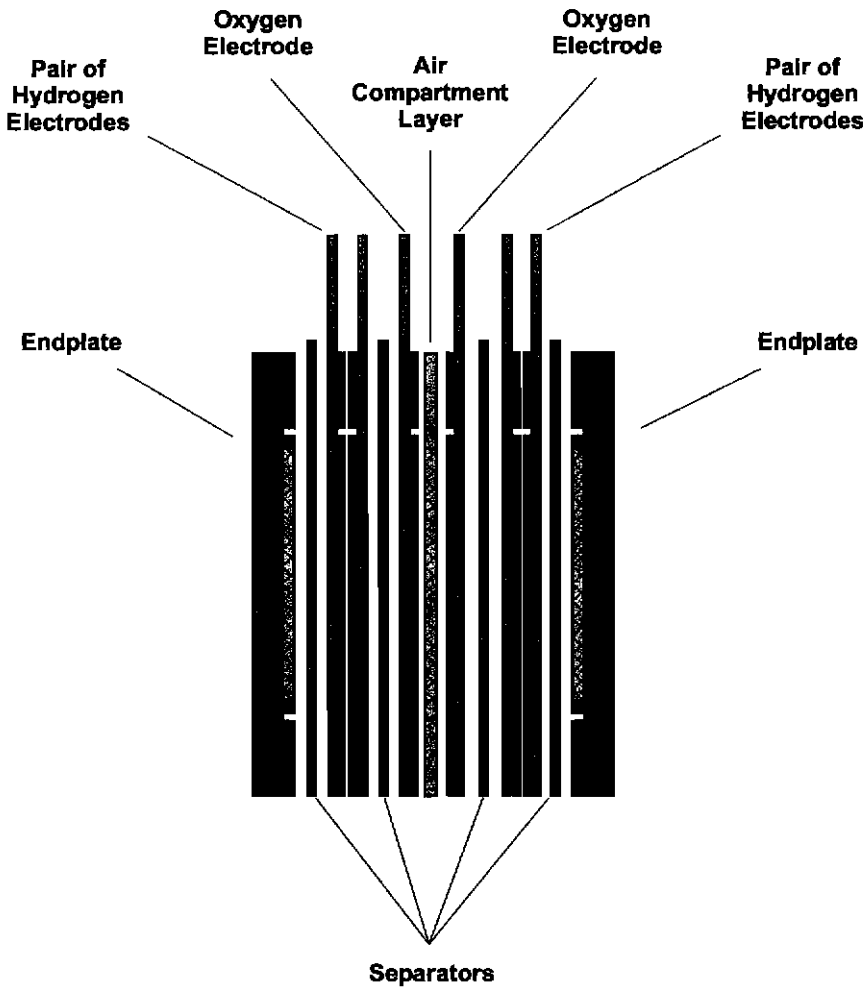


**Figure 3-20:** Schematic representation of the design of Fuel Cell 0096 and 0101

Figure 3-20 shows the design of Fuel Cell 0096 and 0101. The design of both cells is identical. Only the components used to build the cells vary.

For Fuel Cell 0096 at the hydrogen side four nickel electrodes of type #314 were used and at the oxygen side two silver electrodes with Silflon-catalyst were used. The separator used was an AMS FAS 1100. Due to its construction this cell was a dual cell with both cells connected in parallel. Each cell consists of two hydrogen

electrodes (anode) and one oxygen electrode (cathode). The air compartment layer separates both cells.

**Gaskatel Nr. 0101 – EF FC 1x (4/2/2)**

Fuel Cell 0101 was the second cell built with a gas compartment between the oxygen electrodes for the operation with air. The design of this cell was identical to the design of Fuel Cell 0096 (see Figure 3-20). However, nickel foam was not used and instead a plastic layer with a labyrinth-shaped air distributor was used (see Figure 3-18). The electrodes used were again at the hydrogen side four nickel electrodes of type #314 and at the oxygen side two silver electrodes of type #249. Oxygen electrode #249 was also manufactured with a Silflon-catalyst, but with additional substances. The separator used was again AMS FAS 1100. The further set-up is equal to the one of fuel cell 0096. Each cell consists of two hydrogen electrodes (anode) and one oxygen electrode (cathode). Both cells were connected in parallel. The air compartment layer separates both cells.

## 3.2 Measurement Methods

### 3.2.1 Half Cell

Half cell measurements are carried out to characterise the capacity of an electrode; the relationship between current and voltage is measured. The term half cell originates in the fact, that only one of the individual electrodes, half a fuel cell so to speak, is examined by a suitable positioning of the reference electrode. For gas diffusion electrodes the gas production and the gas consumption can be examined with it.

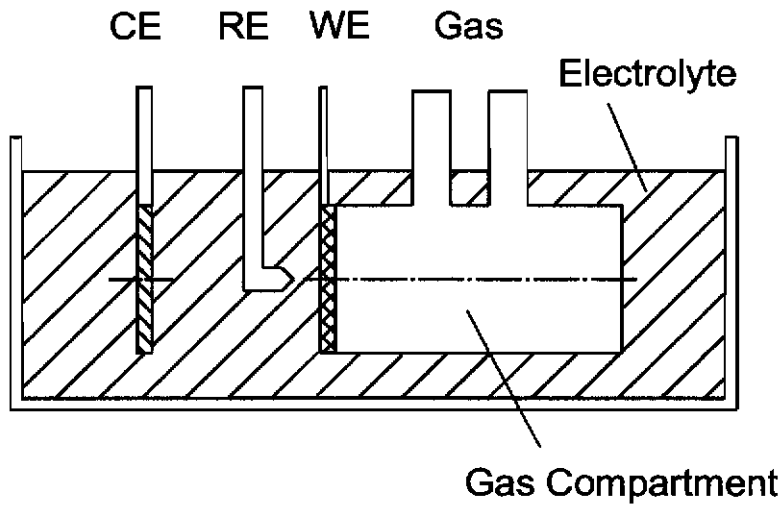


**Figure 3-21:** Schematic construction of a half cell

Figure 3-21 shows the schematic construction of a half cell. The electrode under test (working electrode, WE) is mounted in a bracket. One side is in contact with the electrolyte while the other side is in contact with the gas compartment. The ionic current flow occurs between the working electrode and the counter electrode (CE); the reference electrode (RE) is placed in between. Further explanations on the half cell can be found in the final year project report of J. Grassegger (1993) [3-2]. For this research only the measurement results are significant.

The current and the voltage (electric potential) measured at the half cell give a reference value for the estimation of the operating parameters a fuel cell equipped

with the measured electrodes could reach in operation. In practice, considerable differences can occur between a half cell and a fuel cell, which are due to the construction of the fuel cell.

### 3.2.2 Flow Rate and Tightness Test Stand

Each manufactured fuel cell is tested for the flow rate of the gases and the fluids as well as for tightness before its operation is started. This is to ensure that from the beginning, the fuel cell has no supply problems with the gases or the potassium hydroxide solution and that there are no damages at the separator or faults in the casting. The tests are carried out with compressed air and with de-ionised water.

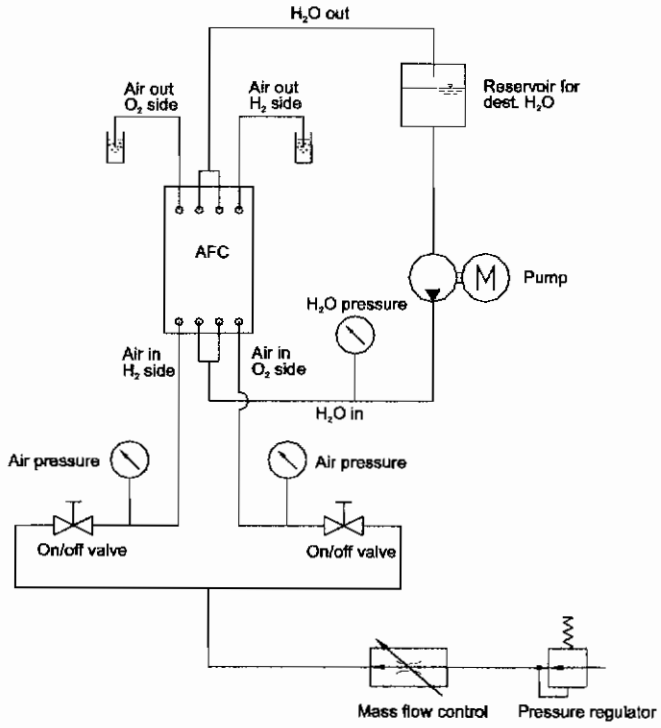


**Figure 3-22:** Flow chart of the flow rate and tightness test stand

The test stand features a tank for the water; the latter is moved by a pump. The pressure and the flow rate are measured at the water side. The pressure and the flow rate are measured at the air side for the oxygen and the hydrogen electrodes. The pressures are measured with tube spring manometers, the water flow is

measured by volume measurement, while a mass flow meter and regulator by Manger & Wittmann is installed in the air supply conduit for the measurement of the air flow rate.

The following measurements are taken:

- flow rate air in dry state
- flow rate air in wet state
- permeation (water) of the separator
- pressure loss at the electrodes
- EloFlux flow

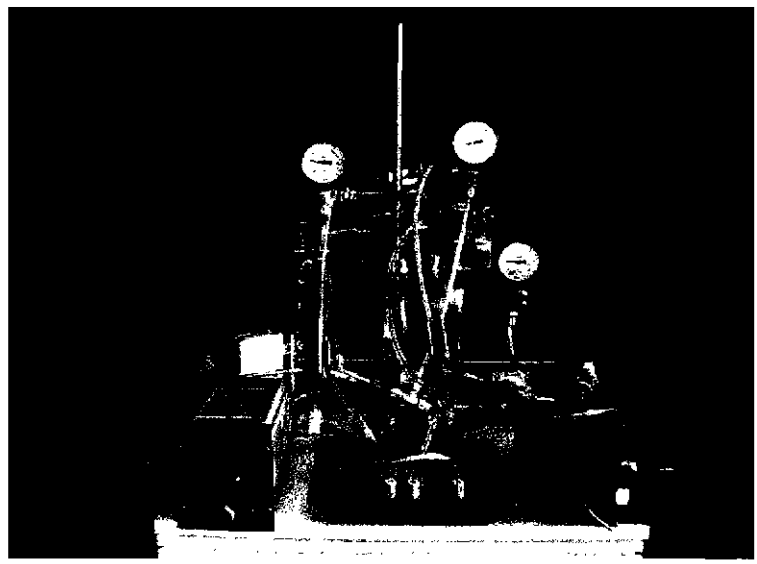

**Figure 3-23:** Flow rate and tightness test stand

### 3.2.3 Fuel Cell Test Stand

After the fuel cells have passed the initial flow rate and tightness test they are activated and tested using the main test stand.

Activating the fuel cell

In order to operate an AFC, firstly the hydrogen electrodes have to be activated. The used electrodes with the catalyst Raney-nickel are processed in a passivated state; the catalyst is previously oxidised using a special procedure. This makes it

possible to process it while exposed to air; pure Raney-nickel would spontaneously combust when exposed to oxygen (air). The catalytic activity is almost completely lost through the oxidation and hence the catalyst has to be reactivated. For the activation process the cell is heated up to a temperature of more than 50 °C and supplied only with hydrogen; the oxygen side remains unsupplied [3-3, 3-4]. Under the influence of the temperature and the hydrogen the nickel oxide is reduced and is converted to nickel. This process takes several hours. By means of a hydrogen reference electrode, which is built into the KOH-circulation, the electric potential of the hydrogen electrode is measured. This gives an indication whether the $H_2$-electrodes are active yet.

Operating the fuel cell

In order to operate an AFC the gases hydrogen and oxygen are required as well as KOH as electrolyte. The gases are supplied by high-pressure cylinders and the inlet pressure is adjusted to the required value with pressure reducers on the cylinders. After the cell the gases are conducted through a fluid separator. The pressure in the cell and the gas flow rate through the cell, the so-called purge-rate, are adjusted with a fine tune valve by the EM-Technik company (1–30 l/h). The gas pressure before and after the cell is measured. This set-up is retained at the $H_2$-side for the tests for air operation of the AFC. At the air side, a mass flow rate meter and regulator by Manger & Wittmann (maximum flow rate 1 sl/min) is integrated in the supply conduit before the fuel cell. For examinations of the water circulation a fluid separator / condenser was included after the cell. Since this device consists of glass it is hence operated unpressurised and the fine tune valve for the adjustment of the pressure is placed immediately after the cell. The air is led through the double-walled glass vessel, which can be cooled down to the desired temperature using a thermal bath. The condensate is collected in the vessel and can be taken out via a closable outlet from time to time to take measurements. The KOH solution is pumped in a circulation through the cell. It is supplied from a storage tank to the cell with an electric diaphragm pump (company IWAKI). A hydrogen

reference electrode (Hydroflex, company Gaskatel) is integrated in the supply conduit to the cell. After the cell the potassium hydroxide solution is led back into the container. For these experiments a measuring cylinder is used as container. It is placed on an electronic scale PM16-K by Mettler, which was integrated in the experimental set-up. In order to gain information about the water circulation of the fuel cell, the increase in weight of the electrolyte due to the reaction water produced in operation was measured. The measured data are recorded by the measurement program via an RS-232 interface. The measurement cylinder is closed with a lid equipped with feed-through borings for the supply and drain of the potassium hydroxide solution, in order to minimise the change of electrolyte volume. The supply and the drain were decoupled from the scale as far as possible.
The pressure and the temperature of the KOH can be measured. However, more significant than the KOH temperature is the temperature of the actual cell. For this, Pt 100 temperature sensors were cast into the fuel cell.
For the supply and the drain of the gases and the electrolyte, polyamide conduits and polypropylene clamp ring screw connectors (EM-Technik) were used.
For the experiments of this research, initially an electronic load by Höcherl & Hackl was used. This load can be operated current- or voltage-controlled and is adjusted via a TestPoint measurement program on the PC. This load was later replaced by a current-controlled load provided by Prof. H. Schmidt-Walter.
The measurement value logging is done by a digital multimeter by Prema; the logged values are transferred to a PC, where they are represented by the TestPoint measurement program and saved as text files.
In case the cell has to be heated, this can be achieved by either heating the potassium hydroxide solution or by mounting the cell in between two heating plates. The fuel cells built last feature heating foils (2x12 W) in the endplates, thus reducing the heating effort to a minimum. The cell temperature is measured with a Pt 100 cast into the cell, while the control is achieved with a micro-processor controlled temperature instrument Jumo di eco. This instrument features a limit monitor using toggle relays.

The following table provides an overview of the parameters to be measured as well as the sensors and instruments used for this.

| Measurement Value Logging – Fuel Cell Test Stand | | | |
|---|---|---|---|
| Quantity | Position | Sensor | Manufacturer |
| temperature | fuel cell | Pt 100 | RS |
| pressure | KOH | pressure transducer (additional manometer) | Jumo |
| pressure | $H_2$ | pressure transducer (additional manometer) | Jumo |
| pressure | $O_2$ / air | pressure transducer (additional manometer) | Jumo |
| volume flow | $O_2$ / air | WIGHA 1010 (volume flow regulator) | Manger&Wittmann |
| current | fuel cell | multimeter DMM 5000 | Prema |
| voltage | fuel cell | multimeter DMM 5000 | Prema |
| potential | $H_2$-electrode | Hydroflex (hydrogen reference electrode) | Gaskatel |
| weight | KOH | scale PM16-K | Mettler |

**Table 3-1:** Summary overview of the sensors and meters of the fuel cell test stand

### 3.2.4 Gas Chromatograph (GC)

For the gas analysis a gas chromatograph GC-14A by Shimadzu was used.

Working principle of a gas chromatograph:

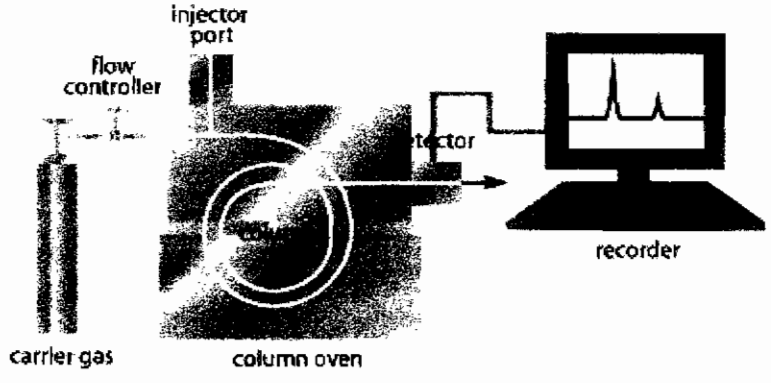


**Figure 3-24:** Working principle gas chromatograph

Every chromatography process is characterised by a mobile and a stationary phase. Differently structured molecules also exhibit different interactions with a solvent,

or, in case of a gas chromatograph, with the carrier gas, i.e. the mobile phase. Often plain nitrogen can be used as carrier gas.

Each substance consequently has a characteristic migration speed through the stationary phase in the column, resulting in a separation of the individual material components of an analysed substance. The components which have already passed the column are detected by, for instance, converting the different thermal conductivity of an emitted gas into an electric signal, which can be transferred to a PC.

The GC records the graph as the difference to the electrical properties of the pure carrier gas, which are measured by a second detector and are used as reference value. Other GC-procedures varying from this scheme exist as well.

The peaks of each graph as recorded by the device correspond to certain known substances. The height of the peak is proportional to the amount of substance of each component. The purpose of the GC-procedure is to enable the exact identification of substances when adjusting certain parameters [3-5].

During the experiments on the long-term operation of the AFC with air the $CO_2$-content of the air was measured, for example, before and after the cell. This allows to make a statement about the absorption of $CO_2$ by the potassium hydroxide solution. Furthermore, the $CO_2$-content of the hydrogen after the cell was measured. Measurements of the $CO_2$-content of the air as well as measurements to determine the $CO_2$ absorption of various electrolytes were carried out as well. For this, the ambient air was led through a washing bottle filled with the respective electrolyte. Potassium hydroxide solution, potassium carbonate and potassium hydrogen carbonate solutions as well as de-ionised water were tested. For the tests, the air was led through a frit into the washing bottle.

### 3.2.5 Diffusion measurement

During other research work at Gaskatel, G. Sauer developed a method to investigate the transport properties by diffusion of several components of the fuel cell [3-6]. Figure 3-25 shows a schematic representation of the test cell for the diffusion measurement. The investigated sample (electrode, separator, etc.) is fixed between two compartments. For the tests concerning this research work compartment 1 was filled with 7.0 M KOH solution, compartment 2 was filled with 3.5 M $K_2CO_3$ solution, both by injection. The pipettes were used to measure a change of volume.

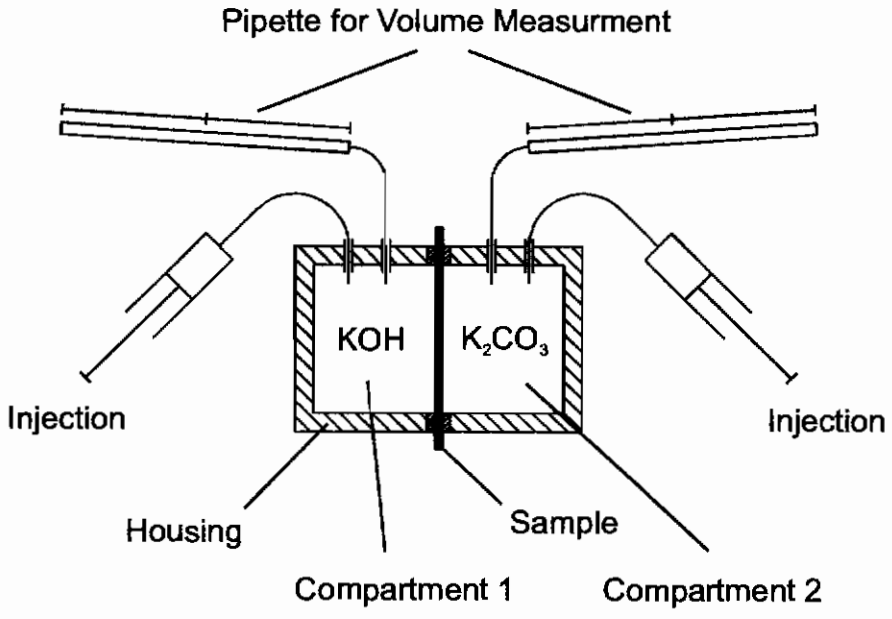


**Figure 3-25:** Schematic representation of the test cell for diffusion measurement

The measurement time was typically 50 minutes. Before and after testing, the concentration of the electrolytes and the carbonate content of the KOH solution were determined by titration.

### 3.2.6 Titration

Titration is a method of chemical analysis which can be used to determine the concentration of a known reactant.

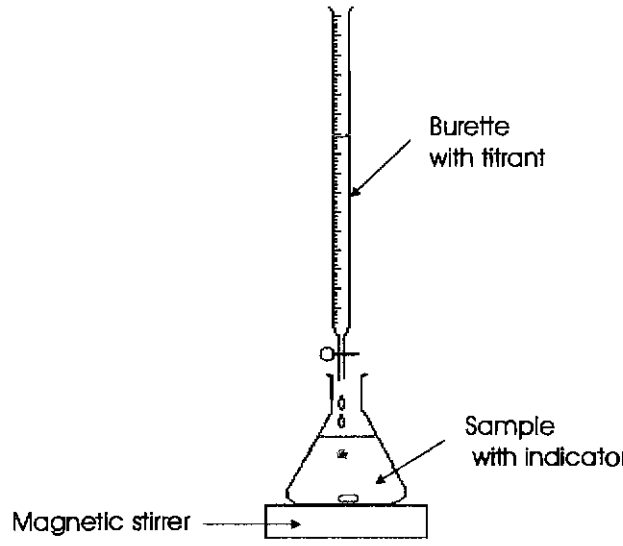


**Figure 3-26:** Schematic representation of a titration setup

A reagent, called the titrant, of known concentration (a standard solution) and volume is used to react with a measured volume of reactant. Using a calibrated burette to add the titrant, it is possible to determine the exact amount that has been consumed when the endpoint is reached. The endpoint is the point at which the titration is stopped. This is classically a point at which the number of moles of the titrant is equal to the number of moles of analyte, or some multiple thereof (as in di- or tri-protic acids). In classic strong acid-strong base titration the endpoint of a titration is when pH of the reactant is just about equal to 7, and often when the solution permanently changes colour due to an indicator.

There are however many different types of titration. During this research acid-base titration was used to determine the carbonate content as well as the carbonate and hydroxide content of the electrolyte.

The titration unit Dosimat 665 from company Metrohm was used during this work.

# 4 Tests, Results and Data

The aim of this research was to examine the long term operation of an AFC with air. For the operation with air, the main focus is the commonly known problem of the incompatibility of the electrolyte KOH with $CO_2$. Furthermore, special attention has to be paid to the water in the cell for long term operation. The experiments carried out on these topics are presented in this chapter.

## 4.1 Half Cell Tests

Various electrodes were tested in a half cell with regards to their performance. A long-run test was initiated with an oxygen electrode (electrode #50). The electrode was operated in oxygen consumption mode and was supplied with unfiltered air. This was a single test only because of the long duration of testing and a limitation of technical measurement equipment. Apart from the long-run tests with the half cell mainly current/voltage characteristics were recorded. With this method electrodes can be characterised with a lower expenditure of time. However, conclusions can be made if the electrode is suitable for the application. A great advantage of the half cell layout is the possibility to change the operating conditions of the electrodes in a very short time with less complexity. Various tests were made to investigate the influence of different operating conditions:

- Variation of temperature
- Increase of the $CO_3^{2-}$ content of the electrolyte
- Operation with pure oxygen or air
- Tests with pretreated electrodes in order to simulate an inclusion of potassium carbonate or potassium hydroxide

### 4.1.1 Long-Run Test with Permanent Load

For the long-run test oxygen electrode #50 with a silver catalyst called Silflon was used. #50 is the manufacturing number of company Gaskatel; Silflon is a

trademark by company Krupp-Uhde, Germany. In the half cell the oxygen electrode was loaded with 0.1 A/cm² for 5400 hours.

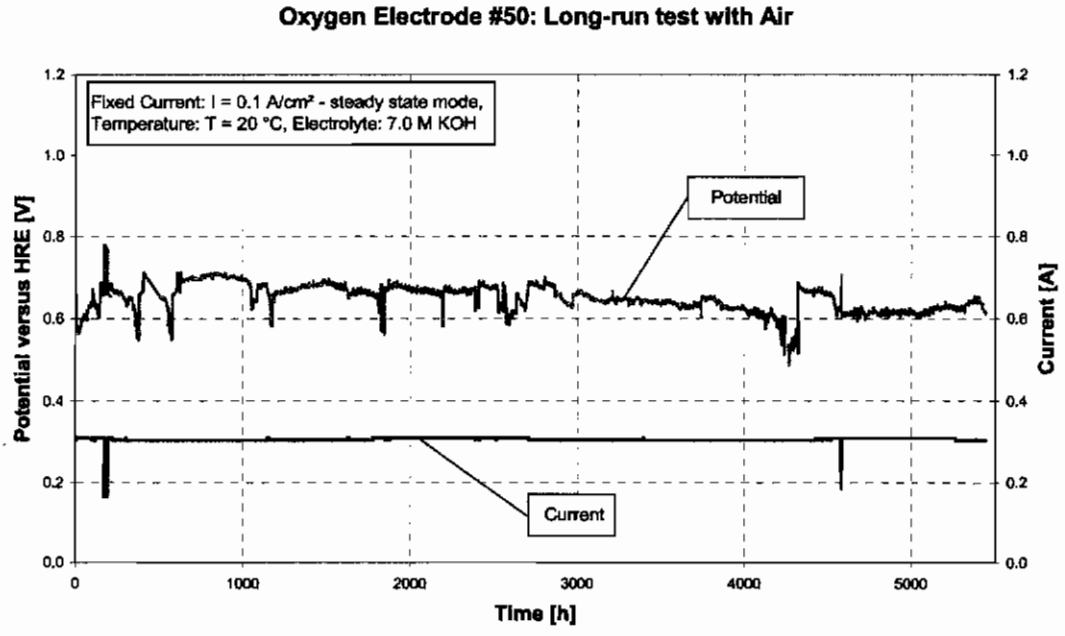


**Diagram 4-1:** Long-run test of an $O_2$-electrode with air (permanent load).
Electrode #50 was operated in the half cell with fixed current I = 0.1 A/cm². Tests were made at room temperature of 20 °C. Electrolyte used was 7.0 M KOH solution. Unfiltered air was supplied with a small compressor (company KNF Neuberger, Germany). HRE: Hydroflex from Gaskatel.

Diagram 4-1 shows the progression of the current and the electric potential for the duration of the measurement. A decline of the electric potential along the total measurement duration could be observed. By neglecting each drop of the electric potential caused by a partly flooded gas compartment and taking an average using linear fits a decline of about 100 mV can be calculated for the total run time. Divided by the run time this is a decline of circa 0.019 mV/h.

### 4.1.2 Long-Run Test with a "Pulsed Load"

Following the experiment with a permanent load, the half cell was filled with fresh 7.0 M KOH and operated further for 1000 hours with a pulsed load (on/off mode). Diagram 4-2 shows the measured values for this test. After starting again,

the electric potential is higher than in the experiment with the permanent load, but it declines again during the progression of the measurement. In summary, the overall operating voltage levels are higher in pulsed mode than when operated in steady state mode.

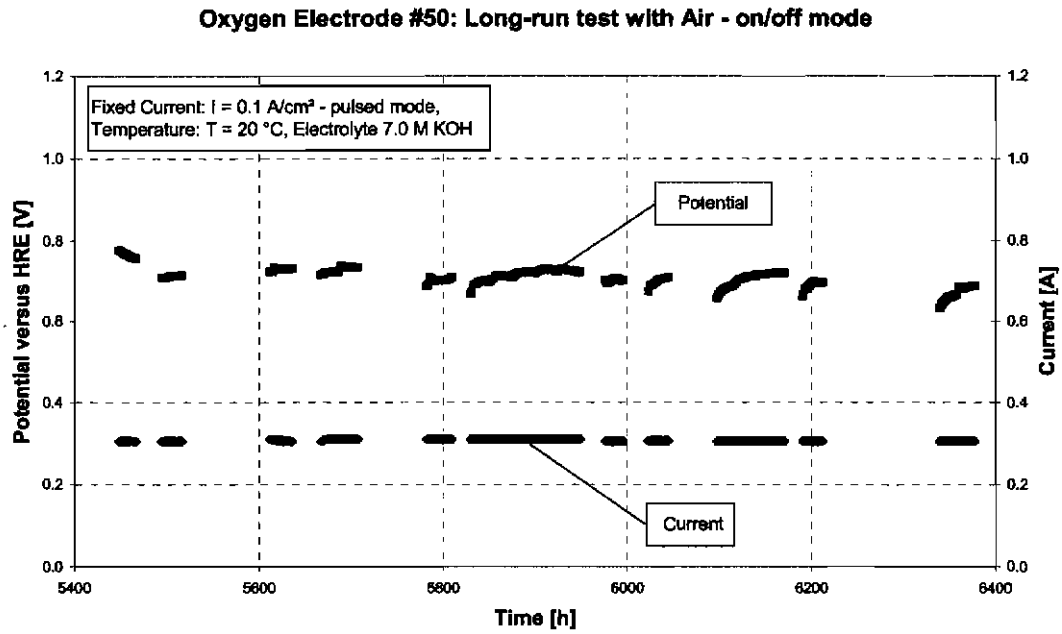


**Diagram 4-2:** Long-run test of an $O_2$-electrode with air (pulsed load).
Continuation of the half cell test shown in Diagram 4-1: Same electrode #50 but renewed electrolyte 7.0 M KOH and pulsed load in place of steady state mode. All settings of the experiment were retained identically.

### 4.1.3 I/V-Characteristics of the Oxygen Electrodes

The following diagrams show the results for three different oxygen electrodes #249 (fuel cell 0101) and Silflon (fuel cell 0096) as used in the manufactured fuel cells and electrode #461. The $O_2$-consumption was examined both with pure oxygen and with unfiltered air at different temperatures and with various electrolytes.

Electrodes #249 and Silfon are both manufactured with Silflon catalyst. The oxygen electrode called "Silflon (fuel cell 0096)" is from an older manufacturing date where no consecutive numbers existed. They are similar except for the use of a pore builder, which was used for electrode #249. The fuel cells build and tested during this project were provided with these electrodes: Electrode "Silflon" was

used in fuel cell Gaskatel No. 0096, electrode #249 was used in fuel cell Gaskatel No. 0101. In addition an electrode with a different catalyst was investigated. Electrode #461 was manufactured with silver oxide ($Ag_2O$) as a catalyst. Gaskatel name for these electrodes is Oxag.

## Effect of Temperature Variation on the Oxygen Electrode

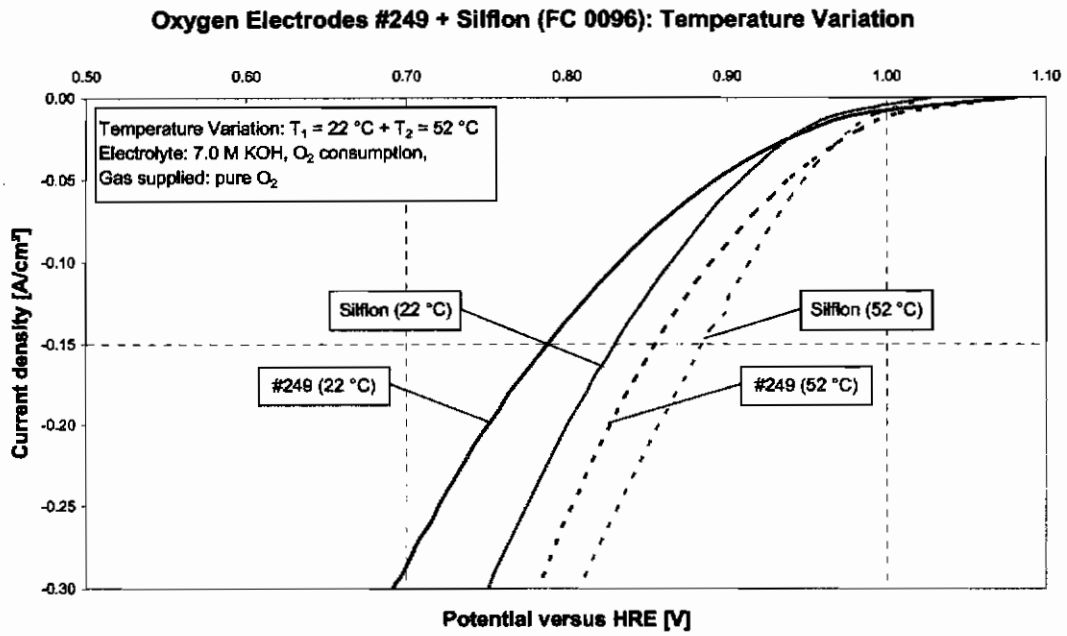


**Diagram 4-3:** I/V Curves of $O_2$-electrodes at 22 °C and 52 °C in KOH consuming $O_2$. Oxygen electrodes #249 and Silflon (FC 0096) were tested in the half cell to investigate the effect of temperature variation. One test at room temperature T=22 °C, second test at T=52 °C. The electrodes were operated in 7.0 M KOH with pure oxygen.

Diagram 4-3 shows the current/voltage characteristics of the electrodes #249 and Silflon. These half cell tests were carried out at room temperature and at higher temperature with 7.0 M KOH as electrolyte; the electrodes were supplied with pure oxygen. The influence of the temperature can be clearly seen. Both electrodes reached a higher electric potential at the same load when the temperature was increased by heating up the electrolyte. The I/V curves are shifted towards a higher potential in the Diagram above.

### Influence of the $CO_3^{2-}$ Content of the Electrolyte

Diagrams 4-4 and 4-5 show the influence of the $CO_3^{2-}$ content of the electrolyte on the oxygen electrodes. An increase of the carbonate content in the electrolyte results in a decrease of the conductivity as the number of $OH^-$ ions is reduced when adding carbonate. So these experiments also show the influence of the electrolyte conductivity on the electrodes. 7.0 M KOH, 3.5 M $K_2CO_3$ and a mixture with a ratio of 50:50 were used as electrolytes. This mixture then consists of 3.5 M KOH and 1.75 M $K_2CO_3$ with only half the number of $OH^-$ ions. To provide a better overview the results for both electrodes are presented separately. The experiments were carried out at room temperature and the electrodes were supplied with pure oxygen.

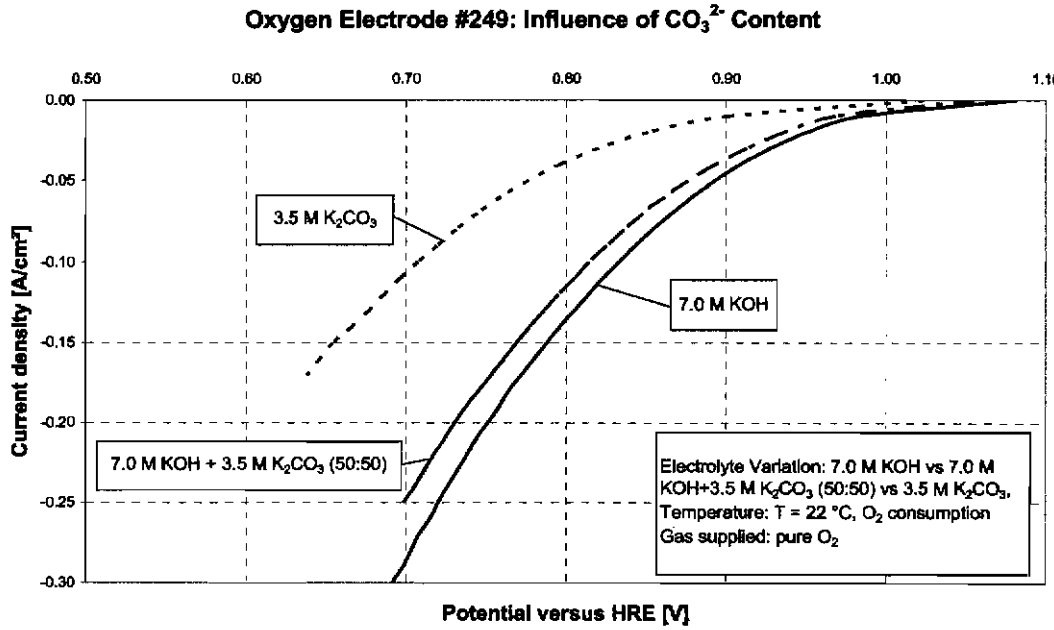


**Diagram 4-4:** I/V Curves of an $O_2$-electrode at 22 °C in various electrolytes, consuming $O_2$. Oxygen electrode #249 was tested in the half cell to investigate the influence of the $CO_3^{2-}$ content of the electrolyte. Electrolytes used were 7.0 M KOH, a mixture of 7.0 M KOH and 3.5 M $K_2CO_3$ (ratio 50:50) and 3.5 M $K_2CO_3$. All tests were made at room temperature with the same electrode, electrolyte was changed. Gas supplied to the electrode was pure oxygen. Potential was measured versus a hydrogen reference electrode, current supplied with a galvanostat (manual variation).

With increasing carbonate content in the electrolyte the electrochemical performance of the electrodes decreases. In a carbonated hydroxide solution both electrodes do not reach the performance as compared to a pure 7.0 M KOH solution.

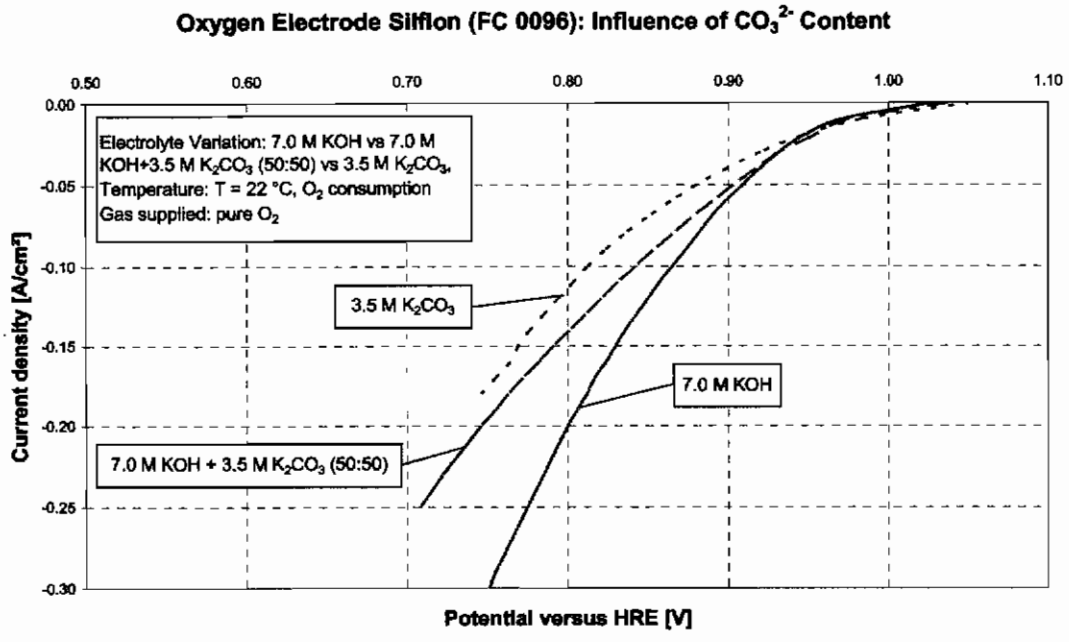


**Diagram 4-5:** I/V Curves of an $O_2$-electrode at 22 °C in various electrolytes, consuming $O_2$. Oxygen electrode Silflon (FC 0096) was tested in the half cell to investigate the influence of the $CO_3^{2-}$ content of the electrolyte. Electrolytes used were 7.0 M KOH, a mixture of 7.0 M KOH and 3.5 M $K_2CO_3$ (ratio 50:50) and 3.5 M $K_2CO_3$. All tests were made at room temperature with the same electrode, electrolyte was changed. Gas supplied to the electrode was pure oxygen. Potential was measured versus a hydrogen reference electrode, current supplied with a galvanostat (manual variation).

For the Silflon electrode this effect is apparently superimposed by another effect, which is reflected in the slope of the measured curve.

### Comparison air operation/oxygen operation: gas diffusion

Diagram 4-6 shows the current/voltage characteristics of the two electrodes with Silflon-catalyst #249 and Silflon (fuel cell 0096) and an Oxag-electrode #461 from the experiment with the carbonated electrolyte. A mixture of 7.0 M KOH and 3.5 M $K_2CO_3$ with a ratio of 50:50 was used. Initially, the electrodes were supplied

with pure oxygen and then with unfiltered air. The flatter progression of the slopes of the measurement curves is clearly visible for air operation. For both electrodes the performance declines, which can be explained with an obstruction of the gas diffusion. Here, the electrode Silflon (fuel cell 0096) performs slightly poorer than electrode #249, which is reflected in the even lower slope of the measurement curve. The Oxag-electrode achieved better values for higher loads than the electrodes with Silflon-catalyst. In the lower load range of less than 100 mA/cm² it has, however, a poorer performance. The difference between the operation with pure oxygen and the operation with unfiltered air has to be considered similar for both catalysts.

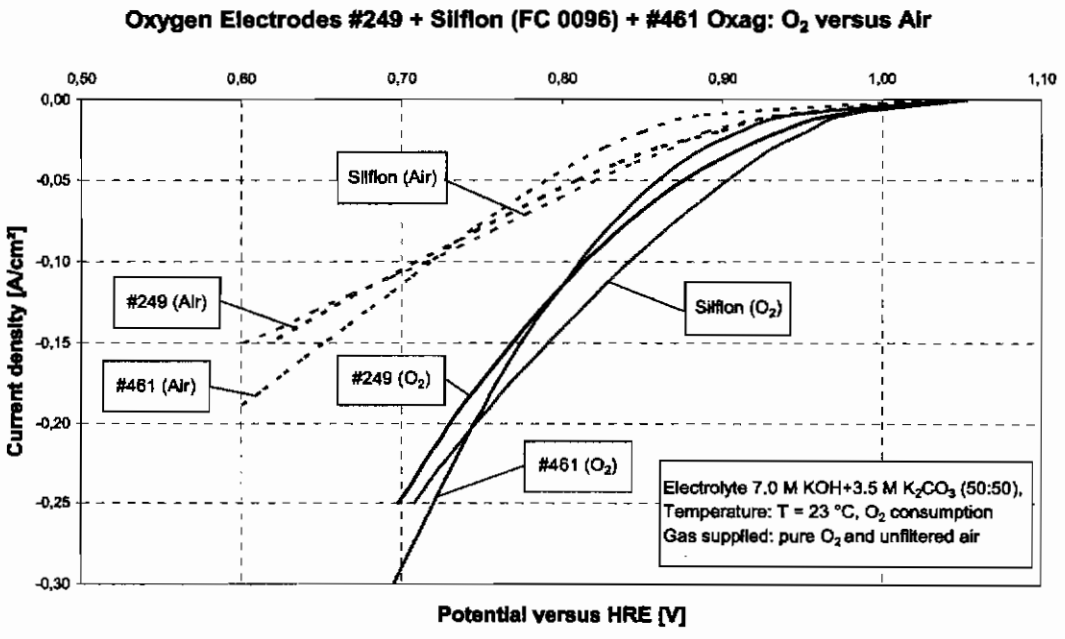


**Diagram 4-6:** $O_2$-electrodes at 23 °C in 50:50 KOH/$K_2CO_3$ for $O_2$ / air-consumption.
Oxygen electrodes #249, Silflon (FC 0096) and #461 were tested in the half cell. Each electrode was first operated with pure oxygen. For the second test unfiltered air was supplied to the electrode in place of oxygen. Electrolyte used was a mixture of 7.0 M KOH and 3.5 M $K_2CO_3$ (ratio 50:50). All tests were made at room temperature. Potential was measured versus a hydrogen reference electrode, current supplied with a galvanostat (manual variation).

## Current/Voltage-Characteristics of the Oxygen Electrode #461 Oxag

Tests were made with oxygen electrode #461 to investigate the difference in electrode performance if another catalyst is used. For electrode #461 a silver oxide catalyst is used, the former described electrodes Silflon and #249 were manufactured using a Silflon catalyst.

Again, the effect of temperature variation was investigated, both for operation with pure oxygen in comparison to operation with unfiltered air. The influence of the $CO_3^{2-}$ content was also investigated by changing the electrolytes.

## I/V-Characteristics of the Oxygen Electrode #461 in 7.0 M KOH

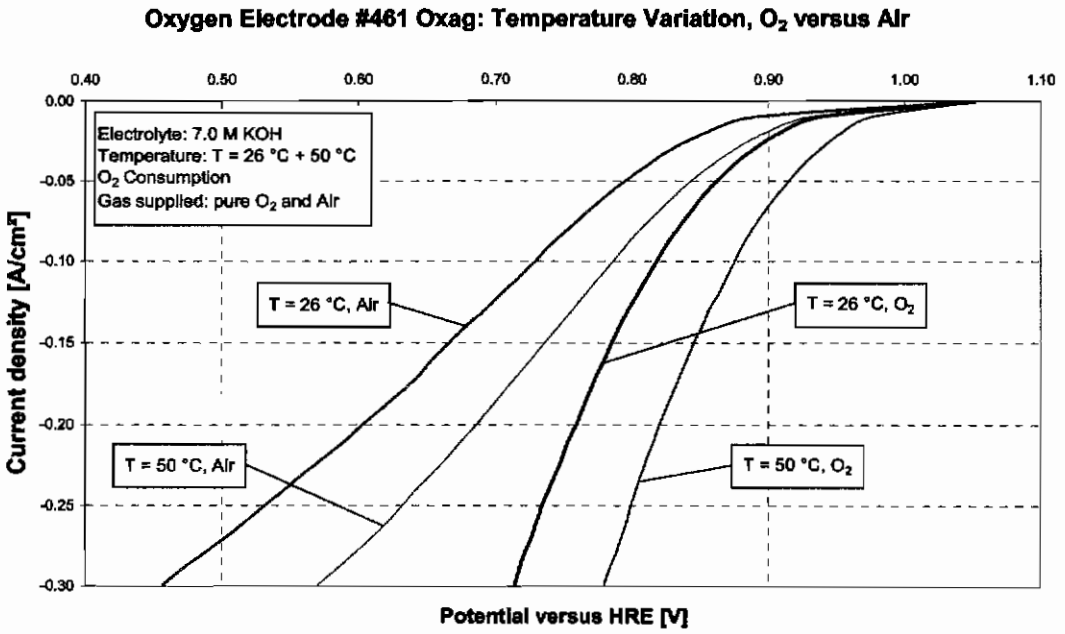


**Diagram 4-7:** Comparison oxygen/air-operation of an $O_2$-electrode in 7.0 M KOH.
Oxygen electrode #461 was tested in the half cell to compare operation with air to operation with pure oxygen. In addition the effect of temperature variation was also investigated. Potential was measured versus a hydrogen reference electrode, current supplied with a galvanostat (manual variation).

In Diagram 4-7 to Diagram 4-9 the current/voltage characteristics of an Oxag-electrode can be seen. For these half cell experiments, the electrode was supplied alternately with pure oxygen and with unfiltered air. The electrolyte was changed in order to simulate carbonation.

Several effects can be shown with these measurements:

In the comparison of air and oxygen operation the lower performance at air operation stands out. Also with an increased gas flow it is not possible to sufficiently supply the electrode with gas. The measurement curves recorded for air operation show a clearly flatter progression. With increasing load the electric potential is stronger reduced than for operation with pure oxygen.

## I/V-Characteristics of the Oxygen Electrode #461 in a mixture of 7.0 M KOH + 3.5 M $K_2CO_3$ (50:50)

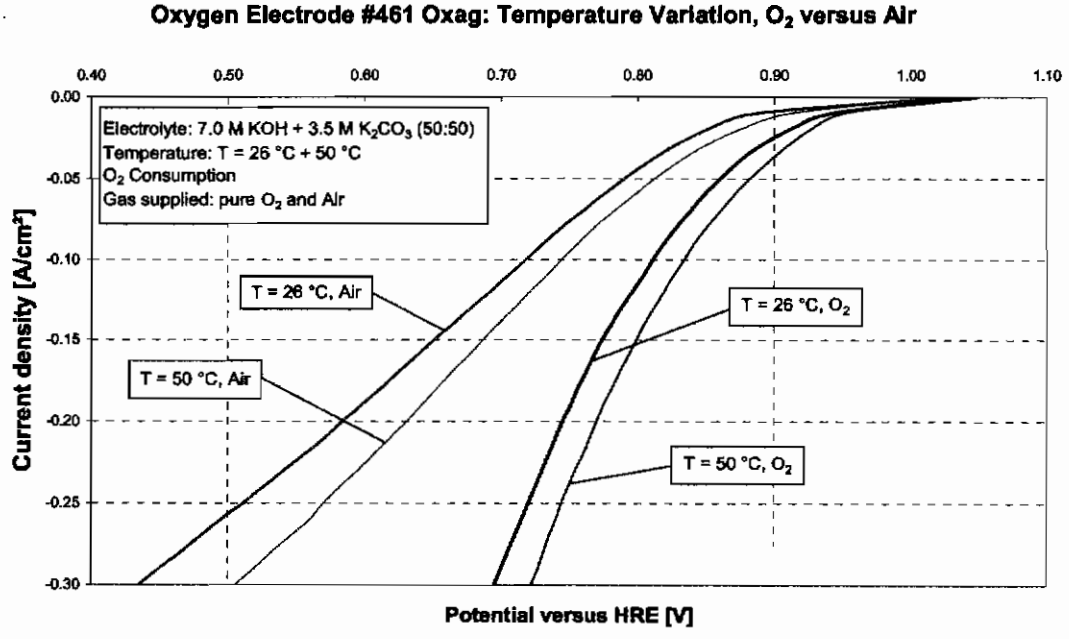


**Diagram 4-8:** Comparison oxygen/air-operation of an $O_2$-electrode in a mix of 7.0 M KOH and 3.5 M $K_2CO_3$ with a ratio of 50:50. Oxygen electrode #461 was tested in the half cell to compare operation with air to operation with pure oxygen. In addition the effect of temperature variation was also investigated. Potential was measured versus a hydrogen reference electrode, current supplied with a galvanostat (manual variation).

Furthermore, the influence of the temperature becomes apparent. An increase in temperature also increases the performance of the electrodes; this is the case for oxygen operation as well as for air operation. However, the effects are different

here: when operating with pure oxygen the measurement curves are merely shifted in parallel, while for operation with air also the slopes of the measurement curves change. For higher temperatures the curve becomes steeper thus indicating that the influence of the temperature is superimposed with another effect.

## I/V-Characteristics of the Oxygen Electrode #461 in 3.5 M $K_2CO_3$

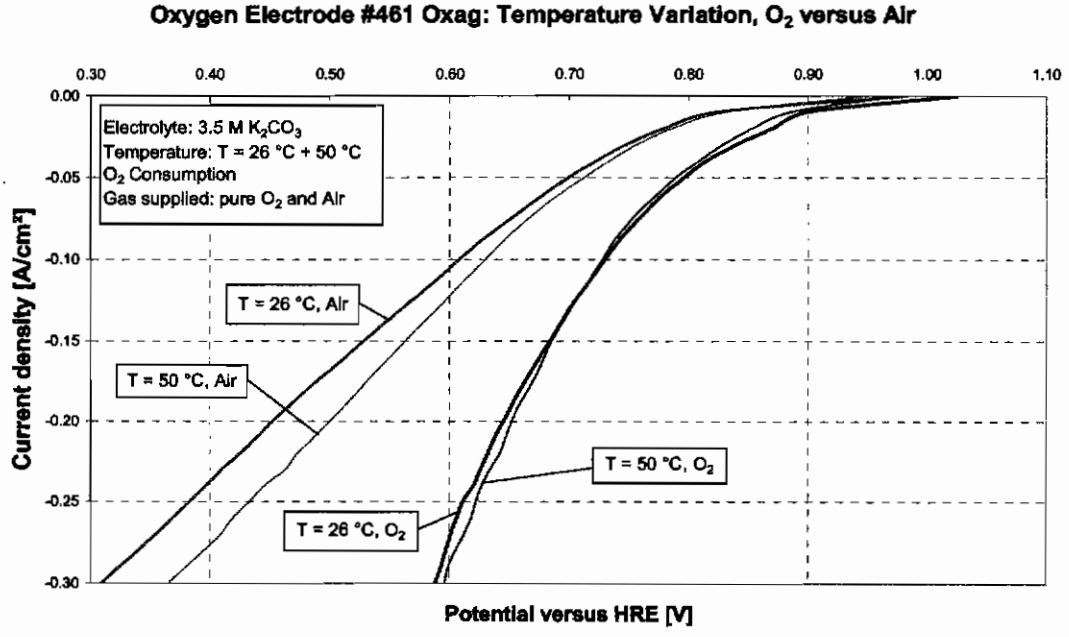


**Diagram 4-9:** Comparison oxygen/air-operation of an $O_2$-electrode in 3.5 m $K_2CO_3$.
Oxygen electrode #461 was tested in the half cell to compare operation with air to operation with pure oxygen. In addition the effect of temperature variation was also investigated. Potential was measured versus a hydrogen reference electrode, current supplied with a galvanostat (manual variation).

It can also be clearly seen that the influence of the temperature decreases with an increasing carbonate content in the electrolyte. For the experiment with a $K_2CO_3$ solution only a marginal difference can be seen. With increasing carbonate content the measured electric potentials decrease when connected to the same load.

## Effect of Temperature Variation on the Oxygen Electrode - Comparison of electrodes #249, Silflon (fuel cell 0096) and #461 Oxag

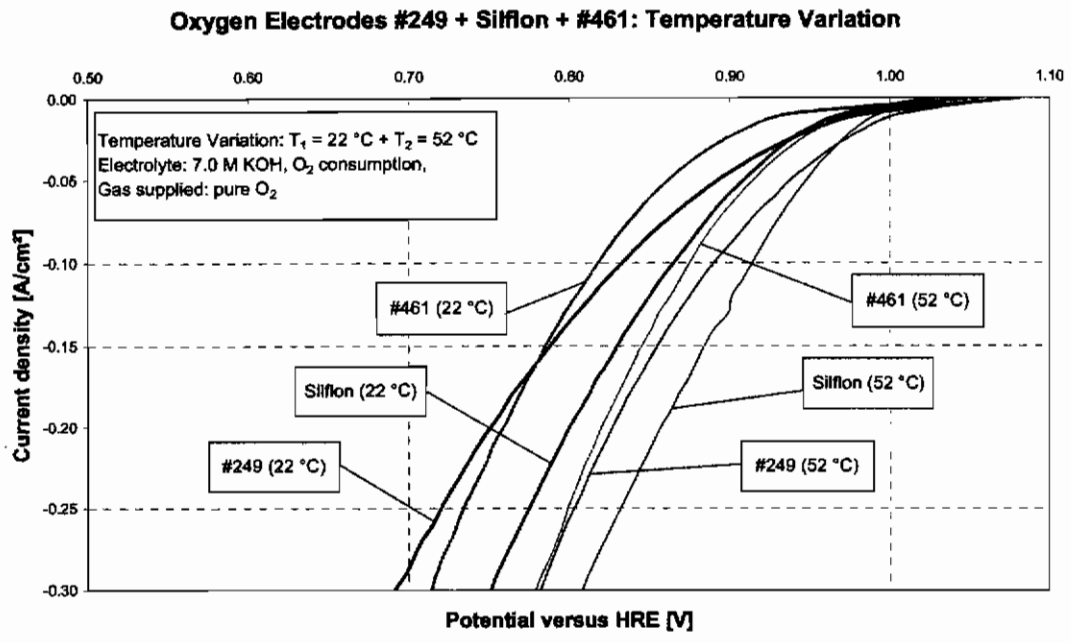


**Diagram 4-10:** I/V Curves of $O_2$-electrodes at 22 °C and 52 °C in KOH consuming $O_2$. Oxygen electrodes #249, Silflon (FC 0096) and #461 were tested in the half cell to investigate the effect of temperature variation. One test at room temperature T=22 °C, second test at T=52 °C. The electrodes were operated in 7.0 M KOH with pure oxygen. Potential was measured versus a hydrogen reference electrode, current supplied with a galvanostat (manual variation).

Diagram 4-10 shows the comparison of two Silflon-electrodes (#249 + fuel cell 0096) with an Oxag-electrode. These electrodes are oxygen electrodes with silver catalysts, the main difference being the actual catalyst. The difference between the two electrodes with Silflon-catalyst is the different composition of the further elements. Electrode #249 has a very porous structure, the Silflon-electrode (fuel cell 0096) additionally contained two different carbons. As can be seen from the recorded measurement values this has an effect on the performance of the electrodes. The two electrodes with Silflon-catalyst exhibit an approximately similar progression with the electrode containing carbon reaching better values. The Oxag-electrode #461 approximately reaches the performance of the Silflon-

electrode #249; while being inferior in the load range up to circa 150 mA/cm², while above this level it reaches a higher electric potential with the same load.

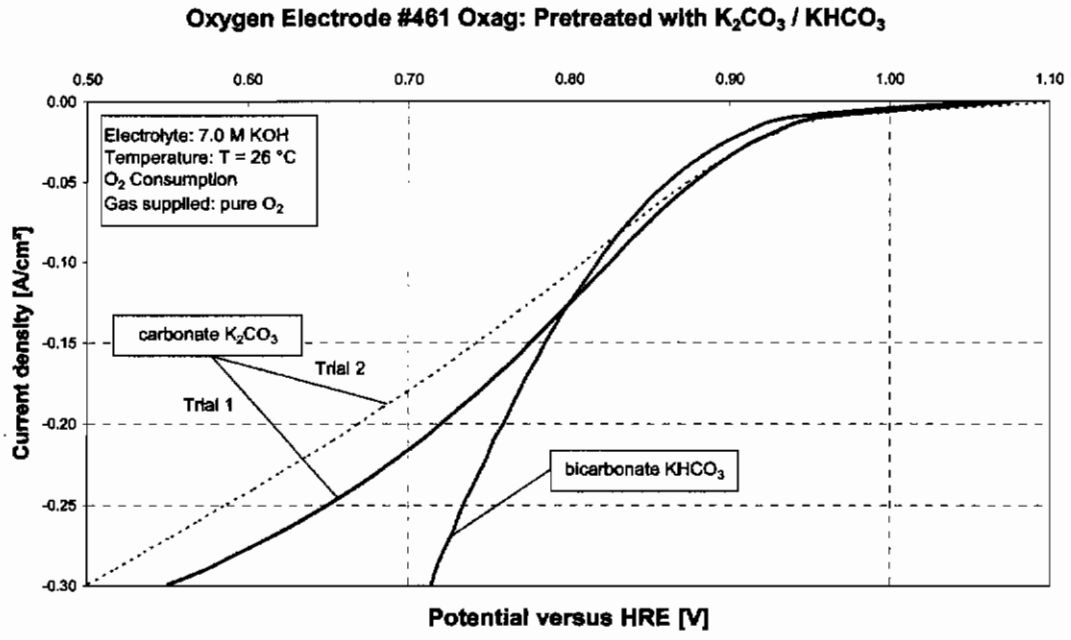


**Diagram 4-11:** $O_2$-electrode pretreated with $K_2CO_3$ and $KHCO_3$ respectively.
Oxygen electrode #461 was tested in the half cell to investigate the influence of carbonate inclusion. The electrode was pretreated with $K_2CO_3$ and $KHCO_3$ respectively. Therefor the samples were soaked in the liquid electrolyte at 70 °C and dried after that in an oven. Tests were made in 7.0 M KOH at a temperature of 26 °C. Gas supplied to the electrode was pure oxygen. Potential was measured versus a hydrogen reference electrode, current supplied with a galvanostat (manual variation).

Diagram 4-11 shows the current/voltage characteristics of two #461 Oxag-electrodes, which were previously soaked in $K_2CO_3$ and $KHCO_3$ solution respectively and dried. The electrode pretreated with $KHCO_3$ can take a load across the entire measurement range and achieves good values. Contrary to this, the performance of the electrode pretreated with $K_2CO_3$ declines rapidly above a load of circa 100 mA. The measurement was repeated (dashed curve), in which case the electrode achieved even worse values. This effect had not become apparent during the long-term experiments with a permanent load in a half cell with

electrode #461 (compare Diagram 4-14), since lower current densities (50–100 mA/cm²) are adjusted for long-term measurements.

In addition to the already shown current/voltage characteristics long-term measurements in a half cell were also carried out with electrode #461.

Diagram 4-12 shows the results of the measurement of an untreated oxygen electrode #461 Oxag in various electrolytes. For the experiment the electrode was operated with pure oxygen and then with unfiltered air from the compressed air network. The half cell was operated for several hours with a preadjusted current. The measurement results show the expected progression; with increasing carbonate content and in particular with an alternation between oxygen and air operation the measured voltage at the hydrogen reference electrode has to decline.

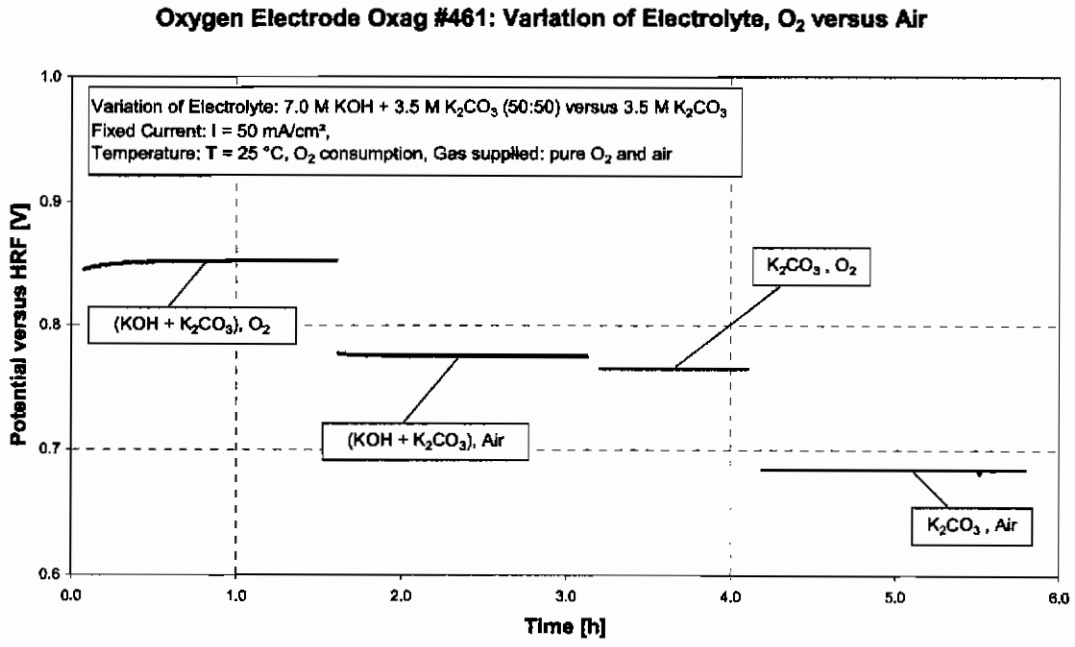


**Diagram 4-12:** $O_2$-electrode in carbonated electrolyte, operation with pure $O_2$ and air.
Half cell test of oxygen electrode #461 with fixed current (I = 50 mA/cm²). The influence of the carbonate content of the electrolyte was investigated. Tests were made in 7.0 M KOH, a mixture of 7.0 M KOH and 3.5 M $K_2CO_3$ (50:50) and 3.5 M $K_2CO_3$. In addition a comparison of operation with pure oxygen and unfiltered air is shown. Potential was measured versus a hydrogen reference electrode.

### 4.1.4 Experiments with pretreated Oxygen Electrodes

In order to examine the influence of carbonate formation or hydroxide formation on the electrodes specially pretreated oxygen electrodes were examined in a half cell:

- electrode I for 24 h at 70 °C in 7.0 M KOH, dried at 70 °C
- electrode II for 24 h at 70 °C in 3.5 M $K_2CO_3$, dried at 70 °C

This procedure was developed to achieve an inclusion of carbonate or hydroxide crystals in the electrode pores. All samples were soaked for 24 h in the electrolyte at 70 °C and than dried in an oven at 70 °C. It may occur that the decline of the performance is ascribed to the formation of carbonate, when white precipitates were detected. However, without further examinations it cannot be stated whether the precipitate is dried potassium hydroxide or potassium carbonate. For that reason carbonate formation was investigated as well as hydroxide formation.

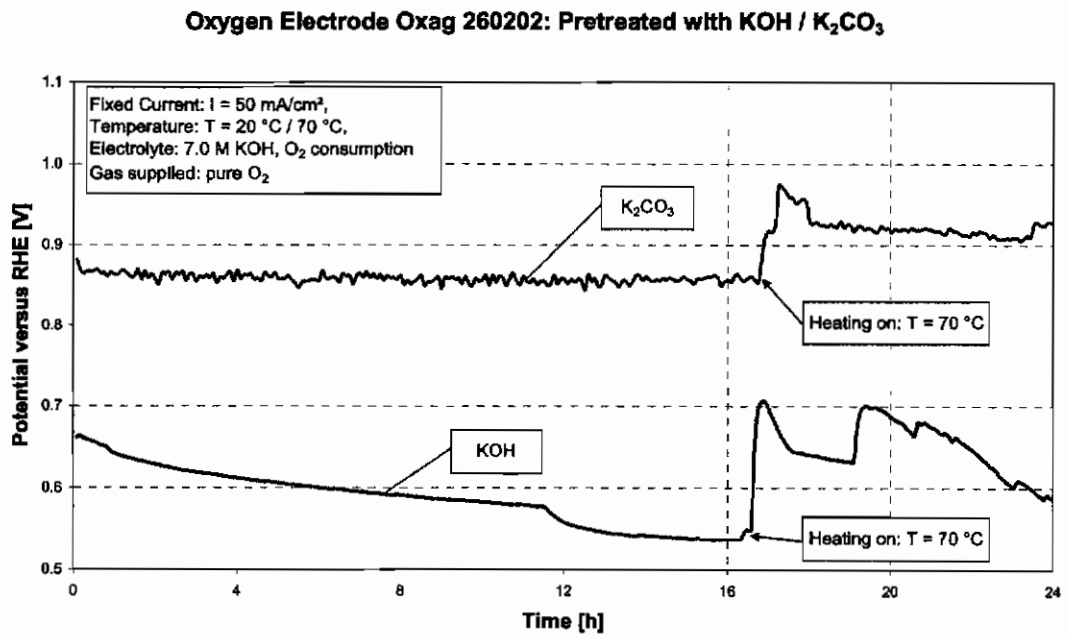


**Diagram 4-13:** $O_2$-electrodes pretreated with KOH and $K_2CO_3$ respectively.
Oxygen electrode Oxag 260202 was tested in the half cell to investigate the influence of carbonate inclusion. The electrode was pretreated with $K_2CO_3$. In addition the inclusion of hydroxides was investigated also. Therefore the samples were soaked in the liquid electrolyte at 70 °C and dried after that in an oven. Tests were made in 7.0 M KOH at a temperature of 20 °C and 70 °C respectively. Gas supplied to the electrode was pure oxygen. Voltages measured versus a hydrogen reference electrode, current supplied with a galvanostat.

Diagram 4-13 shows the measured electric potential for oxygen consumption at a fixed current of I=50 mA/cm². A tested electrode had been previously soaked in potassium hydroxide solution and dried. However, at the beginning of the measurement this electrode could not be loaded, since even for low currents with galvanostatic measurement the electrode switched from oxygen consumption to hydrogen production. The therefore initially potentiostatically taken measurements resulted in a voltage of 370 mV. The current increased over the duration of 4 h to circa 80 mA/cm². Following this, the experiment was started again and the data shown in Diagram 4-13 was recorded. The continuously declining electric potential can be clearly seen at 20 °C as well as at 70 °C. The measured electric potential for an oxygen electrode also has to be rated as poor. Without any treatment of the electrode sample an electric potential of circa 850-900 mV (or even more) at the same load had to be expected at least.
Also shown are the results of the half cell measurement with an oxygen electrode that was previously soaked in a $K_2CO_3$ solution and then dried. The electric potential measured at the hydrogen reference electrode declined during the measurement duration by circa 20 mV at 20 °C and by circa 15 mV at 70 °C respectively. The reached values are at a very good level, which was unexpected. This is an indication that either no carbonate was deposited in the electrode or that the electrode was not affected by it.

For a comparison of the measurement results and for their verification the experiment was repeated. An oxygen electrode with similar composition but from a different lot was used. In a half cell an untreated electrode was tested as well. The measurement of this electrode was meant as a reference for all measurements with pretreated electrodes. It can be assumed that the untreated electrode will deliver the best performance characteristics. In addition, an electrode was tested, which previously had been soaked in a $KHCO_3$ solution and then dried. The recorded data are presented in Diagram 4-14. The voltages measured at the hydrogen reference electrode are, in comparison to the previous measurement, at a slightly

higher level. At a load of I=50 mA/cm² and a temperature of T=20 °C all the pretreated electrode samples reached a potential versus HRE of about 900 mV or even more. The untreated electrode sample reached a minimum of 890 mV at the same load.

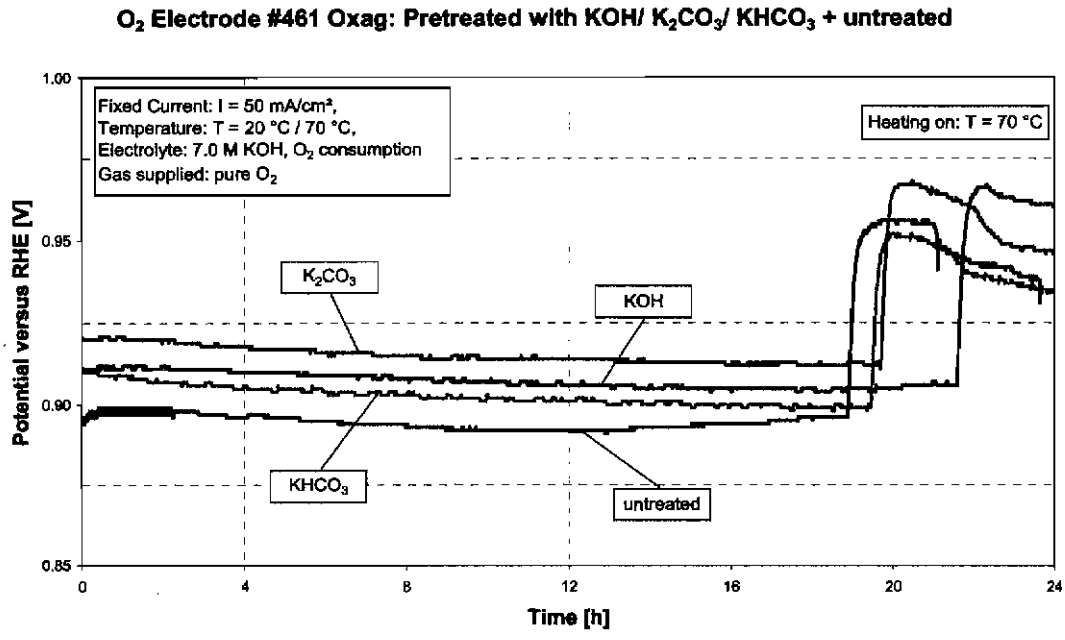


**Diagram 4-14:** $O_2$-electrodes untreated and pretreated with different electrolytes.
Half cell tests of oxygen electrode #461 with fixed current (I = 50 mA/cm²) to investigate the influence of carbonate inclusion and hydroxide inclusion. The electrode samples were pretreated with $K_2CO_3$, $KHCO_3$ and KOH. Therefore the samples were soaked in the liquid electrolyte at 70 °C and dried after that in an oven. In addition the measurement result of an untreated electrode is shown. Tests were made in 7.0 M KOH at a temperature of 20 °C and 70 °C respectively. Gas supplied to the electrode was pure oxygen. Voltages measured versus a hydrogen reference electrode, current supplied with a galvanostat.

For the measurement of electrode #461 also no negative effects due to the pretreatment with the carbonate solutions could be detected. The serious effects of the pretreatment with KOH could not be demonstrated with this experiment. Contrary to the expectations, the untreated electrode delivered the poorest values in this comparison. All electrodes exhibited a slight decline in voltage over the experiment duration.

## 4.2 Flow Rate and Tightness Tests

The resulting values of the flow rate and tightness tests were logged and are used for fault detection and the comparison of the manufactured fuel cells, in particular if modifications of the design or the used parts were implemented. All tests are done with de-ionised water and compressed air.

| **Test chart flow measurement and tightness** | | | |
|---|---|---|---|
| Date: 2004/12/13 | | Gaskatel Nr.: 0096 | |
| Name: Schudt | | Block-Code: EF BZ 1x(4/2/2) | |
| | | | |
| air flow dry (p_air = 0.25 bar) | | | comment |
| $H_2$-electrode | 31.7 | % of 1 sl/min | air bubbles also through $O_2$ and KOH outlet |
| $O_2$-electrode | 100.0 | % of 1 sl/min | air bubbles also through $H_2$ and KOH outlet |
| | | | |
| air flow wet (p_air = 0.25 bar) | | | comment |
| $H_2$-electrode | 9.7 | % of 1 sl/min | no air bubbles through $H_2$ and KOH outlet |
| $O_2$-electrode | 100.0 | % of 1 sl/min | no air bubbles through $H_2$ and KOH outlet |
| | | | |
| $H_2O$ flow (p_$H_2O$ = 0.25 bar) | | | comment |
| total | 6.72 | ml/sec | |
| | | | |
| air flow wet (p_air = 0.30 bar + p_$H_2O$ = 0.25 bar) | | | comment |
| $H_2$-electrode | 11.2 | % of 1 sl/min | no air bubbles through $H_2$ and KOH outlet |
| $O_2$-electrode | 100.0 | % of 1 sl/min | no air bubbles through $H_2$ and KOH outlet |
| | | | |
| permeability for water through Separator | | | comment |
| $H_2O$ to $H_2$-electrode | 0.023 | ml/sec | upper $H_2$ outlet |
| $H_2O$ to $O_2$-electrode | 0.017 | ml/sec | upper $O_2$ outlet |
| | | | |
| decrease of pressure | | | comment |
| $H_2$-electrode | 2.5 | mbar/min | |
| $O_2$-electrode | 2.8 | mbar/min | |
| | | | |
| EloFlux- flow | | | comment |
| in front/out rear | - | ml/min | incapable of measurement |
| in rear/out front | - | ml/min | incapable of measurement |

**Table 4-1:** Data of the Flow Rate and Tightness Test with Fuel Cell 0096

The tests with fuel cell 0096 show that the cell has no obvious problems caused by mechanical failures. A gas flow of 100 % or 1 sl/min for the oxygen electrode indicates the integrated gas compartment for the operation with air in between the

oxygen electrodes. For the hydrogen electrode a smaller gas flow is measured. The measured value is normal as there is only a tiny gas flow structure on the surface of the electrode.

| **Test chart flow measurement and tightness** | | | |
|---|---|---|---|
| Date: 2005/2/26 | | Gaskatel Nr.: 0101 | |
| Name: Schudt | | Block-Code: EF BZ 1x(4/2/2) | |
| | | | |
| air flow dry (p_air = 0.25 bar) | | | comment |
| $H_2$-electrode | 40.5 | % of 1 sl/min | air bubbles also through $O_2$ and KOH outlet |
| $O_2$-electrode | 43.6 | % of 1 sl/min | air bubbles also through $H_2$ and KOH outlet |
| | | | |
| air flow wet (p_air = 0.25 bar) | | | comment |
| $H_2$-electrode | 12.3 | % of 1 sl/min | no air bubbles through $O_2$ and KOH outlet |
| $O_2$-electrode | 10.0 | % of 1 sl/min | no air bubbles through $H_2$ and KOH outlet |
| | | | |
| $H_2O$ flow (p_$H_2O$ = 0.25 bar) | | | comment |
| total | 2.33 | ml/sec | after drilling KOH port: 7.14 ml/sec |
| | | | |
| air flow wet (p_air = 0.30 bar + p_$H_2O$ = 0.25 bar) | | | comment |
| $H_2$-electrode | 11.4 | % of 1 sl/min | no air bubbles through $O_2$ and KOH outlet |
| $O_2$-electrode | 13.1 | % of 1 sl/min | no air bubbles through $H_2$ and KOH outlet |
| | | | |
| permeability for water through Separator | | | comment |
| $H_2O$ to $H_2$-electrode | 0.017 | ml/sec | upper $H_2$ outlet |
| $H_2O$ to $O_2$-electrode | 0.011 | ml/sec | upper $O_2$ outlet |
| | | | |
| decrease of pressure | | | comment |
| $H_2$-electrode | 1.7 | mbar/min | |
| $O_2$-electrode | 0.7 | mbar/min | |
| | | | |
| EloFlux- flow | | | comment |
| in front/out rear | - | ml/min | incapable of measurement |
| in rear/out front | - | ml/min | incapable of measurement |

**Table 4-2:** Data of the Flow Rate and Tightness Test with Fuel Cell 0101

The gas flow for the hydrogen electrode of fuel cell 0101 as well is normal. But for the gas flow on the oxygen side there seems to be a hindrance. A value of 11.4 % or 0.11 sl/min is poor. A flow rate of almost 100 % was expected. All the other measured values are standard.

## 4.3 Tests with the Fuel Cells

In order to operate the fuel cell, the nickel electrodes at the hydrogen side first have to be activated. A current/voltage characteristic (scan) is subsequently recorded for each cell. This is usually done with oxygen and allows to compare the cells.

### 4.3.1 Activation Phase of an AFC

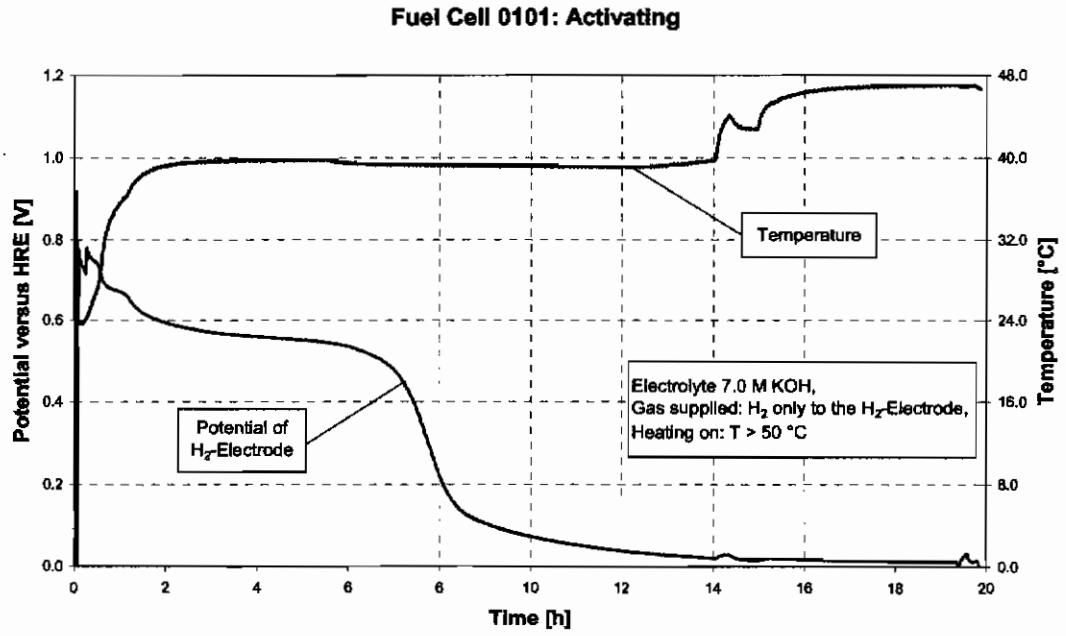


**Diagram 4-15:** Activation phase Fuel Cell 0101.
For the activation the fuel cell is supplied with $H_2$ to the $H_2$-electrodes only. The temperature is implied by heating foils which are situated inside the endplates of the fuel cell. The potential of the $H_2$-electrodes versus a hydrogen reference electrode is measured. The potential is an indication for the activity of the $H_2$-electrode.

Diagram 4-15 shows the activation phase of an EloFlux-AFC while the electric potential at the hydrogen electrode is measured. In the non-active state a mixed electric potential of circa 911 mV is measured. During the activation the measured voltage is reduced to the hydrogen potential ($Pot_{H2}$ = 0.0 V) due to the reduction of the nickel oxide. The measured curve shows the expected progression; initially the electric potential changes slowly, after circa 7 hours an auto-catalytic reaction starts and the electric potential changes very quickly. At t=14 h and t=14.5 h

respectively the temperature limit was increased in order to increase the cell temperature to approximately 50 °C.

### 4.3.2 Fuel Cell 0068 - EF Fuel Cell 1x (4/2/2)

Fuel Cell 0068 is a common EloFlux-AFC without adaptations for the operation with air. At the hydrogen side four nickel electrodes of type #314 were used and at the oxygen side two silver electrodes with Silflon-catalyst were used. The separator used was a PALL Supor 800 with 0.8 $\mu$m pore size.

#### I/V Curve with Fuel Cell 0068 in pure oxygen

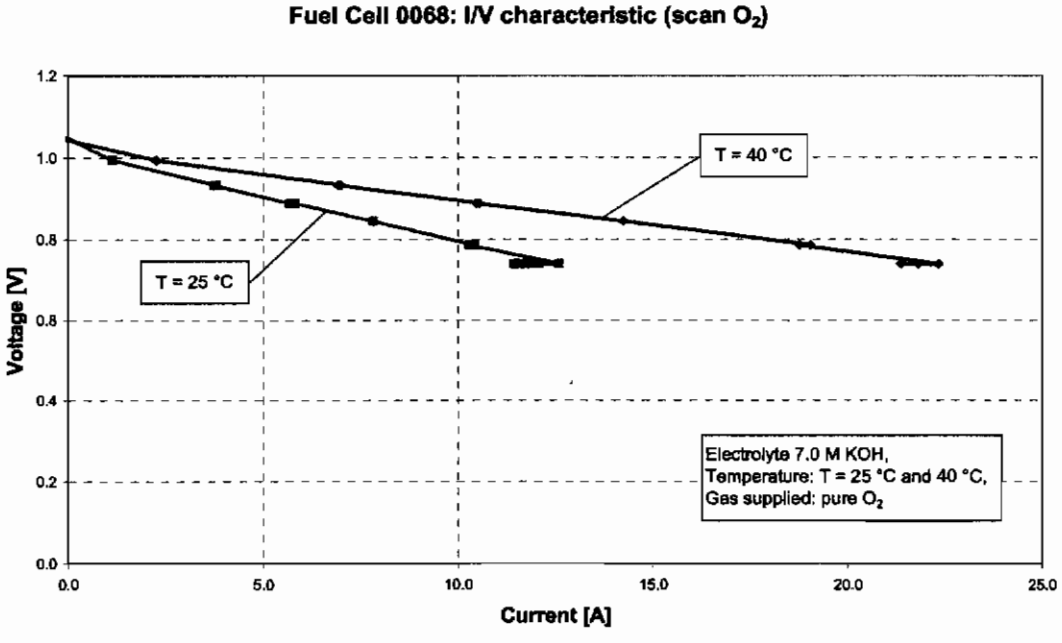


**Diagram 4-16:** Fuel Cell 0068 – current/voltage characteristic in $H_2/O_2$-operation

The current/voltage characteristics shown in Diagram 4-16 were recorded at a high and a low temperature. As expected, at higher temperatures, a higher performance can be achieved. At 40 °C the cell reached 22.3 A at 0.73 V compared to 12.6 A at 0.74 V and 25 °C. Diagram 4-16 shows the measured values. The values measured at a high temperature correspond to a load of circa 110 mA/cm². It can be seen that the current values declined for low as well as for high temperatures at a predetermined voltage.

## Long-term measurement with Fuel Cell 0068 operated with air

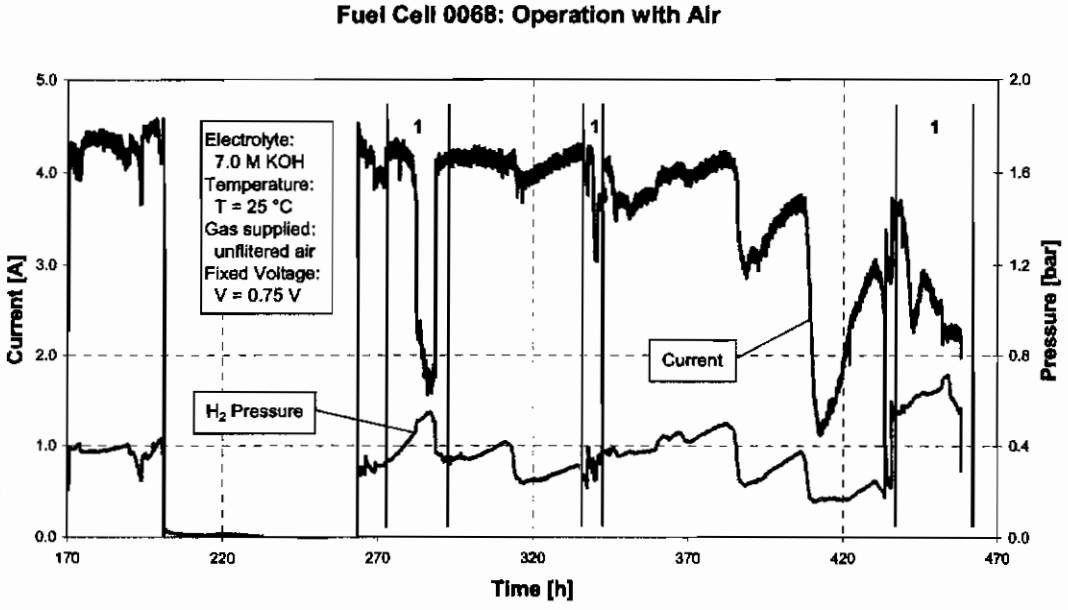


**Diagram 4-17:** Fuel Cell 0068 – long-term measurement with air at fixed voltage V=0.75 V

Diagram 4-17 shows the results of the long-term measurement with air. A constant voltage of 0.75 V was adjusted for the electronic load for this measurement. The experiment was carried out at room temperature. Up to t=170 h into the operation the cell was activated and current/voltage characteristics was recorded respectively. From t=170 h the cell was operated with air from the compressed air network. In the range of t=200–260 h the cell was not loaded. Over the duration of the experiment a decline of the current becomes apparent. It is also visible that there is a relationship between the hydrogen pressure and the performance of the cell. The current rapidly declines with increasing hydrogen pressure in the ranges marked with |1|. As expected, the current increases with increasing hydrogen pressure in all other ranges.

### 4.3.3 Fuel Cell 0096 – EF Fuel Cell 1x (4/2/2)

Fuel Cell 0096 was the first cell featuring a special gas compartment for air operation. For this, a frame with an inserted nickel foam as an air distributor was placed between the oxygen electrodes (see Section 3.1.5). At the hydrogen side four nickel electrodes of type #314 were used and at the oxygen side two silver electrodes with Silflon-catalyst were used, like for cell 0068. The separator used was an AMS FAS 1100. Due to its construction this cell was a dual cell with both cells connected in parallel.

#### I/V Curve with Fuel Cell 0096 in pure oxygen

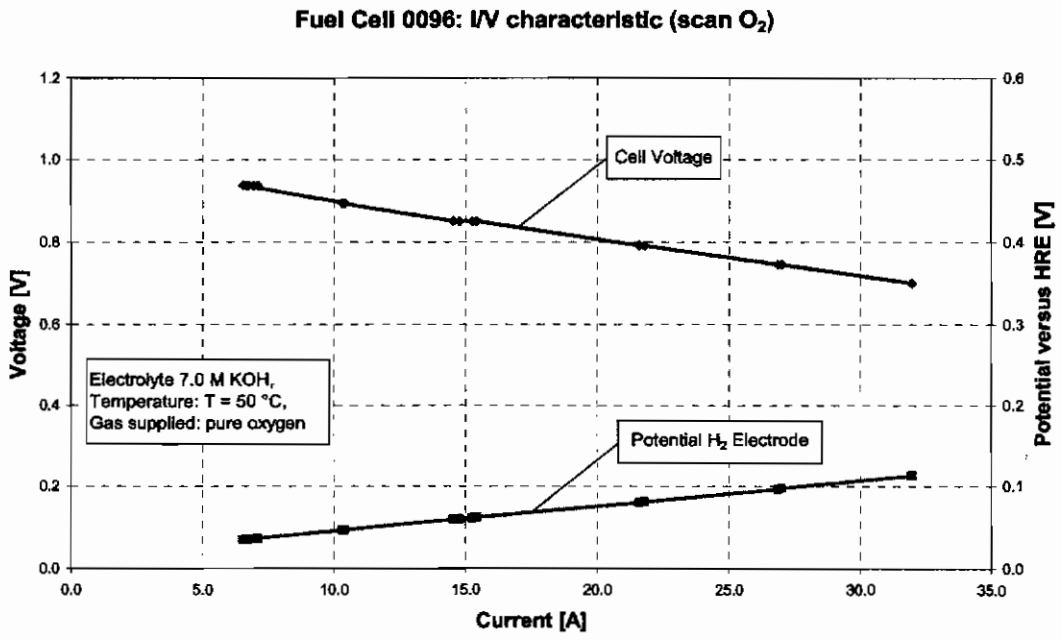


**Diagram 4-18:** Fuel Cell 0096 – current/voltage characteristic for $H_2/O_2$-operation

Here, the current/voltage characteristic was recorded at 50 °C (Diagram 4-18). Additionally, the electric potential of the hydrogen electrodes was measured with a hydrogen reference electrode integrated into the electrolyte circulation. The cell was loaded with a maximum current density of 160 mA/cm², while the cell voltage was 0.7 V. These values are very good and with 114 mV the electric potential of the $H_2$-electrodes is not critical.

## Long-term measurement with Fuel Cell 0096 operated with air

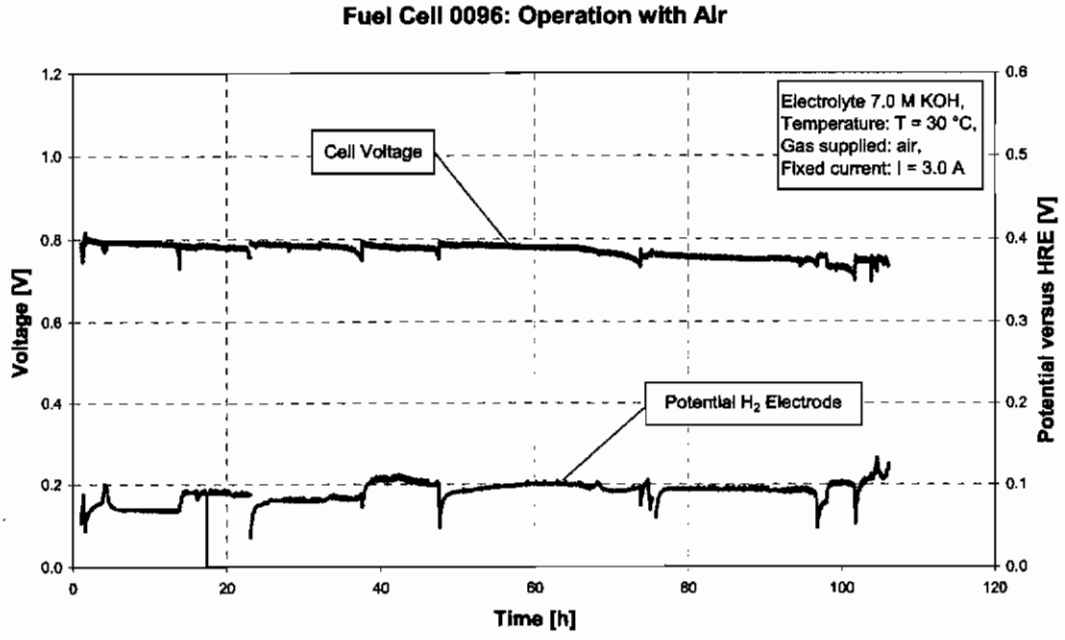


**Diagram 4-19:** Fuel Cell 0096 – long-term measurement with air at fixed current I=3.0 A

Diagram 4-19 shows the progression of the cell voltage and the electric potentials of the $H_2$-electrodes of the long-term measurement of Fuel Cell 0096. The current was adjusted to 3.0 A for this measurement, the operating temperature was 30 °C. In the diagram only the actual operating hours with a load are represented. The actual duration of the experiment was circa 170 hours; the load was switched off in between in order to not leave the experiment unattended. It repeatedly occurred that the air supply of a cell was disrupted. This procedure was deemed suitable in order to avoid possible damages of the cell.

As can be seen, the cell voltage declined by circa 50 mV over the experiment duration. The electric potential of the $H_2$-electrodes increased continuously during the experiment duration. This indicates a problem with the $H_2$-electrodes.

The experiments with this cell were discontinued, since with increasing experiment duration the air distributors were blocked by potassium hydroxide and the $O_2$-electrodes could hence not be supplied with gas any more.

### 4.3.4 Fuel Cell 0101 - EF Fuel Cell 1x (4/2/2)

Fuel Cell 0101 was also fitted with a gas compartment between the oxygen electrodes for the operation with air. However, nickel foam was not used and instead a plastic layer with a labyrinth-shaped air distributor was used (see Section 3.1.5). The electrodes used were again at the hydrogen side four nickel electrodes of type #314 and at the oxygen side two silver electrodes of type #249, which is also a Silflon-catalyst, but without any additional substances. The separator used was an AMS FAS 1100. The further set-up is equal to the one of fuel cell 0096.

#### I/V Curve with Fuel Cell 0101 in pure oxygen and air

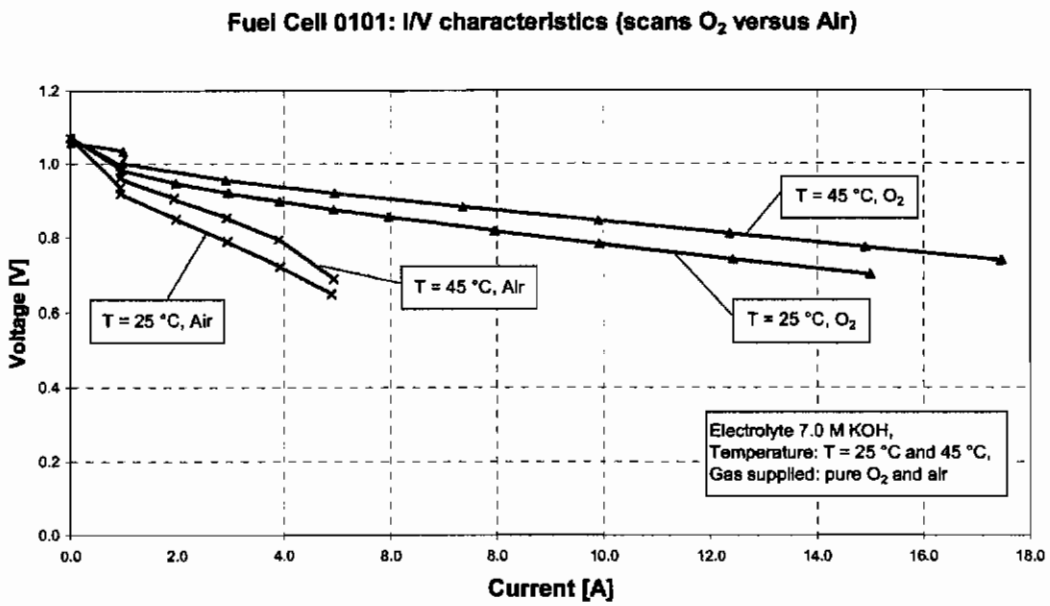


**Diagram 4-20:** Fuel Cell 0101 - current/voltage characteristic for $H_2/O_2$ and $H_2$/air-operation

Diagram 4-20 shows the current/voltage characteristics of fuel cell 0101. In this case, the cell was operated with $O_2$ as well as with air while varying the temperature as well. The measurements were taken at 20 °C and 45 °C. This cell produced significantly lower current values at a cell voltage of 0.7 V. A possible reason could be the new air distributor which covers parts of the electrode surface. This may cause a decrease of active electrode area.

## Long-term measurement with Fuel Cell 0101 operated with air – Effect of Temperature Variation on the Extraction of Reaction Water

For the long-term measurements fuel cell 0101 was supplied with unfiltered air. The cell was loaded with a fixed current of 3.0 A.

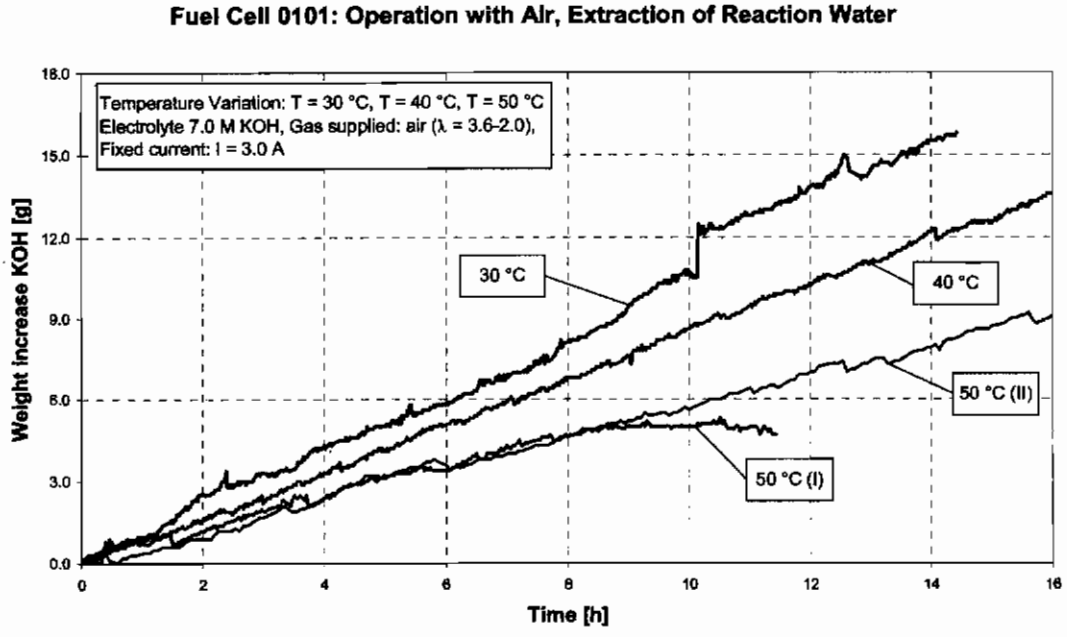


**Diagram 4-21:** Fuel Cell 0101 – long-term measurement with air at different temperatures. Investigation of the influence of temperature variation on the extraction of the water produced by the reaction. The fuel cell was supplied with unfiltered air and operated with a fixed current (I=3.0 A). Temperatures of 30 °C, 40 °C and 50 °C were adjusted. The experiment at 50 °C had to be repeated.

Using this cell, experiments were performed to extract the water of reaction using the air flow as a function of temperature. For that reason the weight of the electrolyte KOH solution was measured with a scale. For operation with a fixed current it is easily possible to calculate the mass of water produced by the reaction. By comparing the measured weight with the calculated values, conclusions can be made, how the water of the reaction was extracted from the cell. For this experiment the cell was operated at a temperature of 30 °C, 40 °C and 50 °C. The measurement results are presented in Diagram 4-21. The slope of the measurement

curves for the weight increase of the KOH solution becomes flatter the higher the temperature was adjusted. This shows that the rate of reaction water that was extracted from the cell via the air increases with increasing temperature. At a temperature of 50 °C the experiment shows an unexpected result. The slope of the measuring curve progresses initially linearly. After approximately 8 hours of operation the curve started to draw near a horizontal run. That behaviour theoretically indicates that all the produced reaction water was extracted via the air. As shown in Diagram 4-22 at the same time the hydrogen pressure declined.

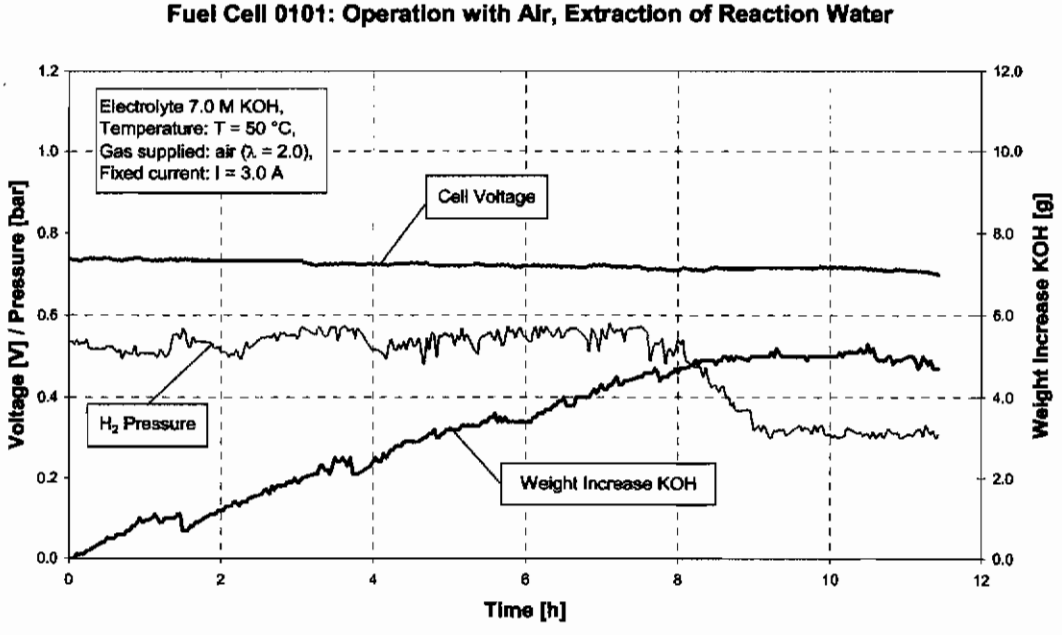


**Diagram 4-22:** Fuel Cell 0101 – first long-term measurement with air at 3.0 A and 50 °C. The fuel cell was supplied with unfiltered air and operated with a fixed current (I=3.0 A). A temperature of 50 °C was adjusted. During the experiment a decline of hydrogen pressure occurred.

This change of the operation parameters obviously had an influence on the electrolyte system of the fuel cell. The experiment was repeated again, since the decline of the $H_2$ pressure occurred by itself and was not intended. The slope of the measuring curve again is flatter than in the experiment at 40 °C.

Furthermore, it could be observed during the experiments, that the cell voltage declined over the experiment duration (see Diagram 4-23). Initially, the cell voltage during the 30 °C experiment was constant. However, in the experiments with temperatures of 40 and 50 °C a continuous decline can be seen. For the first 50 °C experiment from the beginning on the voltage was below the voltage measured during the first experiment, even though the voltage should be higher at a higher temperature. The voltage declined even further during the repetition of the 50 °C experiment, but progressed constant over the experiment duration.

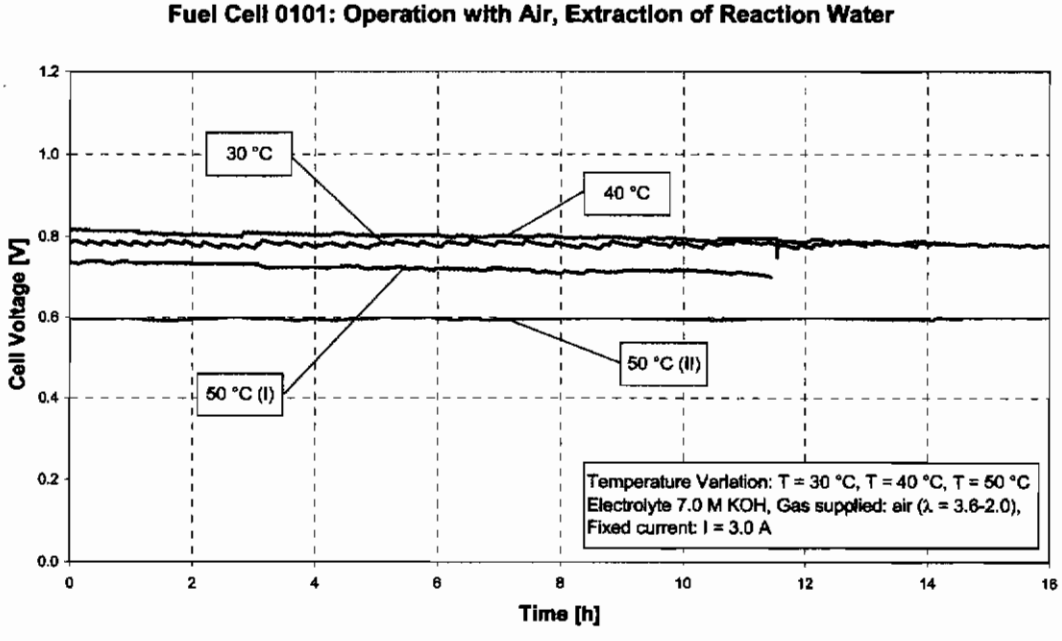


**Diagram 4-23:** Fuel Cell 0101 – long-term measurement with air at 3.0 A.

With an increasing operating time, however, the air flow rate declined. This effect could not be corrected during the measurements. Due to the poor air flow rate the experiments were discontinued at that stage.

## 4.4 Gas Analysis with the Gas Chromatograph

For the analyses of the $CO_2$-problem of the AFC, a gas analysis was carried out with the Gas Chromatograph (GC) in order to gain information about the concentration and location of the $CO_2$ introduced into the cell. The measurements were taken in the fuel gas itself as well as in the exhaust gas of the fuel cell.

### 4.4.1 Calibration Curves and Gas Purity

Initially, calibration curves were recorded using gas from commercial high-pressure gas cylinders, as they were later used for the operation of the fuel cell. According to the supplier the purity of the samples was 99.9 %. Hydrogen was used as the carrier gas for the analysis of oxygen, carbon dioxide and water. For the analyses at the hydrogen side nitrogen was used as carrier gas.

**Calibration data for $O_2$ and $CO_2$ in $H_2$-carrier gas**

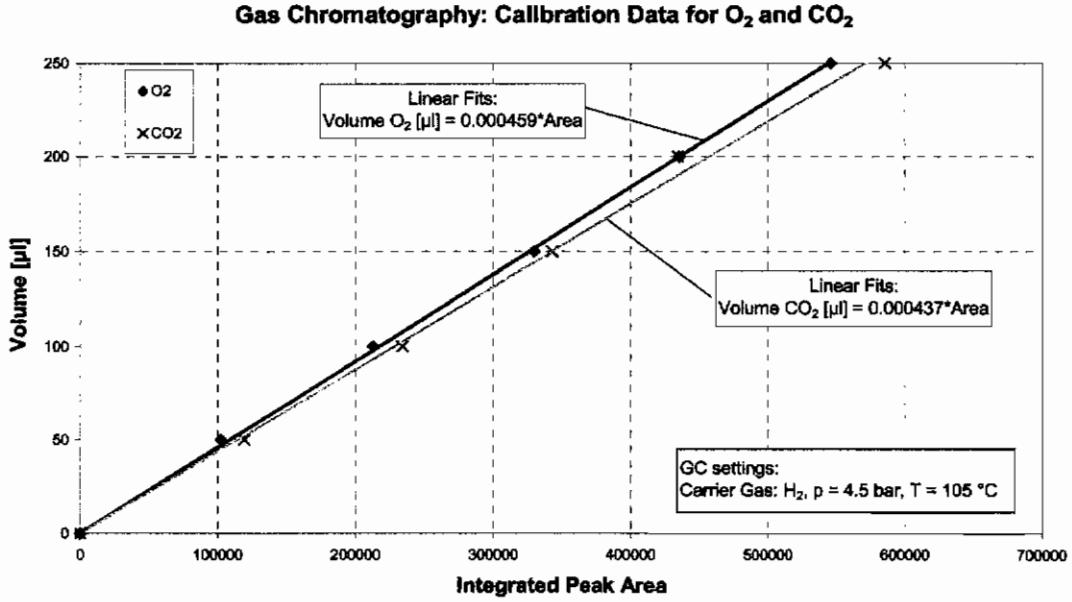


**Diagram 4-24:** Calibration data for $O_2$ and $CO_2$ in $H_2$-carrier gas

## Calibration data for $H_2O$ in $H_2$-carrier gas

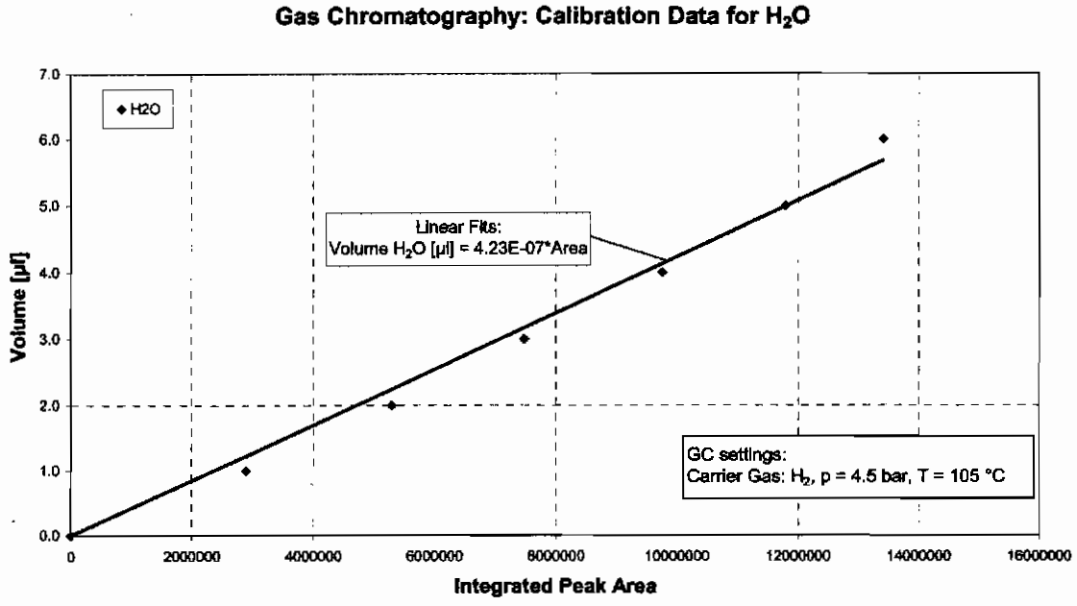


**Diagram 4-25:** Calibration data for $H_2O$ in $H_2$-carrier gas

## Calibration data for $H_2$ and $CO_2$ in $N_2$-carrier gas

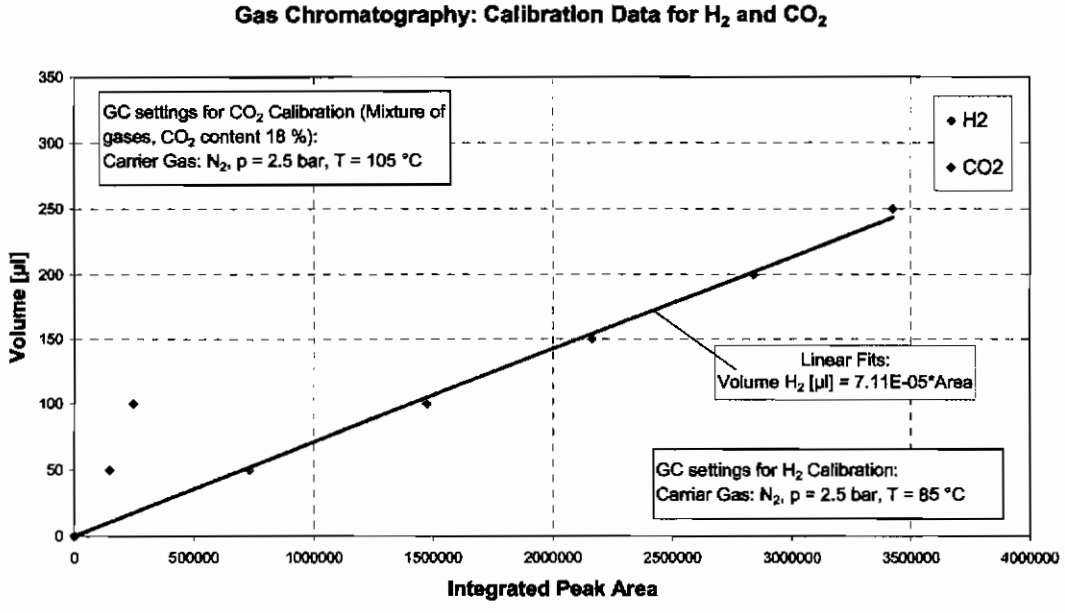


**Diagram 4-26:** Calibration data for $H_2$ and $CO_2$ in $N_2$-carrier gas

### 4.4.2 Retention time of the Components

In the following tables the retention times for the investigated gases are presented. The values correspond to the settings of the calibration data measurement.

| GC settings: | p=4.5 bar, T=105 °C | p=1.25 bar, T=65 °C |
|---|---|---|
| Component | Retention time [min] | |
| $O_2$ | 1.55 | 2.37-2.41 |
| $CO_2$ | 1.60 | 3.61-3.71 |
| $N_2$ | 1.44 | 2.30 |
| $H_2O$ | 2.80 | 12.70 |

**Table 4-3:** Retention Times for the investigated components in $H_2$ carrier gas

| GC settings: | p=2.5 bar, T=85 °C | p=1.25 bar, T=65 °C |
|---|---|---|
| Component | Retention time [min] | |
| $O_2$ | 2.60 | 3.77-3.88 |
| $CO_2$ | 3.60 | - |
| $H_2$ | 2.36 | 3.47-3.59 |
| $H_2O$ | 5.24 | 24.5-25.1 |

**Table 4-4:** Retention Times for the investigated components in $N_2$ carrier gas

### 4.4.3 Fuel Cell 0096 - EF Fuel Cell 1x (4/2/2)

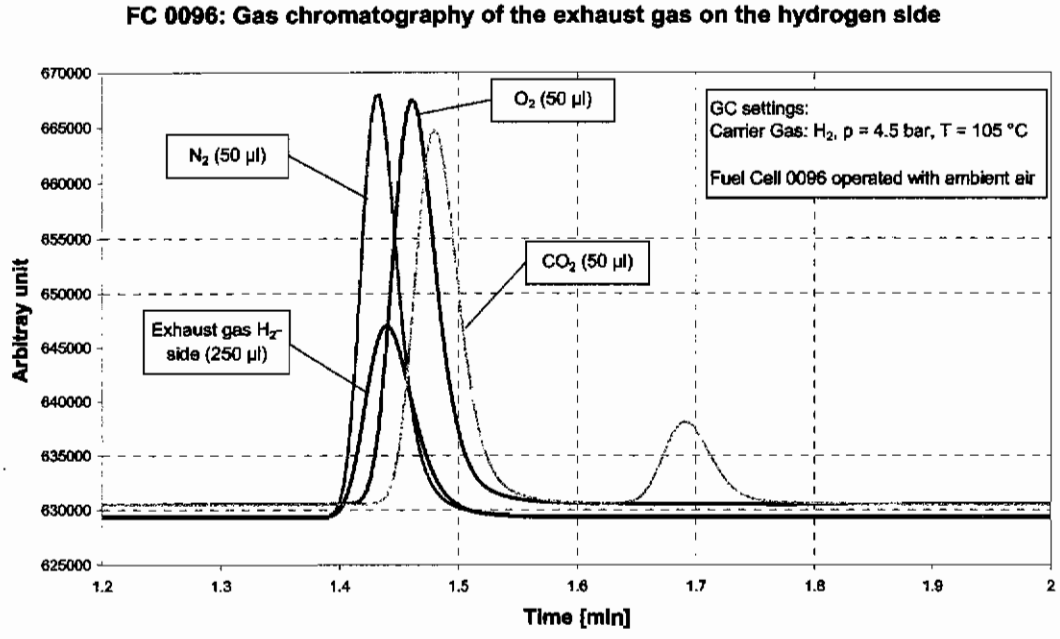


**Diagram 4-27:** Gas analysis of the exhaust gas at the hydrogen side for air operation

## Zoom into Diagram 4-27

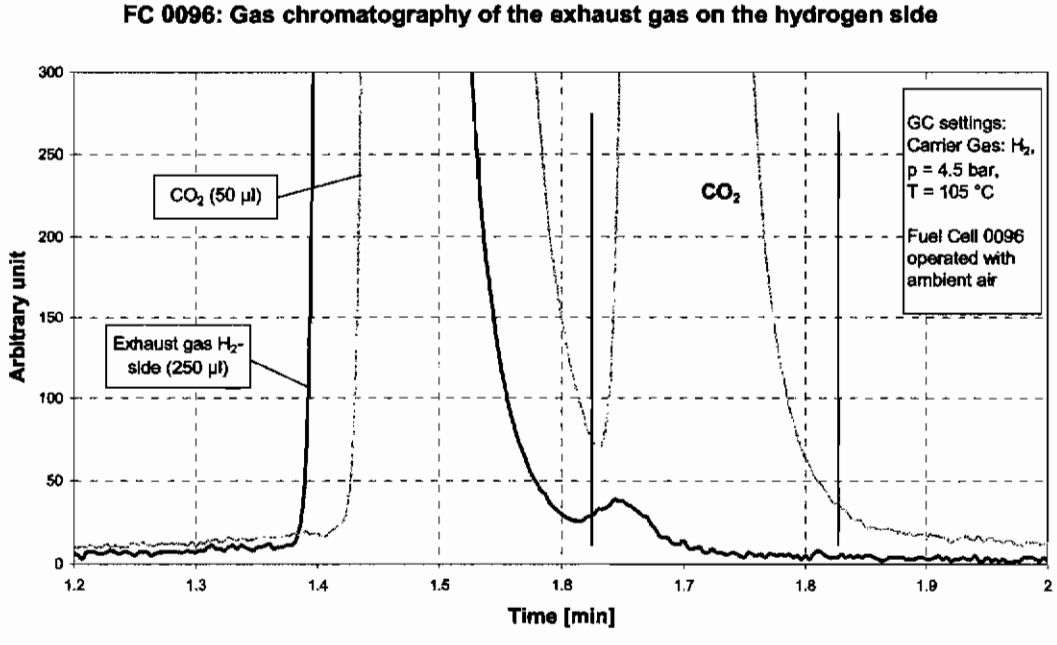


**Diagram 4-28:** Gas analysis of the exhaust gas at the hydrogen side for air operation

Diagram 4-27 and Diagram 4-28 show the results of an exhaust gas analysis at the hydrogen side of an air-operated fuel cell 0096. For a comparison of the measurement values the calibration data for $H_2$, $N_2$ and $CO_2$ are given as well. In Diagram 4-28, the measurement values are with respect to zero and a smaller section was presented. Traces of a substance could be identified which might be $CO_2$. It could have been migrated from the oxygen side to the hydrogen side. In the hydrogen supplied to the fuel cell $CO_2$ could not be detected.

### 4.4.4 Fuel Cell 0101 - EF Fuel Cell 1x (4/2/2)

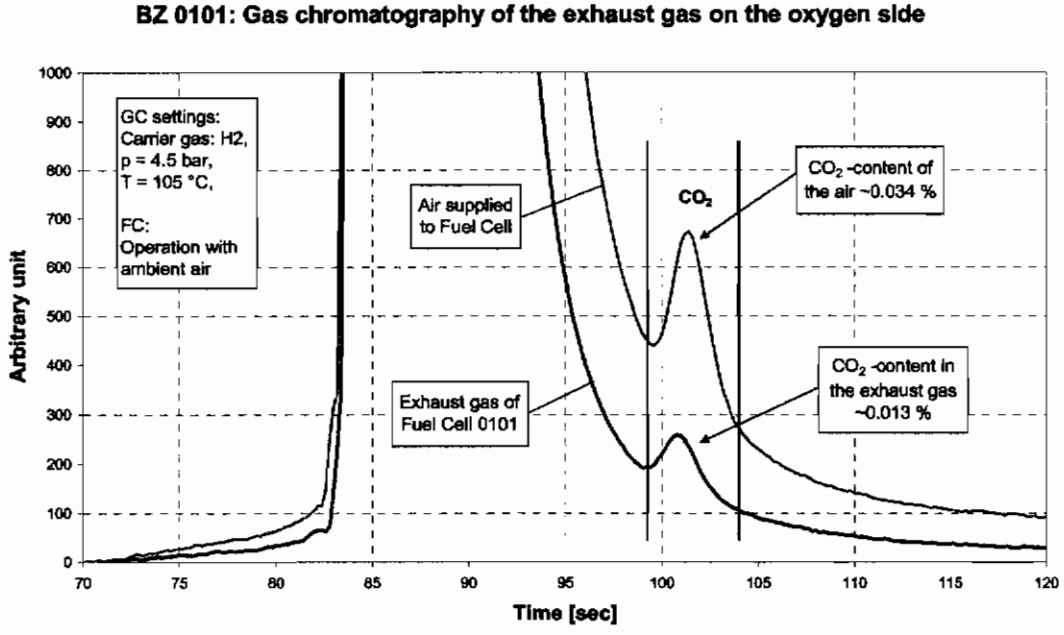


**Diagram 4-29:** Gas analysis of the exhaust gas at the oxygen side for air operation

Diagram 4-29 shows the result of the exhaust gas analysis at the oxygen side of the fuel cell 0101. For comparison a sample of the compressed air network used to supply the cell in operation was examined. The air was supplied to the cell unfiltered. It can be seen, that the $CO_2$-content in the exhaust gas of the fuel cell is lower than in the supplied air. This leads to the conclusion that circa 62 % of the inserted $CO_2$ remained in the cell.

### 4.4.5 Base Analysis: Reaction of $CO_2$ with various Electrolytes

Ambient air was tested with the GC with regards to its $CO_2$-content. To get more information about the interaction of the $CO_2$ contained in the air with various electrolytes (KOH-, $K_2CO_3$- and $KHCO_3$-solution), the air supplied to the GC was alternately supplied directly and through a fritted wash bottle filled with the electrolyte under study. In addition a test was made with a wash bottle filled with deionised water.

**Ambient Air led through 3.5 M $K_2CO_3$ solution.**

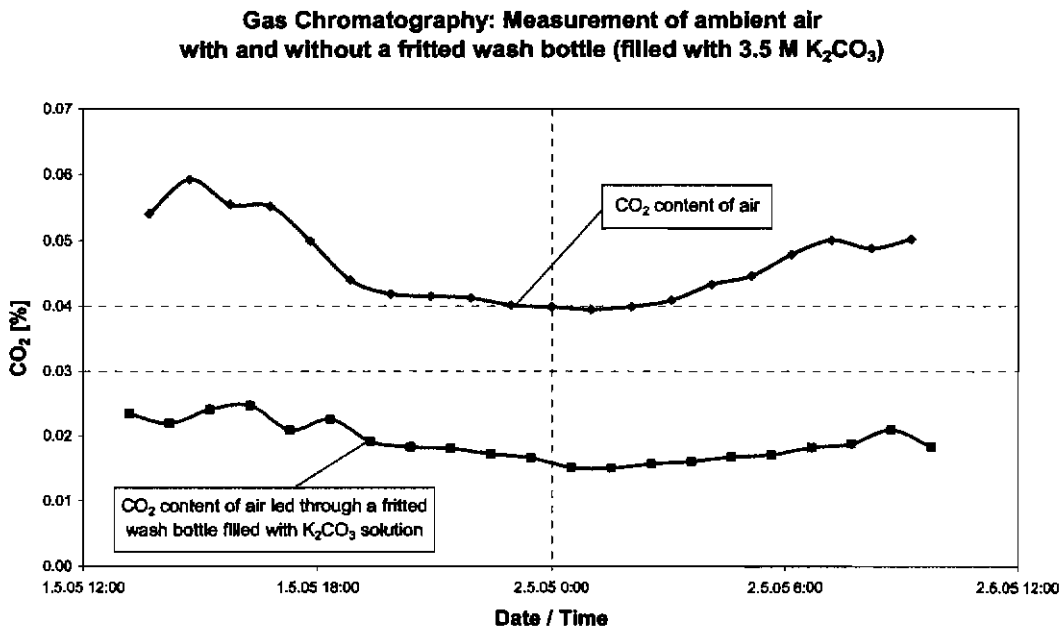


**Diagram 4-30:** GC-measurement to investigate $CO_2$-absorption in a $K_2CO_3$ solution. Ambient air was supplied to the GC alternately directly or through a fritted wash bottle filled with 3.5 M $K_2CO_3$ solution. The $CO_2$ content was measured.

The results shown in Diagram 4-30 were to examine the interaction of a $K_2CO_3$ solution with air which was conducted through the solution. The aim was to show whether $CO_2$ was absorbed by the solution. For this the air was analysed directly in the GC. Both measurement curves exhibit a similar progression; however, the

$CO_2$-content after the washing bottle was consistently reduced by more than half of the previous value.

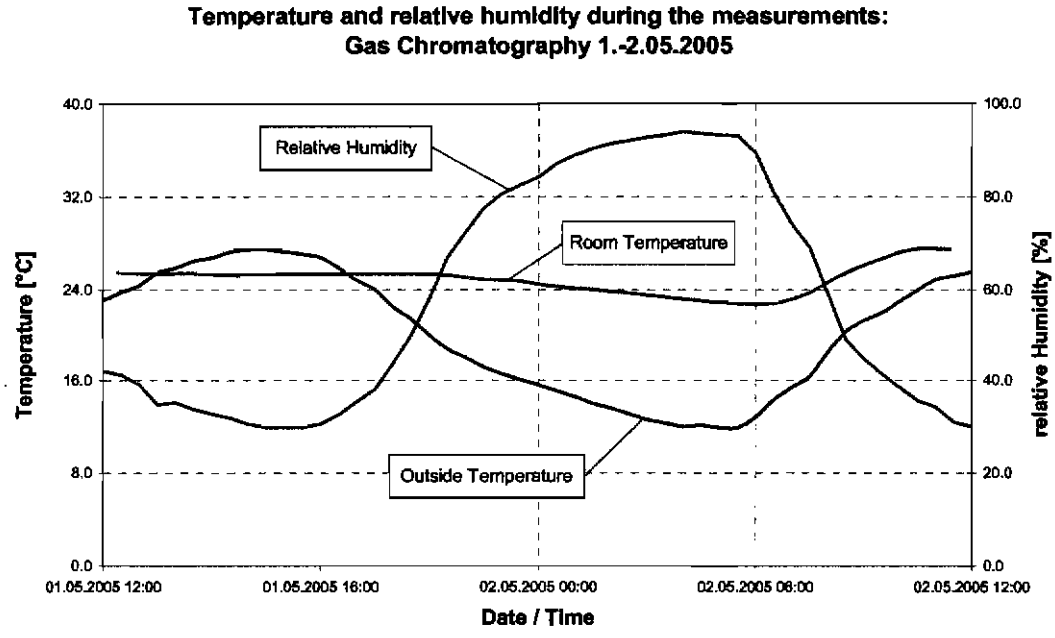


**Diagram 4-31:** Values of Temperature and Air Humidity during the GC-measurement. Room temperature was measured in the laboratory. The values of the outside temperature and the relative humidity of the air were measured at a gauging station of the HLUG ("Hessisches Landesamt für Umwelt und Geologie" – Hessian State Office for Environment and Geology). The gauging station is located approximately in 500 m distance to the laboratory.

Additionally, the outside temperature, the temperature in the laboratory and the relative humidity were recorded in order to illuminate eventual influences on the $CO_2$-content (Diagram 4-31).

### Ambient Air led through 2.0 M $KHCO_3$ solution

In a further experiment air was conducted through a washing bottle with a 2.0 M $KHCO_3$ solution (Diagram 4-32).

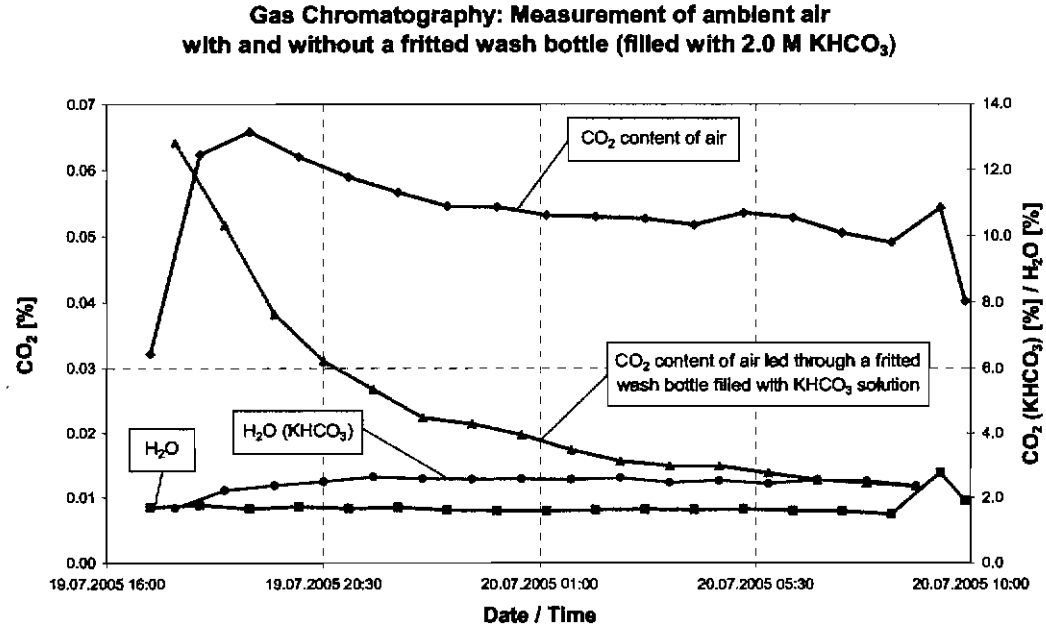


**Diagram 4-32:** GC-measurement on $CO_2$-absorption in a $KHCO_3$ solution.
Ambient air was supplied to the GC alternately directly or through a fritted wash bottle filled with 2.0 M $KHCO_3$ solution. The $CO_2$ content and the $H_2O$ content of the air was measured during the experiment.

The measurement values of the $CO_2$-content of air are in the same range as the ones measured in other experiments. The first values of this measurement curve are very low, so that it can be assumed that these values are measurement errors, whereas the measurement curve of the $CO_2$-content of the air conducted through the washing bottle exhibits an unexpected progression. The values measured at the beginning are very high but also decline very rapidly with time. Nevertheless, even the later values are clearly above the measurement results of the $CO_2$-content of air; in the progression of the measurements they converge to a value of 2 %. Similar to previous experiments a higher water proportion in the sample was measured which was due to conducting the air through the washing bottle.

### Ambient Air led through 7.0 M KOH solution

A concluding experiment was initiated in the series of GC-measurements, where ambient air was conducted through a washing bottle with a 7.0 M potassium hydroxide solution. The measurement results are presented in Diagram 4-33.

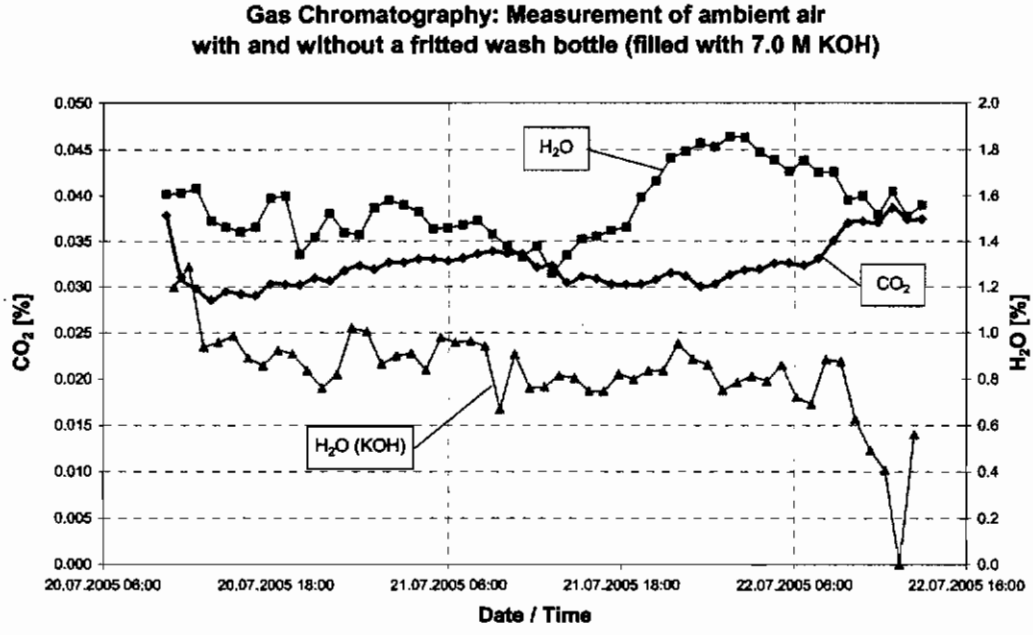


**Diagram 4-33:** GC-measurement on $CO_2$-absorption in potassium hydroxide solution. Ambient air was supplied to the GC alternately directly or through a fritted wash bottle filled with 7.0 M KOH solution. The $CO_2$ content and the $H_2O$ content of the air was measured. In the air conducted through the wash bottle no $CO_2$ was detectable.

In case the air was conducted through the washing bottle the GC could not detect any $CO_2$ in the probe. The values for the $CO_2$-content of air are slightly lower than in the previous measurements, but their range is around the average $CO_2$-content of air, which is 0.035 %.

Different from the previous measurements the results for the water contents showed in the analysed samples. The values for the air which was conducted through the washing bottle were significantly lower than for the directly measured air.

## Ambient Air led through de-ionised Water

Apart from the experiments with electrolytes in the washing bottle another experiment with de-ionised water in the washing bottle was carried out.

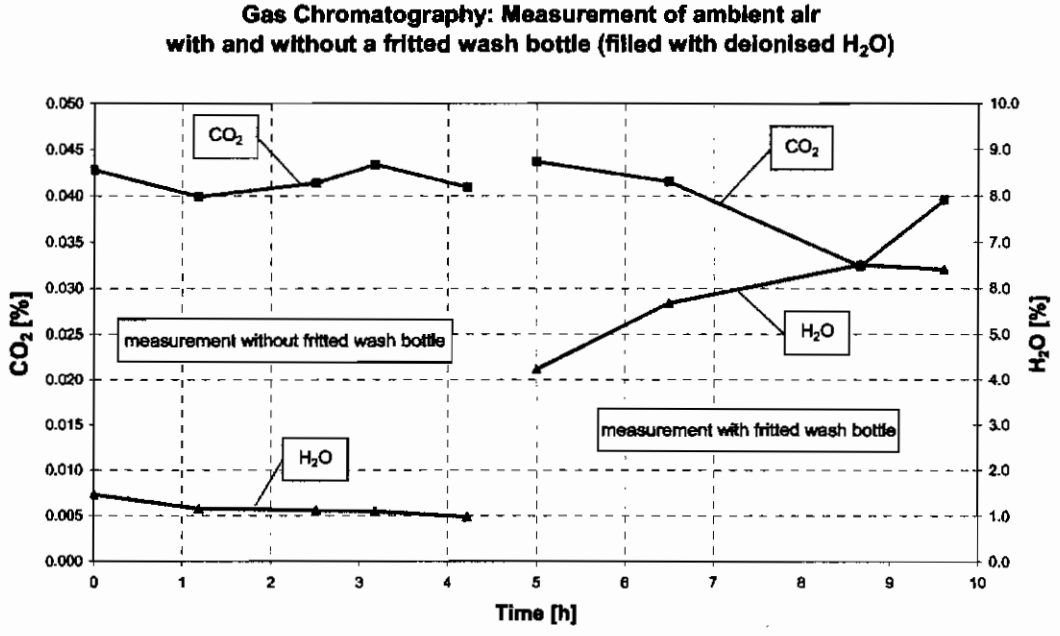


**Diagram 4-34:** GC-measurements on $CO_2$-absorption in de-ionised water

In case the air was conducted through a washing bottle with de-ionised water the measured $CO_2$-content decreased only marginally, whereas the water content of the sample increased. When conducting the air through the washing bottle the air could have absorbed water. This means that $CO_2$ could also be dissolved in the water vapour which is removed by the air. With the selected settings of the GC it might be possible that $CO_2$ dissolved in water passed the GC without being detected.

## 4.5 Diffusion Measurement

Table 4-5 shows the results of the diffusion measurement carried out to examine the transport properties of carbonate. Two oxygen electrodes with different catalysts were tested. Electrode #418 was manufactured using silver oxide ($Ag_2O$) as catalyst. Electrode #366 is a remake of the Silflon electrode which was used to build Fuel Cell 0096. Here Silflon is used as catalyst.

| Diffusion Measurement KOH/$K_2CO_3$ | | | | |
|---|---|---|---|---|
| Electrode | Before Measurement | | After Measurement | |
| | $c_S$ (KOH) | $c_S$ ($K_2CO_3$) | Carbonate content in KOH | $c_E$ ($K_2CO_3$ in KOH) |
| | [M] | [M] | [g/l] | [M] |
| **#418 Oxag** | 6.73 | 3.39 | 10.01 | 0.072 |
| **#366 Silflon** | 6.77 | 3.43 | 51.52 | 0.370 |

**Table 4-5:** Results of the diffusion measurement of two oxygen electrodes carried out to examine the carbonate transport

Both electrode samples were mounted in the test cell for the diffusion measurement. The electrode sample separates the two compartments of the cell. At the beginning of the experiment one compartment was filled with 7.0 M KOH solution, the other compartment was filled with 3.5 M $K_2CO_3$ solution. The start-concentration ($c_S$) of the electrolytes was determined by titration. When the experiment was finished, the electrolyte concentration was determined again. Also the carbonate content in the KOH solution was determined by titration ($c_E$).

The values of the measurement show that electrode #366 enabled a higher rate of carbonate transport by diffusion. The transport rate of electrode #418 was 5.15 times smaller.

## 4.6 Titration

During this research work acid-base titration was used to determine the carbonate content as well as the carbonate and hydroxide content of the electrolyte. For each analysis the titration unit Dosimat 665 (company Metrohm) was used.

### Titration Method

Carbonate reacts with an acid according the exemplary equation:

$$Na_2CO_3 + 2HCl \rightarrow 2NaCl + H_2O + CO_2 \uparrow \qquad \text{Eq. (4-1)}$$

In solution the base $CO_3^{2-}$ reacts with acid following the equation $CO_3^{2-} + 2H_3O^+ \rightarrow 3H_2O + CO_2 \uparrow$ (Eq. 4-2). Carbonate can be titrated directly using an acid, just like hydroxide. The determination is made with methyl orange as the indicator.

For the determination of hydroxide and carbonate the method of Winkler [4-1] was used. First the total alkali content (hydroxide and carbonate) in the base was determined by titration with methyl orange as the indicator. In a second sample the carbonate ions were precipitated by adding barium chloride: $K_2CO_3 + BaCl_2 \rightarrow 2KCl + BaCO_3 \downarrow$ (Eq. 4-3). In a next step the hydroxide which was still dissolved was titrated with oxalic acid ($c(C_2H_2O_4) = 0.05\ M; 0.1\ N$) and phenolphthalein as the indicator. The amount of oxalic acid used for the titration gave the mass of alkali metal hydroxide. The difference between the total alkali content and the content of hydroxide gave the mass of carbonate [4-2].

## 4.7 Other Quantities

The following table presents the composition of the oxygen electrodes that were used during the research.

| Electrode Composition | | | | | |
|---|---|---|---|---|---|
| **Electrode** | **Catalyst** | **PTFE** | **Activated carbon** | **Graphite** | **Pore builder** |
| #165 | 95 % Silflon | in catalyst | 5 % | - | 80 % |
| #249 | 100 % Silflon | in catalyst | - | - | 80 % |
| #355 | 100 % Silflon | in catalyst | - | - | 80 % |
| #366 | 85 % Silflon | in catalyst | 10 % | 5 % | - |
| Silflon (BZ 0096) | 85 % Silflon | in catalyst | 10 % | 5 % | - |
| Oxag 260202 | 90 % $Ag_2O$ | 5 % | 5 % | - | - |
| #461 (Oxag) | 90 % $Ag_2O$ | 5 % | 5 % | - | - |
| #418 | 85 % $Ag_2O$ | 10 % | 2 % | 3 % | - |

**Table 4-6:** Composition of some selected oxygen electrodes

# 5 Discussion of the Measurement Results

In this chapter the measurement results of the experiments presented in Chapter 4 are discussed. Initially, the half cell tests are covered which primarily served the examination of the basics and the selection of the electrodes. This is followed by a discussion of the results with the fuel cells and the measurements with the gas chromatograph.

## 5.1 Half Cell Tests

### 5.1.1 Long-Run Test with Permanent Load and "Pulsed Load"

The results of the long-run measurement with the half cell were a fundamental turning point in the progression of this project. Over the 5400 hours duration of the experiment with oxygen electrode #50 operated with air no significant decline of the performance could be detected. The electrode was loaded with a fixed current of 100 mA/cm² in steady state mode. The electric potential measured versus a hydrogen reference electrode (HRE) declined by circa 10 % (start: circa 700 mV, end: circa 730 mV) over the measurement duration. It can be assumed that the decline was caused by the formation of potassium carbonate in the electrolyte and hence a decrease in the conductivity. As a matter of fact the electrode was not damaged by the carbonate. After changing the potassium hydroxide solution the electrode was operated for another 1000 hours with pulsed load and achieved even better results compared to the previous test. In case the decline of the electric potential during the first experiment had been caused by parts of the pore system being congested by carbonate, the improvement cannot be explained by the change of the electrolyte. If the carbonate crystallises it cannot be simply washed out of the pores again. A simple explanation for this behaviour is, however, closely related to the formation of potassium carbonate. The formation of potassium carbonate due to the introduced $CO_2$ causes a decrease in the concentration of $OH^-$ ions in the electrolyte and hence a decline in the conductivity. Exchanging the electrolyte would eliminate this effect, which was

confirmed by the experiment. Further attempts to explain this found in the technical literature indicate a reduction of the active area and increasing transport restriction as the cause of the decline of the electrochemical performance. The aging and disintegration of the PTFE is also given as a possible cause [5-1].

With this observation it appeared possible to operate the AFC with unfiltered air without an electrolyte regeneration process. Therefore, the development work for an electrodialysis cell were discontinued as this procedure is too laborious when solely used for the extraction of the reaction water

During the literature review it became clear that other institutes also came to this conclusion. Apparently, certain electrodes are not damaged by the formed carbonate. As an example the research of the DLR is mentioned here [5-2]. Different from the presented research the $CO_2$-content of the supplied air was additionally increased. On the one hand it can be concluded that some electrodes can operate under even worse conditions. On the other hand increasing the $CO_2$-content could also falsify the measurement in so far as this does not correspond to real conditions. For this reason it was decided to carry out all experiments with ambient air as this is also closer to the intended application.

Further long term experiments were carried out in a half cell with different oxygen electrodes. Two oxygen electrodes with Silflon-catalyst (#165 + #355) and two oxygen electrodes with silver oxide ($Ag_2O$) catalyst (Oxag 260202 + #418) were investigated. During the measurement a problem occurred with the technical measurement equipment. The computer crashed and for indefinite time the electrode samples were loaded with 500 $mA/cm^2$. The electrode samples could be operated subsequently but it was not clear if they suffered damage of that operating failure. Because of the long duration of these tests the experiment was not repeated. For that reason the experiment is only discussed in terms of the carbonate formation in the electrolyte and the electrodes respectively. After each measurement series the electrolyte used as well as the electrode itself were examined with regards to their carbonate content. The carbonate measurement was done by titration. This is very easy to do for the electrolyte. After an

operation time of 1000 hours with a load of 50 mA/cm² the measurements resulted in a carbonate content of circa 50 g/l in the potassium hydroxide solution. However, in the 7.0 M potassium hydroxide solution used for the tests circa 15 g/l carbonate were already measured despite the fact that the solution was stored in a sealed container. All values for the carbonate content were measured by titration. The analysis of the carbonate contents in the electrodes was more laborious and was hence only carried out after the completion of the measurements. The electrodes were extracted from the cell, dabbed and weighed. Following this, they were soaked in "$CO_2$-free", de-ionised water in order to flush out the electrolyte from the electrode. To support this process the sample was placed in an ultrasonic bath. After this treatment the electrode was reweighed and the weight difference was used as the basis for further calculations. Then the carbonate content of the solution was determined by titration. In the following table some basic values for the calculation of the carbonate content of the electrolyte stored in the electrodes are presented.

| Electrode | Volume of the flushed sample | Carbonate content in the flushed sample | Electrolyte Volume in the Electrode |
|---|---|---|---|
| #418 | 60 ml | 0.414 g/l | 0.064 ml |
| Oxag | 80 ml | 0.529 g/l | 0.074 ml |

**Table 5-1:** Base values for the calculation of the carbonate content of the electrolyte stored in the electrodes operated in the half cell. The carbonate content in the flushed sample was measured by titration. Electrolyte Volume stored in the electrode is calculated based on the weight difference of the electrode sample before and after it was flushed in de-ionised water. For the conversion of the weight into volume the density at 25 °C of the electrolyte 7.0 M KOH solution of $\rho_{KOH} = 1.29$ g/ml was used.

The calculation of the carbonate content of the electrolyte stored in the electrode #418 is shown below:

$$Carbonate\ Content\ \#418 = \frac{60ml}{0.064ml} \cdot 0.414 \frac{g}{l} = \underline{\underline{388 \frac{g}{l}}} \qquad \text{(Eq. 5-1)}$$

From the calculations for the mass flushed from the electrode a carbonate content of 390–570 g/l for the electrolyte in the different electrodes resulted. Up to then, the run-time was also 1000 hours at 50 mA/cm² in operation with unfiltered air. However, these values have to be seen critically as they rather state orientation values. It is, for instance, not proven, that a complete exchange took place of the electrolyte in the electrode with the solution to be analysed. The calculated values for the carbonate content in the analysed electrodes are in the range of the experimentally determined solubility limit for $K_2CO_3$ in 7.0 M KOH, which is 461 g/l (at 25 °C) [5-3]. It can, however, be assumed that the carbonate remained in solution, since the concentration of the electrolyte KOH in the electrode was circa 1.0 M (measured by titration). At this concentration the solubility limit is significantly higher (compared with the solubility limit of $K_2CO_3$ in water, which is 1135 g/l at 25 °C) [5-4]. Under those conditions the solubility limit would not yet have been exceeded.

In order to further refine the observations of the long-run test in the half cell, in a further step fuel cells with suitable electrodes were manufactured and operated with unfiltered air.

### 5.1.2 I/V-Characteristics of the Oxygen Electrodes

For the selection of suitable electrodes again experiments with the half cell were used. The current/voltage characteristics were recorded and the electrodes were operated under various conditions:

- different electrolytes: KOH, KOH/$K_2CO_3$ 50:50, $K_2CO_3$
- different temperatures: 20 °C and 50 °C

In order to be able to compare the results each test was carried out with unfiltered air as well as with pure oxygen.

#### Effect of Temperature Variation on the Oxygen Electrode

As expected, it became apparent that a higher operating temperature improves the performance. All electrodes exhibited higher measured electric potentials at the same current when the temperature was increased. Higher temperatures enhance

the reaction as the activation energy is reduced. An operating temperature of 50–60 °C would hence be recommended for the cell. The slope of the linear range of the recorded measurement curve is a measure of the capacity of the electrode. The steeper the slope the smaller is the decline of the potential at a higher current. The intersection of this line with the x-axis is then the "actual" resting potential of the electrode. Comparing the experiments where only the temperature was modified, while the electrolyte and the gas supplied were kept the same, showed that also the slope of the measurement curve mostly stayed the same. The measurement curves were merely shifted (in parallel) towards higher electric potentials. This behaviour was exhibited by the tested Silflon-electrode in fuel cell 0096 (see Diagram 4-3). In case the slope becomes steeper with increasing temperature it can be assumed, that apart from the influence of the temperature other limiting factors are present. This can be explained with the electrode properties. If the electrode is too hydrophilic, a strong wetting of the electrode with the electrolyte inhibits a sufficient gas supply. In case the electrode is too hydrophobic, as small gas overpressure is sufficient to drive the electrolyte out of the electrodes. In both cases the capacity of the electrode declines. For electrode #249 it can be stated that due to its composition the electrode is very hydrophobic. Caused by the high contents of pore builder a very porous structure is established during the manufacturing. A small overpressure of circa 20 mbar is sufficient to drive the electrolyte KOH out of the pore system.

**Influence of the $CO_3^{2-}$ Content of the Electrolyte**

It is clearly visible that the slope of the measurement curves partly change dramatically, if a mixture of KOH and $K_2CO_3$ or a pure $K_2CO_3$ solution is used instead of KOH. This is caused by a lowering of the electrolyte conductivity. Calculations were made for the theoretical voltage drop in the half cell caused by the different conductivities of the electrolytes used. The values of conductivity were measured with a conductivity meter "Konduktometer 703" from company Knick, Germany.

Calculation of the theoretical Voltage Drop for 7.0 M KOH at I = 100 mA/cm²:

$$V_{Drop,KOH} = I \cdot R = I \cdot \frac{1}{\kappa} \cdot \frac{l}{A} \qquad \text{(Eq. 5-2)}$$

$$V_{Drop,KOH} = 0.314\ A \cdot \frac{1}{0.8208}\frac{cm}{S} \cdot \frac{0.1\,cm}{3.14\ cm^2} = 0{,}0122\ V \qquad \text{(Eq. 5-3)}$$

where:

| | | |
|---|---|---|
| $V_{Drop,KOH}$ : | voltage drop for electrolyte KOH |
| $I$ : | current in A |
| $R$ : | resistance in Ω |
| $\kappa$ : | electrical conductivity in S/cm |
| $l$ : | total length of the conductor in cm |
| $A$ : | cross-section of the conductor in cm² |

The following table provides an overview of the values for the electrical conductivity (at 20 °C) and the theoretically resulting voltage drops in the half cell for the corresponding electrolytes:

| Electrolyte | Conductivity | Theor. Voltage Drop | ΔV for 7.0 M KOH |
|---|---|---|---|
| | [mS/cm] | [mV] | [mV] |
| 7.0 M KOH | 820.8 | 12.2 | - |
| KOH + $K_2CO_3$ (50:50) | 559.2 | 17.9 | 5.7 |
| 3.5 M $K_2CO_3$ | 251.0 | 39.8 | 27.7 |

**Table 5-2:** Overview of the electrical conductivity (at 20 °C) and the resulting voltage drop in the half cell experiments for different electrolytes. Electrical conductivity was measured with a conductivity meter (Konduktometer 703, Knick, Germany). Current density for the calculation: I = 0.1 A/cm². In addition the differential voltage to the values of 7.0 M KOH are presented as well.

The effect of the voltage drop may have quite significant consequences in the half cell; however, in the actual fuel cell the consequences are not quite as severe, as the distance between the electrodes is small. Admittedly, the conductivity of the

electrolyte also influences the penetration, i.e. the regions of the electrodes which are mainly involved in the electrochemical reaction. In case the conductivity declines (and thus the activation polarisation resistance) the penetration also declines. This equals a reduction of the active reaction zone and the capacity of the electrode deteriorates [5-5]. This explains the poor measurement results of electrode #249, as represented in Diagram 4-4. In the half cell experiment with 3.5 M $K_2CO_3$ the achieved values are significantly worse than for electrodes with the same catalyst. This shows that the penetration is also influenced by electrode properties such as the porosity. The electrode Silflon (FC 0096) with the same Silflon-catalyst, but an otherwise different composition, exhibits much better results in this experiment (see Diagram 4-5). However, the steeper slope of the measurement curve for a higher load with this electrode from the experiment with 3.5 M $K_2CO_3$ cannot be explained with these considerations. A possible explanation is the wetting of the electrode, or rather of the catalyst. It is not sufficient to determine how much electrolyte was absorbed by the electrode, since this does not yield with certainty how much electrolyte was actually in contact with the catalyst, i.e. the reaction zone. Currently a method is under development to determine the ion exchange capacity (IEC) using titration. This is meant to allow conclusions with regards to the wetting of the catalyst. At the current state, however, the measurement results cannot be considered reliable yet.

**Comparison air operation/ oxygen operation**

Losses also have to be accepted when changing from oxygen operation to air operation. This is caused by the fact that the electrode is not sufficiently supplied with oxygen. The other constituents of air can act as inert gases and thus partly block the access to the reaction zones of the electrode; the gas diffusion is hence inhibited. Another factor which can also have a negative effect on the performance of the electrodes for air operation is the higher gas flow rate compared to the operation with pure oxygen. The higher flow rate results in a higher gas pressure thus changing the operation conditions for the electrode. The measurement results of this experiment are presented in Diagram 4-6. It is also possible, that the

electrodes dry out due to the high gas flow rate. An increase in concentration of the potassium hydroxide solution due to the extraction of water can result in damages. Initially, this would lead to an enhanced corrosion and can finally result in precipitation of potassium hydroxide crystals, which would also block the porous structure of the electrodes.

Similar experiments were carried out with oxygen electrode #461 which contained silver oxide as the catalyst. Diagrams 4-7 to 4-9 show the measurement results of the experiments with electrolytes with a varying carbonate content. The electrodes were each supplied with pure oxygen and with unfiltered air respectively, both at a low and an increased temperature. This electrode type also exhibited the already mentioned effects. The decline of the temperature influence for higher carbonate concentrations in the electrolyte for oxygen operation is clearly visible. As already mentioned the temperature influences the conductivity of the electrolyte. The conductivity, in return, influences the penetration. These factors all influence the performance of the cell. It is also noteworthy, that the measurement curves are flatter when operating with unfiltered air. This shows very clearly, that there is a problem with the gas supply. The amount of oxygen required to maintain a certain adjusted current cannot diffuse into the reaction zones in the electrode. This behaviour can be described as critical-current behaviour. It is also very distinctive in Diagram 4-11. Here, electrode #461, pretreated with $K_2CO_3$, cannot be loaded above a current density of circa 100 mA/cm² without significant losses, even when operated with pure oxygen. In order to verify the findings the experiment was repeated, with, however, even poorer results. Diagram 4-12 shows the results of the long-term measurements with electrode #461. The electrode was loaded with 50 mA/cm² while the carbonate content in the electrolyte was varied. For the operation pure oxygen and unfiltered air were used alternately. The electric potential decreases with an increasing carbonate content, which can be explained by the conductivity and the penetration. The difference between the operation with oxygen and with air is clearly visible. Here, the decline in capacity for air operation is also due to insufficient oxygen supply.

The formation of carbonates in the electrolyte became very clear during the half cell experiments. Since this effect also occurred during the operation with pure oxygen, it can be assumed that the introduction of $CO_2$ did not or not only take place via the supplied oxidants. The effect is rather due to the construction of the half cell. The electrolyte volume is very small and the container is open to the atmosphere. The gas development at the counter electrode also seems to influence the $CO_2$-absorption (compared to stirring the electrolyte). However, the electrodes did not suffer damages due to this and changing the electrolyte resulted in a performance like the initial performance. Therefore, different half cells were used for the long-run tests, featuring a larger electrolyte volume which did not have direct contact with the ambient air. It should be noted, that depending on the set-up of the system even for conventional operation of the AFC with pure gases the formation of carbonate has to be anticipated, which could be confirmed with measurements [5-6].

### 5.1.3 Experiments with pretreated Oxygen Electrodes

The half cell tests with previously carbonated oxygen electrodes yielded interesting results as well (Diagram 4-13 and 4-14). This experiment was carried out to show the influence depositing potassium carbonate, potassium hydrogen carbonate and potassium hydroxide on the electrodes. As a comparison an untreated electrode sample of the same lot and same consistency was tested. There was no visual difference between neither the untreated nor the pretreated electrode or between the pretreated electrodes itself. Only when handling them did it became apparent that the pretreated electrodes were more brittle than the untreated. The tests showed that the electrodes previously soaked in carbonate solutions did not suffer any apparent disadvantages through this treatment. They could be loaded similarly and could be operated with constant results over the whole experiment duration. Contrary to this, the electrode treated with potassium hydroxide solution achieved comparatively poor values. The electrode also had to be exposed to a higher gas pressure. This observation could lead to the conclusion that the drying of the KOH is the actual problem and not the formation of

carbonate. This behaviour could be interpreted in the following manner: potassium hydroxide solution has a particularly high ability to creep. In case an electrode is soaked with KOH the catalyst grains become enclosed by the KOH like a film. During the drying a hard crust of potassium hydroxide is formed. It is also possible that KOH itself intrudes into rather hydrophobic regions, i.e. into the gas pores. There, hydroxide-ions are deposited. Potassium hydroxide is very hygroscopic. The electrode tends to "drown" when it comes in contact with liquid electrolyte. In order to clear the gas pores of the electrode a higher gas pressure is required. However, even then it is not ensured that the electrode will be supplied sufficiently with reaction gas. An explanation for the initially very poor values would be the certain time that is required to dissolve the crusts until gas as well as electrolyte can reach the reaction zone. The lower electric potential can be seen as evidence that it was indeed not possible to clear all gas pores from the electrolyte thus resulting in a loss of reaction zones. Another effect also caused by the drying of the potassium hydroxide solution could be the reason for the effect. Due to the drying the concentration of the potassium hydroxide solution increases, the water evaporates leaving solid potassium hydroxide. The higher the concentration of the solution increases the higher the corrosive effect on the electrode, which can finally lead to the total destruction of the electrode. Diagram 5-1 shows the mean activity coefficients of potassium hydroxide solution at different concentrations [5-7].

The progression of the curve clearly shows that the activity of the potassium hydroxide solution increases disproportionally quickly in the range used for the experiments. In operation and in particular during the drying process of the electrodes the initial concentration of 7.0 M rapidly increases to a significantly higher concentration. In theory, a fuel cell loaded with 1.0 A and in which no matter transport takes place would exhibit a KOH concentration of over 20.0 M after only circa 35 minutes [5-11].

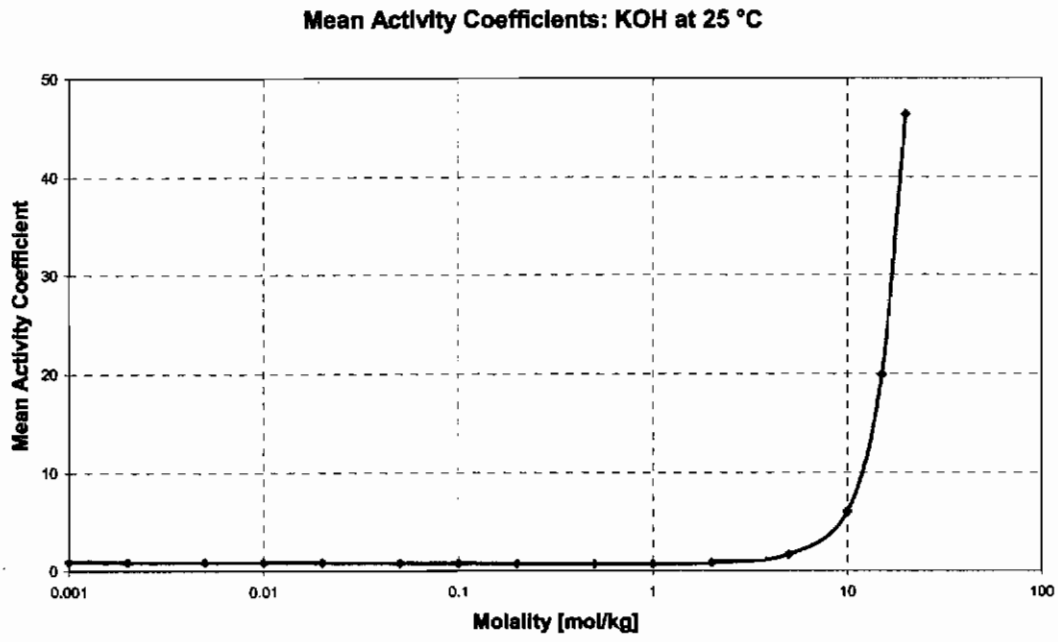


**Diagram 5-1:** Mean Activity Coefficients of KOH at 25 °C as a function of the molality

In this range, particularly under the influence of an increased temperature, the potassium hydroxide solution is very corrosive and KOH could also precipitate. Therefore, an oxygen electrode was operated in a half cell with a 20.0 M potassium hydroxide solution in a further experiment. The electric potential dropped after a short time. After the completion of the measurement it could be seen, that particles were dislodged from the electrode.

Due to this the half cell measurements with pretreated electrodes was repeated again with the result, that the effect of the dried potassium hydroxide on the electrode as it occurred in the first experiment did not occur again (Diagram 4-14). It is noteworthy that the electrode pretreated with KOH delivered poorer results than the electrode from the same lot which was pretreated with $K_2CO_3$. The worst results for this experiment were delivered by the untreated electrode. It should be noted that not every electrode section delivers absolutely identical results which is due to the manufacturing process of the electrodes and the consistency of the individual constituents of the electrodes. The results of the four half cell measurements with one electrode type are in the range of circa 25–30 mV if the values of the electrode with the highest capacity are compared to the electrode

with the lowest capacity. The electrode exhibiting a significant performance drop after the drying of KOH originate from an older lot and where stored for several years. All other measurement results from the experiments are at a similar level as the electrodes with identical composition that were only produced recently.

The results of the half cell experiments indicate that the depositing of carbonate has no negative effects on the performance of the electrode. Material was actually deposited in the electrodes, which was verified by the embrittlement and the weight increase of the sample pieces. The titration of the electrolyte extracted from the electrodes also yielded an increased carbonate content. It is likely that during the filling of the half cell with potassium hydroxide solution the dried carbonate was dissolved again and could thus be flushed out of the electrode. With an according mass transfer the electrode will not suffer any damage from the carbonate, whereas the electrode can be severely damaged by drying potassium hydroxide solution. The drying process increases the concentration of the potassium hydroxide solution. This effect is stronger the purer the potassium hydroxide solution. The formation or introduction of carbonate decreases the KOH concentration, so that the concentration stays low even when drying. Above a concentration of 10.0 M the electrode is increasingly destroyed through corrosion which is an irreversible process. White precipitates visible externally were probably deemed to be carbonate in a premature judgement in earlier experiments. There is no visual difference between dried carbonate and dried potassium hydroxide. The question arises whether the commonly known carbonate problem of the AFC is probably based on a wrong assumption. It is, however, hard to believe that no-one would have tried to detect the carbonate. During the research for this thesis no sound references could be found in the literature describing such investigations. In the chapter about the $CO_2$-problem two references are given covering the formation of carbonate. This is stated as the cause for the performance decline of the fuel cell in one reference [5-8], while the other stated that it did not have any effect on the cell [5-9]. In the first case the fuel cell was operated from the start with a 12.0 M potassium hydroxide solution, which - according to the presented research - can already damage the electrodes

due to corrosion. Therefore, the results of this investigation have to be considered questionable from today's viewpoint.

Another indication of the corrosion problem being due to high concentrations of potassium hydroxide solution are indicated indirectly in the final year project report of J. Helmke [5-10], where a change of the catalyst surface is pointed out which occurs during the reduction of Silas-electrodes (Oxygen electrodes with silver catalyst and asbestos). This change is attributed to the different current strengths used for the reduction of the electrodes. Images of the electrodes taken with a scanning electron microscope clearly show the different structures of the electrodes. This effect could also be caused by corrosion due to the presence of different concentrations of the potassium hydroxide solution caused by different current strengths.

## 5.2 Experiments with the Fuel Cells

### 5.2.1 Fuel Cell 0068 - EF Fuel Cell 1x (4/2/2)

The first experiments with a fuel cell operated with air were carried out with a conventionally manufactured AFC which did not feature any adaptations for a larger gas flow rate (Fuel Cell 0068). Initially, it was noticeable that for high loads the recorded current/voltage characteristics exhibited a current drop for fixed voltages. This was initially explained with the hydrogen electrodes not being completely activated. Further examinations indicated, however, that the problem is due rather to the diffusion properties of the electrodes. The experiments and detailed results are presented in the work of G. Sauer [5-11]. The test results with fuel cell 0068 were quite promising in so far as the cell delivered a constant power over a span of more than 100 hours when operated with unfiltered air. However, the cell had a mechanical problem. In case the pressure difference between gases was too high the air supply was suppressed by the increasing $H_2$-pressure. This effect is presented in Diagram 4-17 in the ranges marked with |1|. For this reason this experiment will not be discussed in greater detail. It was, however, shown that the operation with air can be realised.

Further fuel cells were manufactured featuring an appropriate gas compartment between the oxygen electrodes thus ensuring the sufficient supply with air oxygen. It was also possible to work with a sufficient air excess which was particularly important for the experiments on the extraction of the reaction water. From the recorded current/voltage characteristics it can be seen that the cells did not have any faults initially and achieved a good performance.

### 5.2.2 Fuel Cell 0096 – EF Fuel Cell 1x (4/2/2)

The first fuel cell especially built for air operation featured an air distributor made of nickel foam (see Section 3.1.5). For the long-term measurement with air the cell was operated galvanostatically at 3.0 A. The overall experiment duration was slightly over 100 hours and during this time the cell voltage dropped by circa 50 mV. This behaviour is consistent with the results of the half cell measurements. During the long-term measurements also a decline of the cell voltage occurred which was explained with the drop of the electrolyte conductivity. This effect could be reversed by changing the potassium hydroxide solution. However, this did not succeed in the fuel cell which could be due to the more complicated construction resulting in a poorer mass transport.

The first experiments concerning the water in the cell were carried out by varying the temperature and the air flow rate. At the time of the experiment a continuous measurement data logging was not available. When the cell was operated with a fixed voltage of 0.75 V (~7.0 A) at 50 °C an increase of the electrolyte fluid level was observed, even for such high flow rates of 12 sl/h ($\lambda$=8). Accordingly, the concentration of the potassium hydroxide solution declined. Increasing the flow rate to 30 sl/h ($\lambda$=20) lowered the fluid level and the concentration increased. Since the concentration increased above the initial concentration the gas flow must have extracted more water than was produced in the cell during operation. With the heating switched off it was found that the high gas flow cooled down the cell thus resulting in a lower performance.

After a certain operating time without any noticeable problems and with a constant power delivery a decline of the current at a fixed voltage could be observed. This behaviour is thought to have the same causes as were observed in the half cell experiment with electrodes previously soaked in potassium hydroxide solution and then dried. After an initial long-run measurement over a circa 150 h period the fuel cell was switched off in between the experiments. The gas supplies were also disconnected from the fuel cell. As a possible consequence the fuel cell could become completely soaked with KOH. This process is accelerated by using a special method to shut down the cell. For this the oxygen supply is closed off and the cell is supplied only with hydrogen until no current is delivered any more. This method was used to prevent oxygen to intrude into the hydrogen side thus oxidising the $H_2$-electrode during the inactive state. However, from today's viewpoint this method is totally unsuitable and should not be used any more. Although the electrode of the tested fuel cell had not been dried as in the half cell experiment it has to be assumed that the pore system was nevertheless completely flooded with KOH. This enabled the hydroxide ions to even be deposited in the otherwise hydrophobic regions. If the electrode then gets in contact with electrolyte again previously hydrophobic, electrolyte rejecting gas pores could now be flooded with KOH. If gas cannot reach these regions a reduction of the triple-phase boundaries necessary for the reaction is caused. The electrode performance then drops or in the worst case the electrode could be destroyed. In principle it should be possible to press the electrolyte from the gas pores using a high gas overpressure. However, in particular for air operation with a gas compartment this is not possible as the air flow at the outlet would have to be reduced. Due to the low oxygen portion in air this method would very soon interrupt the supply of fresh oxygen.

To repair this damage the cell was taken from the test stand and the gas compartment was flushed with distilled water. This was also meant to flush the electrodes. The idea was to remove the hydroxide ions in this manner which otherwise would "drown" the electrode. Following this the cell was dried in an oven. The intention was, that the hydrophobic gas pores in the completely dried

electrode would be totally free of fluids and that the initial pore distribution would thus have been restored when restarting. It was, however, not possible to reach the initial performance values with this method. Moreover, a separator was damaged during the drying procedure in the oven. This is another proof that it is not possible to flush the cell or its components respectively in such a way that all deposited ions are removed.

A further effect which occurred over time was a decrease of the gas permeability of the air distributor. Occasionally the gas supply to the electrode was completely disrupted. This problem could initially be solved by changing the direction of the gas flow and later by flushing the gas compartment with de-ionised water. In order to investigate the cause the gas compartment was rebuilt in a simple set-up and supplied with air. If previously potassium hydroxide solution was conducted through the nickel foam then the hydroxide was now dried by the air flow. In the supply channel towards the air distributor and in the nickel foam itself, soon white deposits could be seen which decreased and eventually stopped the flow rate (see Figure 5-1).

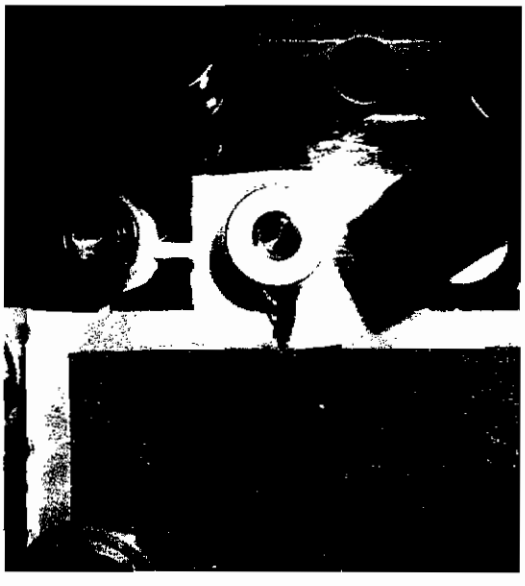

**Figure 5-1:** Gas supply channel blocked by crystals of dried up KOH solution.

The formed crystals were analysed and identified to be potassium hydroxide and not the suspected carbonate deposits as assumed in previous analysis. This finding led to the assumption that also in previous analyses dried potassium hydroxide was wrongly thought to be carbonate.

### 5.2.3 Fuel Cell 0101 - EF Fuel Cell 1x (4/2/2)

The control of the water flow of the fuel cell was more difficult than anticipated. As presented in Chapter 4, fuel cell 0101 was used for experiments to extract the water of reaction using the air flow as a function of temperature (see Diagrams 4-21 to 4-23). For these experiments the weight increase of the electrolyte caused by the water of the reaction was measured. Here the results are presented again in addition with the theoretical weight increase of the KOH solution calculated by using Faraday's Law:

$$m = \frac{I \cdot t \cdot M}{z \cdot F} \qquad \text{(Eq. 5-4)}$$

where:

- $m$: mass in kg
- $I$: current in A
- $t$: time in s
- $M$: molar mass in kg/kmol
- $z$: number of electrons
- $F$: Faraday-Constant $F = 96484{,}56 \frac{C}{mol}$

If the measured weight increase is lower than the theoretical (calculated) weight increase the water of reaction was extracted by the air flow.

The experiments were conducted at temperatures of 30 °C, 40 °C and 50 °C during the long term measurements with unfiltered air. The cell was loaded with a fixed current I=3.0 A.

## Long-term measurement with Fuel Cell 0101 operated with air at 30 °C

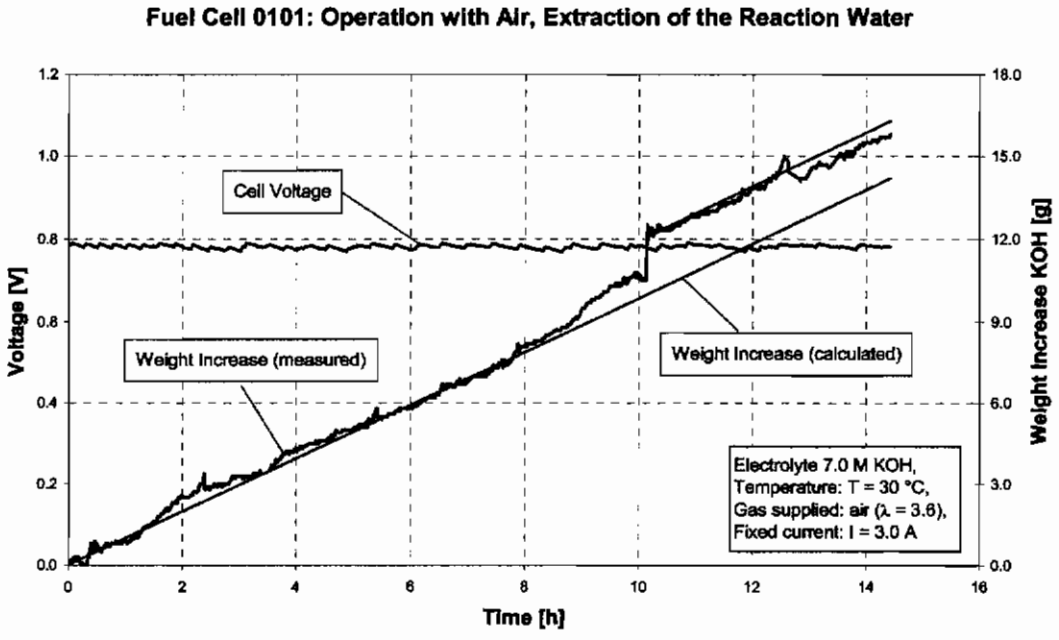


**Diagram 5-2:** Fuel Cell 0101 – long-term measurement with air at 3.0 A and 30 °C

## Long-term measurement with Fuel Cell 0101 operated with air at 40 °C

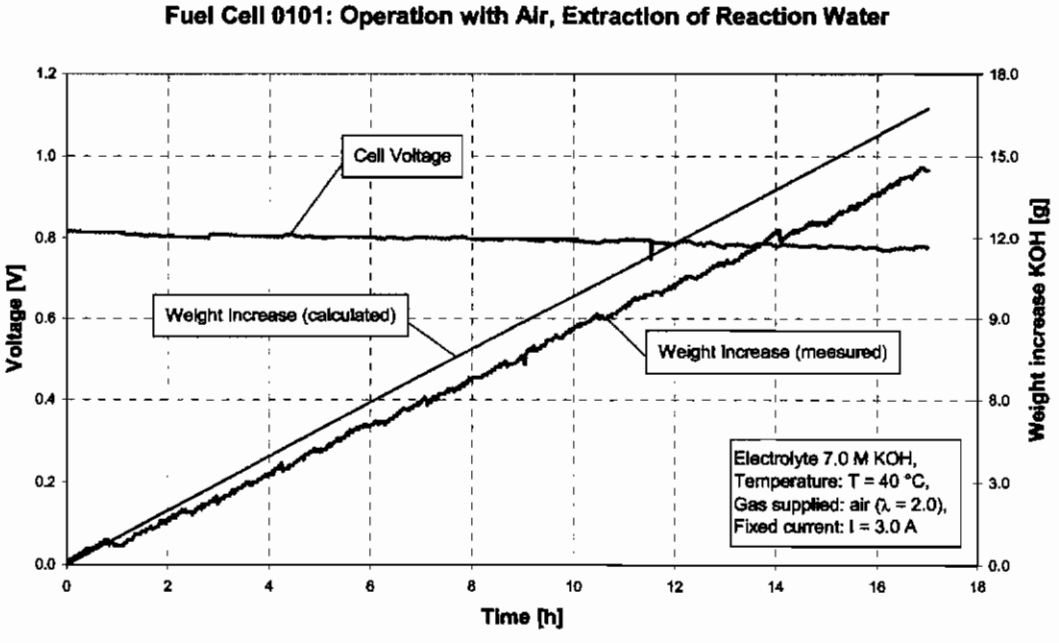


**Diagram 5-3:** Fuel Cell 0101 – long-term measurement with air at 3.0 A and 40 °C

## Long-term measurement with Fuel Cell 0101 operated with air at 50 °C

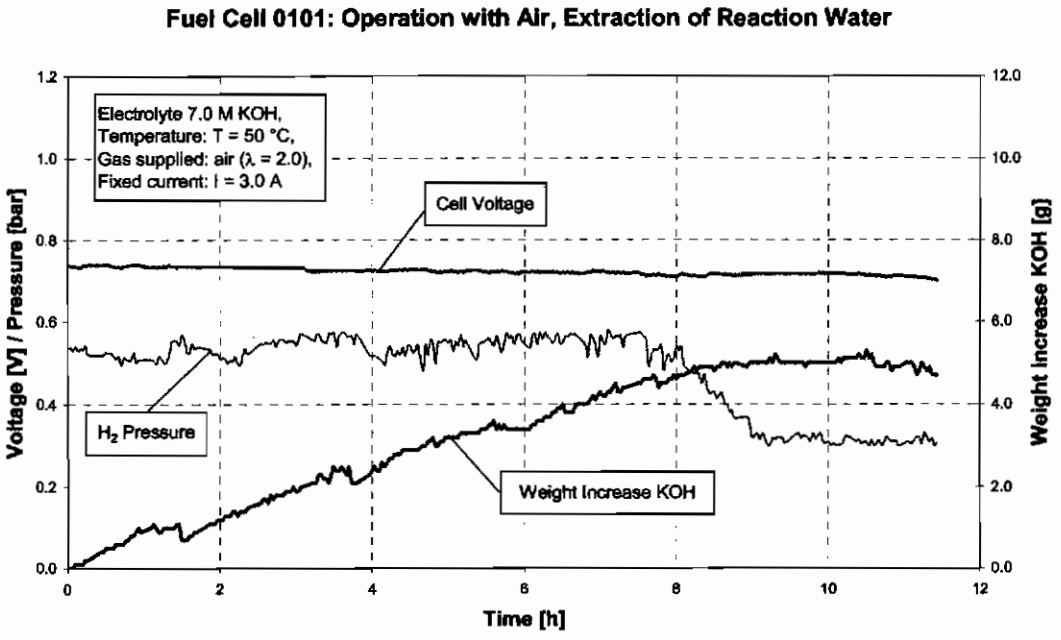


**Diagram 5-4:** Fuel Cell 0101 – long-term measurement with air at 3.0 A and 50 °C

## Repetition of the long-term measurement at 50 °C

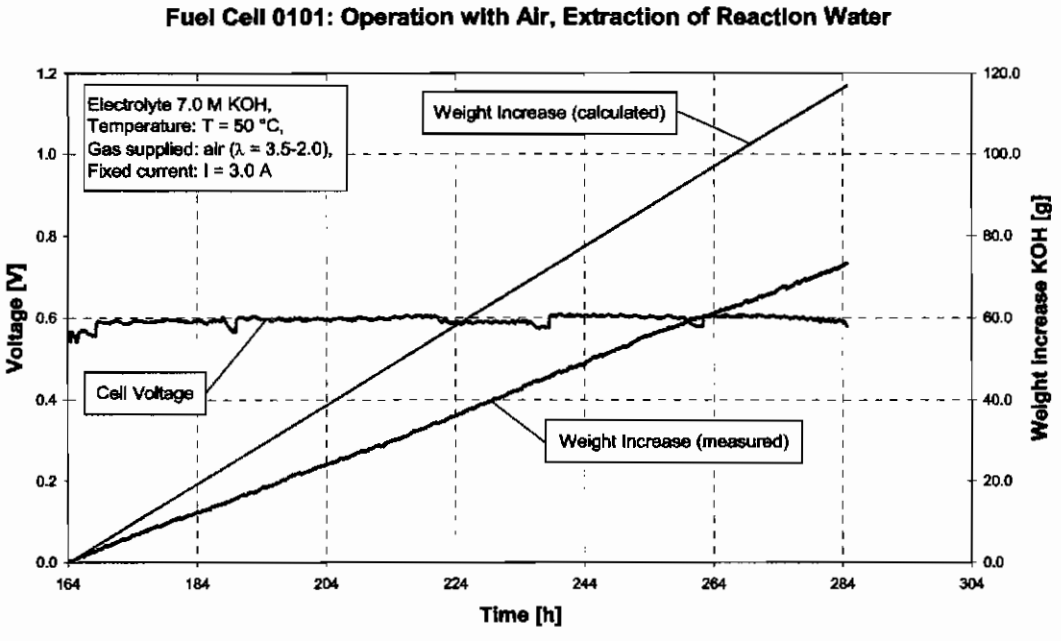


**Diagram 5-5:** Fuel Cell 0101 – repetition of the long-term measurement with air at 3.0 A and 50 °C

The experiment at 30 °C shows that the reaction water was extracted from the cell entirely via the electrolyte (Diagram 5-2). The step at a run time of about 10 hours was caused by accident. An electrolyte tube came to lie on the scale. As it did not change the conclusion of this experiment, the measurement was not repeated.
At an operating temperature of 40 °C a portion of the reaction water was already extracted via the air (Diagram 5-3); this portion was even larger in the experiment with an operating temperature of 50 °C (Diagram 5-4).
At a temperature of 50 °C the increase of the reaction water in the electrolyte progressed initially linearly; the progression of the curve was, however, flatter than in the theoretical consideration. From t=7.6 h onwards the hydrogen pressure declined and as a consequence of that no reaction water could be extracted via the electrolyte. This experiment was repeated again, since the decline of the $H_2$ pressure occurred by itself and was not intended. The results are presented in Diagram 5-5. The produced reaction water was still extracted to a 60 % extent with the electrolyte, while 40 % was extracted via the air flow. Due to the poor air flow rate the experiments were discontinued at that stage.

Although it was possible to increase the portion of the produced reaction water which was extracted from the cell via the air flow by increasing the temperature, the reaction water could not be completely removed via the air flow. On the one hand this is because the flow rate of air could not be adjusted to values larger than $\lambda=3.5$. The flow rate was limited and even input pressures of above 1.0 bar could not achieve an improvement. With an increasing operating time, however, the air flow rate declined more and more. This effect could not be corrected for during the measurements. In order to solve this problem the cell would have to be opened. It is possible that electrode material was displaced from the mesh or that resin intruded into the supply channel during the casting. From the beginning fuel cell 0101 had a poorer performance than the previously built fuel cell 0096 which can be explained with the modifications applied to the air distributor in the gas compartment.

The labyrinth-shaped frame (see Figure 5-2) inserted in the gas compartment to support the electrodes covers parts of the active areas. Even though it was ensured that the loss of active area was kept small, circa 25 to 30 % of the active area were covered. The assumption that gas could diffuse into the covered regions and also react there was proven wrong.

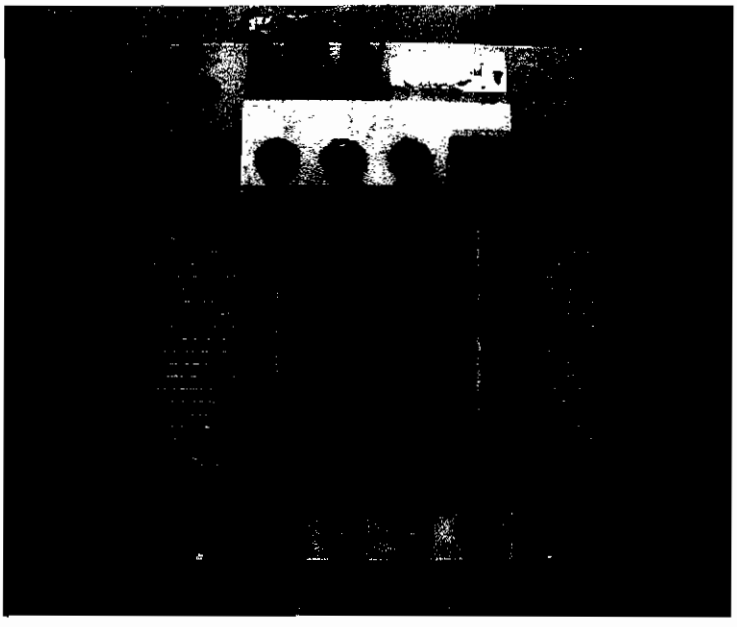

**Figure 5-2:** Gas compartment with labyrinth-shaped air channel used as an air distributor

Additionally, the pore system of the oxygen electrode could have been damaged when pressure-mounting the individual parts. It was nevertheless possible to carry out experiments at different temperatures in order to examine the influence on the extraction of the reaction water. At an operating temperature of 50 °C after all 40 % of the produced reaction water could be removed from the cell via the air flow. The remaining part was extracted from the cell via the electrolyte which was measured via the weight increase of the electrolyte. As already mentioned the measurements had a limited use in so far as the desired air excess (see Table 2-1) could not be adjusted.

A further observation of the experiments was the decline of the cell voltage over the experiment duration. At the beginning of the measurements the cell was operated with a fixed current of 3.0 A at a voltage of approximately 0.8 V. This value remained constant over a duration of 50 hours. However, with increasing

experiment duration the cell voltage decreased to approximately 0.6 V (at the same current) and remained constant at this level. Meanwhile the cell was not loaded for about 200 hours, so that the already mentioned effect of the electrodes being soaked with KOH could take place thus depositing hydroxide ions. It is also possible that during operation a very high KOH-concentration occurred in the electrode, so that parts of the electrode could have been destroyed through corrosion. The performance drop was in any case irreversible, even changing the potassium hydroxide solution did not restore the initial performance values.

In further experiments with a lower current density it was found that the produced reaction water inhibited the reaction inside the hydrogen electrode. For the operation at a room temperature of circa 22 °C the water of the reaction was removed from the cell via the electrolyte. The attainable cell power was, however, very low. It could be shown that by increasing the current density (which in return increases the temperature) and by increasing the $H_2$-flow rate the performance of the cell could be significantly improved. It could also be seen then that the reaction water was now removed from the cell via the hydrogen. This behaviour led to the conclusion that the electrodes employed caused problems for the water transport in the cell and therefore water extraction via the electrolyte was hindered [5-11].

## 5.3 Measurements with the Gas Chromatograph

Initially, basic data were collected with the gas analysis. The measured calibration values are for comparison and to verify the later measurement results from the fuel cell experiments. Experiments were carried out where ambient air was conducted through various electrolytes and through de-ionised water respectively. This was done to examine the $CO_2$-absorption of the different fluids. Depending on the time of the day and the weather conditions the $CO_2$-content of air exhibits fluctuations. The average value for the $CO_2$-content in air is 0.034 %. In order to carry out the experiments under realistic conditions the analysed air was taken from the ambient and not from the existing compressed air network. When

conducting the air through a washing bottle with a $K_2CO_3$ solution (Diagram 4-32) a smaller amount of $CO_2$ was measured with the GC than compared to the measurement of air without a washing bottle. The measured amount of water behaves reciprocally to that which is due to the fact that the air absorbs water from the $K_2CO_3$ solution. Through this mechanism $CO_2$ dissolved in the water could pass through the GC column without appearing in the measured results. Attempts to counteract this effect by varying the settings of the GC were attempted, but it is not possible to state with certainty that this succeeded. On the other hand the $CO_2$ in the air could have reacted with the $K_2CO_3$ solution ($KHCO_3$ + KOH) thus forming further carbonate in the solution. However, during the experiment a saturation did not occur and no carbonate precipitated. The carbonate content in the solution was measured before and after the measurement by titration. Over the experiment duration the carbonate content increased from 475.9 g/l to 497.7 g/l. Both values are clearly below the solubility limit of 1135 g/l (at 25 °C) for $K_2CO_3$ in water [5-4]. According to an approximating calculation the air volume flow through the washing bottle was circa 0.46 l/min over the experiment duration. This does not match with the real values as the adjusted air volume flow was only 0.07 l/min. The increase of the carbonate content is hence not only due to the absorption of $CO_2$ from the air. The detected water extraction from the solution caused an increase of the concentration.

In the following experiment the washing bottle was filled with de-ionised water (Diagram 4-33). Here, only a minor difference of the $CO_2$-content of the samples was measured, but an increase of the water portion in the sample conducted through the washing bottle could be detected. For this experiment it can also be assumed that the decrease of the $CO_2$-content was caused by $CO_2$ being dissolved in water. An analysis of the water by titration was not carried out as this experiment does not correspond to the typical fuel cell conditions. It was more important to see whether there were severe differences in the experiments with different electrolytes. In the next experiment air was conducted through a washing bottle with a 2.0 M $KHCO_3$ solution (Diagram 4-34). This measurement yielded a

different result. After the washing bottle much higher $CO_2$-values were measured than without the washing bottle and the $CO_2$-content approached a value of 2 % during the progression of the measurement. This effect could be explained if $CO_2$ escaped as a gas from the solution. It is also noteworthy that at the beginning of the measurement values of slightly above 13 % were measured, which declined quickly in the following measurements. In case a reaction takes place where $CO_2$ escapes from the solution it is possible that $CO_2$ accumulates in the washing bottle after the air was conducted into it and before the first sample was loaded into the GC. After a certain time an equilibrium is established and from then on the measurement results are at the same level. Similar to the experiment with $K_2CO_3$ solution a higher water content was detected when the air was conducted through the washing bottle. After the experiment the content of the washing bottle was examined by titration. The $KHCO_3$-concentration declined from the initial 2.0 M to 1.58 M. After the experiments a $K_2CO_3$-content of 0.24 M was measured. The last experiment in this series was done with a washing bottle with a 7.0 M potassium hydroxide solution (Diagram 4-35). In this experiment no $CO_2$ could be detected behind the washing bottle. It can be assumed that the entire $CO_2$ from the air had reacted with the potassium hydroxide. Different from the previously described experiments the water content after the washing bottle was now lower than without the washing bottle. It is commonly known that potassium hydroxide is used as a drying agent. In this respect this result can be explained with the strong hygroscopic properties of KOH.

In further experiments the exhaust gas of the fuel cell operated with unfiltered air was analysed. The analysis of the supplied air and the exhaust gas at the oxygen side yielded a different $CO_2$-content (Diagram 4-30). This result is to be expected when assuming that the $CO_2$ reacts in the fuel cell or rather in the electrode and thus does not leave the cell again. The most likely scenario would be the reaction with potassium hydroxide to form potassium carbonate. Further experiments yielded, on the other hand, that during the progression of a day quite different $CO_2$-concentrations of the air could be measured. The maximum deviation between two subsequent measurements ($\Delta t = 30$ minutes) was 17 % with respect to

the initial value. The following assumption could hold as well: $CO_2$ could be solved in the water vapour, which is absorbed by the air from the electrode when flowing through the gas compartment, and could pass the GC without being analysed. A wide range of different adjustments were performed with the GC; it was, however, not possible to find a solution confirming or contradicting the suspicion. It is thus difficult to make a sure statement about the fate of the $CO_2$.
The detection of $CO_2$ in the exhaust gas of the fuel cell at the hydrogen side (Diagrams 4-28 and 4-29) was on the other hand unusual. In the supplied hydrogen no $CO_2$ could be detected. It should be considered that only a very small amount of $CO_2$ was detected. Anyway, the question is where the $CO_2$ originated from. A crack in the separator could be the cause, but in this case $CO_2$ would have to be detected continuously at the hydrogen side. The fact that the pressure at the hydrogen side is higher than at the air side also contradicts this assumption. A fault during the measurement could also be the cause; despite the greatest care taken this cannot be totally excluded. During the literature research for this work indications were also found describing an occurrence of $CO_2$ at the hydrogen side not originating from the supplied gas. In a patent by J. Giner so-called carbonate and $CO_2$-transport mechanisms are described respectively [5-12]. The air supplied to the fuel cell was enriched with $CO_2$, while a saturated $K_2CO_3$ solution was used as electrolyte. For the cathode the following reaction equation is stated:

$$\tfrac{1}{2} O_2 + 2\,CO_2 + H_2O + 2e^- \rightarrow 2\,HCO_3^{2-} \qquad \text{(Eq. 5-5)}$$

The carbonate $CO_3^{2-}$ ($HCO_3^{2-}$) is now to be transported to the anode in the fuel cell by diffusion and migration; at the anode the following reaction takes place:

$$H_2 + 2\,HCO_3^{2-} \rightarrow 2\,CO_2 + 2\,H_2O + 2e^- \qquad \text{(Eq. 5-6)}$$

The electrodes tested in the half cell performed better if the supplied gas was enriched with $CO_2$.

These assumptions could also explain the measurements. However, it can be questioned that the described transport mechanism should be a continuous process and hence $CO_2$ could have been detected in exhaust gas at the hydrogen side at any time. This, however, could not be demonstrated with the measurements.

## 5.4 Diffusion Measurement

Two oxygen electrodes with different catalysts were tested to investigate their carbonate transport properties by diffusion. Oxygen electrode #418 used silver oxide ($Ag_2O$) as a catalyst, for electrode #366 Silflon was used as the catalyst. The results of the diffusion measurement are presented in Table 4-5.

The results of the measurement show that electrode #366 enabled a higher rate of carbonate transport by diffusion. The transport rate of electrode #418 was 5.15 times smaller. Obviously it was possible to influence the transport properties by changing the composition of the electrodes.

However, at that state of investigating the transport properties by diffusion it is hard to make secure conclusions. These were the first tests, further test have to be done.

# 6 Conclusion and Future Work

The aim of the presented research was to operate an alkaline fuel cell with air and hydrogen as the fuel instead of pure oxygen and hydrogen. The long-term operation was envisaged while the maintenance effort was to be kept low at the same time.

When using air as the fuel gas for long-term operation the following problems arise for an AFC:

- Formation of potassium carbonate

  The $CO_2$ contained in the air reacts with the electrolyte KOH to form potassium carbonate. The latter can precipitate and block the pore system of the gas diffusion electrodes which leads to a destruction of the AFC.

- Formation of reaction water

  The reaction of hydrogen and oxygen in an AFC produces water, the so-called reaction water. The reaction water dilutes the electrolyte thus causing a decrease of the conductivity and the performance of the cell declines. A volume increase would also cause the storage tank to overflow after some time.

In order to achieve a stable long timescale operation both problems have to be solved. Of the various available possibilities to achieve this initially the electrodialysis process was chosen as it is suited to solve both problems. During the experiments it became apparent that the manufactured cells did not suffer any disadvantages from the introduced unfiltered air. The extraction of the reaction water was the remaining problem. It was decided to remove the reaction water via the air flow.

Apart from that, several modifications of the fuel cell itself were achieved during the work on this project. The initial faults occurring when manufacturing the cells could be overcome with these modifications.

The crucial factor for air operation is the consistency of the oxygen electrodes. Appropriate electrodes were manufactured and initially tested in a half cell. This allowed to obtain some basic insights; a long-run test was carried out, for instance,

over several 1000 hours using unfiltered air. The half cell measurements are an aid when selecting the electrodes, but they do not replace the test in the fuel cell as the conditions are quite different.

For the operation of the fuel cell with air, in particular the gas supply system of the cell had to be adjusted to the new conditions. When operated with air, a significantly larger amount of gas was conducted through the cell as compared to the operation with pure oxygen. For this, a special gas compartment between the oxygen electrodes was developed and integrated into the cell. A series of experiments were carried out with these cells. In order to examine the effects of the $CO_2$, gas analyses were conducted using a gas chromatograph. The supplied gas as well as the exhaust gas at both the air and the hydrogen sides were analysed. Most importantly was the location of the $CO_2$. For this reason the electrolyte used in the cell was also analysed with regards to its potassium carbonate content.

For the examination of the removal of the reaction water experiments were carried out where the temperature as well as the air volume flow rate were varied.

Concluding it can be stated, that with a suitable choice of electrodes no disadvantages are to be expected as a consequence of the formation of carbonate. The measurements yielded that the increase of carbonate is beneficial to the long-term stability with respect to the electrode activity. The partly drastic effects on the life time and performance of alkaline fuel cells are hence not caused by the formation of carbonate. It has rather to be assumed that the electrodes and thus the fuel cell itself are destroyed through corrosion. Responsible for this is the concentration increase of the electrolyte potassium hydroxide solution during the operation of the fuel cell. A sufficient matter transport in the electrodes has to be ensured. It would also be advisable to use a lower electrolyte concentration from the start.

With respect to the extraction of the reaction water it became clear that it is not possible to achieve this via the air flow. Even though experiments could show that the principle of the approach is working, the side effects of this method lead to considerable problems. On the one hand the drying out of the oxygen electrodes

enhances the concentration increase of the potassium hydroxide solution and hence amplifies the destruction through corrosion. On the other hand a totally different behaviour with regards to the water in the cell is imposed by the operating parameters of the fuel cell that need to be set. It appears sensible to enable the reaction water extraction via the electrolyte and provide for a sound matter transport through the components of the fuel cell. As further work, a procedure should be realised to keep the potassium hydroxide solution at a certain concentration level. Different methods to achieve this were already illustrated in Section 2.4.3; of these methods the reaction water extraction through evaporation probably requires the least effort.

To prevent the drying up of the oxygen electrodes during air operation tests should be made with a PTFE foil between the electrode and the air compartment. Gas can pass the PTFE foil to ensure the gas supply for the electrode. In contrast, liquid water or potassium hydroxide solution can not pass the PTFE foil. To ensure a proper functioning of the fuel cell it is necessary to have a good interconnection of the electrode and the PTFE foil. A gap in between the components, which eventually could be filled with water, has to be prevented. Laminating could be a possible method for this aim.

It could be shown that an operation of the alkaline fuel cell with unfiltered air can be realised. In the opinion of the authors a carbonate problem does not exist. Special attention should rather be paid on preventing an excessive increase of the KOH concentration. The water cycle of the cell requires further research. A sufficient matter transport needs to be provided for. In this context the electrode properties should be investigated further. Suggestions were made for the reaction water extraction.

# References


[1-1] W. Vielstich, Brennstoffelemente, Verlag Chemie GmbH, Weinheim, 1965

[1-2] M. Cifrain and K. Kordesch, Hydrogen/oxygen (air) fuel cells with alkaline electrolytes, Handbook of Fuel Cells, Wiley, 2003

[1-3] E. Gülzow, M. Schulze, Long-term operation of AFC electrodes with $CO_2$ containing gases, Journal of Power Sources 127 (2004) 243-251

[1-4] Prof. Mirna Urquidi-Macdonald, et al. Design and Test of a Carbon-Tolerant Alkaline Fuel Cell, Pennsylvania State University, 2005

[1-5] Siemens-Varta, Studie, Brennstoffzellen-Antriebsanlage, Ergebnisbericht, Band I, Kap. 2.4.3, 1974

[1-6] K. Mund, Die reversible Elektrodialyse, Dissertation, University of Braunschweig, 1967

[2-1] Philosophical Magazine, Ser. 3, 1839, 14, 127

[2-2] Fuel Cell Handbook, EG&G Technical Services, Inc., 2004

[2-3] A. Winsel, R. Wendtland, Process of operating fuel cell, US Patent 3,597,275, 1971

[2-4] K. Rühling, Untersuchung an neuartigen PTFE-gebundenen Raney-Nickel- und Silberelektroden, Diplomarbeit, University Gesamthochschule Kassel, 1986

[2-5] H. Sauer, Verfahren zur Herstellung einer kunststoffgebundenen Aktivkohleschicht für dünne Gasdiffusionselektroden, Patent DBP DE 29 41 774, 1979

[2-6] A. Winsel, Poröse Gaselektrode, Patent DBP DE 33 42 969, 1983

[2-7] K. Rühling, A. Winsel, Separators for acidic and alkaline batteries, Journal of applied Electrochemistry, 1989

[2-8] M. Cifrain and K. Kordesch, Hydrogen/oxygen (air) fuel cells with alkaline electrolytes, Handbook of Fuel Cells, Wiley, 2003

[2-9] C.E. Kent, R.R. Nilson u. P. Moran, General Electric Rep. No. 63-WA-351, Vortrag Amer. Soc. Mechn. Engr., Nov. 1963 (Zitat aus Brennstoffelemente, Wolf Vielstich, IV.1.1.2.1, S. 162f, Verlag Chemie GmbH, Weinheim, 1965

[2-10] K. Kordesch, Symposium Brennstoffelemente, 136. Nationale Treffen der Amerikanischen Chemischen Gesellschaft, September 1959 (Zitat aus Brennstoffelemente, G.J. Young, Alfred University, New York, Krausskopf-Verlag, Wiesbaden, 1962)

[2-11] Gaskatel GmbH, Brennstoffzellen- und Halbzellenversuche, Kassel, 2004-2005

[2-12] E. Gülzow, M. Schulze, Long-term operation of AFC electrodes with $CO_2$ containing gases, Journal of Power Sources 127 (2004) 243-251

[2-13] Bram de Ruiter, The Dissolution of Carbon Dioxide and the Diffusion of Carbonate Ions in Alkaline Fuel Cells, Helsinki University of Technology, 1990

[2-14] Prof. Mirna Urquidi-Macdonald, et al. Design and Test of a Carbon-Tolerant Alkaline Fuel Cell, Pennsylvania State University, 2005

[2-15] P. Gorérec, L. Poletto, J. Denizot, E. Sanchez-Cortezon, J.H. Miners, The evolution of the performance of alkaline fuel cells with circulating electrolyte, Journal of Power Sources 129 (2004) 193-204

[2-16] K. Kordesch, G. Simader, Fuel Cells and their applications, Berlin, Germany, Wiley-VCH, 1996

[2-17] T K Sanderson, An updated assessment of the prospects for fuel cell-powered cars, DTI, United Kingdom, 2005

[2-18] K. Mund, Die reversible Elektrodialyse, Dissertation, University of Braunschweig, 1967

[2-19] G.F. McLean, T. Niet, S. Prince-Richard, N. Djilali, An assessment of alkaline fuel cell technology, International Journal of Hydrogen Energy 27 (2002) 507-526

[2-20] Appleby AJ, Foulkes FR, Fuel Cell Handbook, Malabar, Florida, Krieger Publishing Company, 1993

[2-21] Ahuja V, Green RK, $CO_2$ removal from air for alkaline fuel cells operating with liquid hydrogen - heat exchanger development, International Journal of Hydrogen Energy 21 (1996) 415-421

[2-22] Ahuja V, Green RK, Carbon dioxide removal from air for alkaline fuel cells operating with liquid hydrogen - a synergistic advantage, International Journal of Hydrogen Energy 23 (1998) 181-185

[2-23] A. Fyke, An investigation of alkaline and PEM fuel cells, Institute for Integrated Energy Systems, University of Victoria, 1995

[2-24] L. Swette et al. Development of single unit acid and alkaline regenerative solid ionomer fuel cells, Intersociety Energy Conversion Engineering Conference Proceedings, Atlanta, GA 1993, 1227-32

[2-25] K. Kinoshita, Electrochemical oxygen technology, New York, Wiley, 1992

[2-26] K. Kordesch, J. Gsellmann, M. Cifrain, Revival of alkaline fuel cell hybrid systems for electric vehicles, Proceedings of Fuel Cell seminar, Palm Springs, 1998

[2-27] A. Winsel, H.J. Schwarz, Belg. Pat. 710675

[2-28] Siemens-Varta, Studie, Brennstoffzellen-Antriebsanlage, Ergebnisbericht, Band I, Kap. 2.4.3, 1974

[2-29] K. Kordesch, G. Simader, Fuel Cells and their applications, VCH Publishers, NY, 1996

[2-30] OUT e.V., Elektromembranverfahren, Abschlussbericht, Berlin, 2004

[2-31] E. Gülzow, M. Schulze, Long-term operation of AFC electrodes with $CO_2$ containing gases, Journal of Power Sources 127 (2004) 243-251

[2-32] Jose D. Giner, Aqueous carbonate electrolyte fuel cell, US Patent 4,781,995, 1988

[3-1] M. Mörbel, Technical Report „Gießharze", Gaskatel GmbH, Kassel 2004

[3-2] J. Grassegger, „Aufbau eines Messstandes für Gasdiffusionselektroden in Halbzellenanordnung und Erprobung von Sauerstoffelektroden", Diplomarbeit, University Gesamthochschule Kassel, 1993

[3-3] A. Kalberlah, „Die Bedeutung des Nickelhydroxyds für die katalytische Aktivität des Raney-Nickel", Dissertation, University of Braunschweig, 1967

[3-4] K. Rühling, „Untersuchungen an neuartigen PTFE-gebundenen Raney-Nickel- und Silberelektroden", Diplomarbeit, University Gesamthochschule Kassel, 1986

[3-5] Chemieplanet Website (www.chemieplanet.de), last accessed 13.11.2005

[3-6] G. Sauer, Fuel Cell design for Techniques and Instruments for Gas hydrates Exploration and Research, Master Thesis, DIT, 2006

[4-1] Winkler, Cl., Praktische Übungen in der Maßanalyse, 5. Auflage, bearb. von Brunck, O., Verlag Felix, Leipzig, 1920

[4-2] Jander, Jahr, Maßanalyse: Theorie und Praxis der Titrationen mit chemischen und physikalischen Indikationen, 15. Auflage, Walter de Gruyter, Berlin, New York, 1989

[5-1] N. Wagner, E. Gülzow, M. Schulze, Long-term investigations of silver cathodes for alkaline fuel cells, Proceedings of the Eighth UECT, Ulm, 20-21 June 2002, Journal of Power Sources

[5-2] E. Gülzow, M. Schulze, Long-term operation of AFC electrodes with $CO_2$ containing gases, Journal of Power Sources 127 (2004) 243-251

[5-3] Gaskatel GmbH, Technical Report, Experimental determination of the solubility of $K_2CO_3$ in 7.0 M KOH solution at 25 °C, Kassel, 2005

[5-4] Küster-Thiel, Rechentafeln für die Chemische Analytik, 103. Auflage, Walter de Gruyter, Berlin, New York, 1985

[5-5] A. Winsel, Verfahrenstechnik poröser Elektroden, Chemie-Ingenieur-Technik, Jahrgang 43 Heft 4, Seite 191-195, 1971

[5-6] Gaskatel GmbH, Determination of the carbonate content in the electrolyte of half cells and fuel cells operated with $H_2/O_2$ and $H_2$/Air by titration, Kassel, 2005

[5-7] Mean Activity Coefficients of KOH at 25 °C, CRC Handbook of Chemistry and Physics, 77th Edition, Page 5-104, CRC Press, 1996

[5-8] C.E. Kent, R.R. Nilson u. P. Moran, General Electric Rep. No. 63-WA-351, Vortrag Amer. Soc. Mechn. Engr., Nov. 1963 (Zitat aus Brennstoffelemente, Wolf Vielstich, IV.1.1.2.1, S. 162f, Verlag Chemie GmbH, Weinheim, 1965)

[5-9] K. Kordesch, Symposium Brennstoffelemente, 136. Nationale Treffen der Amerikanischen Chemischen Gesellschaft, September 1959 (Zitat aus Brennstoffelemente, G.J. Young, Alfred University, New York, Krausskopf-Verlag, Wiesbaden, 1962)

[5-10] J. Helmke, Die Silas-4/4-Elektrode, Herstellung und Verhalten im Lichte des Kugelhaufenmodells, Diplomarbeit, University Gesamthochschule Kassel, 1994

[5-11] G. Sauer, Fuel Cell design for Techniques and Instruments for Gas hydrates Exploration and Research, Master Thesis, DIT, 2006

[5-12] Jose D. Giner, Aqueous carbonate electrolyte fuel cell, US Patent 4,781,995, 1988

# List of Figures

# List of Diagrams

# List of Tables